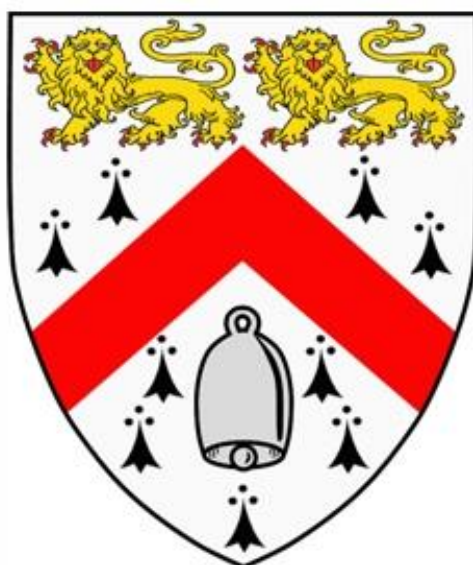


Lipoprotein lipidomics in obesity-associated metabolic and hepatic disorders



Gabriele Mocciaro
Wolfson College

Department of Biochemistry
University of Cambridge

This dissertation is submitted for the degree of Doctor of Philosophy
July 2021

Declaration

This dissertation is the result of my own work and includes nothing which is the outcome of work done in collaboration except as declared in the Preface and specified in the text. It is not substantially the same as any that I have submitted, or, is being concurrently submitted for a degree or diploma or other qualification at the University of Cambridge or any other University or similar institution except as declared in the Preface and specified in the text. I further state that no substantial part of my dissertation has already been submitted, or, is being concurrently submitted for any such degree, diploma or other qualification at the University of Cambridge or any other University or similar institution except as declared in the Preface and specified in the text. It does not exceed the prescribed word limit.

Lipoprotein lipidomics in obesity-associated metabolic and hepatic disorders

Gabriele Mocciaro

Abstract

Over the last few decades, obesity has reached epidemic proportions. Obesity is strongly associated with insulin resistance (IR), hyperglycaemia, mixed dyslipidaemia, and hypertension. These metabolic risk factors, grouped under the definition of the Metabolic Syndrome (MetS), increase the risk of cardiovascular disease (CVD). Non-alcoholic fatty liver disease (NAFLD) is one of the most common co-morbidities of MetS. NAFLD ranges from simple steatosis to more aggressive forms, with the potential to evolve to hepatocellular carcinoma and CVD. Lipoprotein dysmetabolism is crucial to both MetS and NAFLD and few studies have investigated the circulating lipidome, defined as the complete lipid profile in a specific tissue/biofluid, in these conditions. The work contained in this thesis studied the lipoprotein remodelling occurring in two cohorts; MetS cohort including 11 healthy people and 14 MetS subjects and BioNASH cohort including 20 healthy people and 89 biopsy-proven patients across the entire spectrum of NAFLD. To this end, we employed state-of-the-art analytical techniques (mass spectrometry-based) along with molecular biology assays to study the serum and lipoprotein lipidome of these patients.

In the MetS study, we found that the circulating lipidome of MetS was characterised by a phospholipid (PL) dysmetabolism. The latter was driven, at least in part, by a reduced activity of the enzyme lecithin-cholesterol acyltransferase (LCAT). Dysfunctional LCAT could partly mediate the elevated CVD risk in MetS patients. Our study demonstrated, for the first time, the link between reduced LCAT activity and plasma lipidome in MetS.

In the BioNASH cohort, we observed a generalised PL and polyunsaturated fatty acids (PUFA) depletion in NAFLD compared to the control group. By using fast protein liquid chromatography, we isolated HDL and VLDL fractions where we performed lipidomic analyses. As opposed to VLDL, the HDL lipidome was characterised by PL and PUFA depletion. These changes have been reported in hepatic lipidomic studies of NAFLD patients, thus suggesting a close link between peripheral tissues and the liver via HDL.

These results provide the basis for the study of HDL composition as a novel player in the pathogenesis of NAFLD.

In conclusion, these data demonstrate how the study of lipoprotein metabolism in obesity-related metabolic disorders can shed light on novel pathophysiological mechanisms. Further efforts along these lines will clarify the role of LCAT in MetS and CVD alongside establishing the contribution of the HDL lipidome to the liver composition of NAFLD patients.

Publications

1. Hall Z, Chiarugi D, Charidemou E, Leslie J, Scott E, Pelligrinet L, Allison M, **Mocciaro G**, Anstee QM, Evan GI, Hoare M, Vidal-Puig A, Oakley F, Vacca M, Griffin JL. Lipid Remodelling in Hepatocyte Proliferation and Hepatocellular Carcinoma (Hepatology. 2020 May 27)
2. **Mocciaro G**, Bresciani L, Tsiountsioura M, Martini D, Mena P, Charron M, Brighenti F, Bentley S, Harvey M, Collins D, Ray S. Dietary absorption profile, bioavailability of (poly)phenolic compounds, and acute modulation of vascular/endothelial function by hazelnut skin extract (accepted in Journal of Functional Foods)
3. Hinz C, Liggi S, **Mocciaro G**, Jung SM, Induruwa I, Pereira MCDA, Bryant CE, Meckelmann SW, O'Donnell VB, Farndale RW, Fjeldsted JC, Griffin JL. A comprehensive UHPLC ion mobility QTOF method for profiling and quantification of eicosanoids, other oxylipins and fatty acids. (Anal Chem. 2019 May 10)
4. Ducheix S, Peres C, Hardfeldt J, Fra C, **Mocciaro G**, Piccinin E, Lobaccaro JM, Plateroti M, Griffin JL, Ntambi J, Moschetta A. Ablation of Stearoyl-CoA Desaturase 1 in enterocytes drives intestinal inflammation and tumorigenesis that are rescued by dietary oleate. Gastroenterology 2018 Nov;155(5):1524-1538
5. Bhat S, **Mocciaro G**, Ray S. The Association of Dietary Patterns and Carotid Intima-Media Thickness: A Synthesis of Current Evidence (Nutr Metab Cardiovasc Dis. 2019 Dec;29(12):1273-1287)
6. **Mocciaro G**, Ziauddeen N, Godos J, Marranzano M, Chan MY, Ray S. Does a Mediterranean-type dietary pattern exert a cardio-protective effect outside the Mediterranean region? A review of current evidence. (Int J Food Sci Nutr. 2017 Oct 24:1-12)

Preprints (non peer-reviewed)

1. Seyres D, Cabassi A, Lambourne JJ, Burden F, Farrow S, McKinney H, Batista J, Kempster C, Pietzner M, Slingsby O, Huy Cao T, Quinn PA, Stefanucci L, Sims MC, Rehnstrom K, Adams CL, Fray A, Ergüener B, Kreuzhuber R, **Mocciaro G**, D'Amore S, Koulman A, Grassi L, Griffin JL, Ng LL, Park A, Savage DB, Langenberg C, Bock C, Downes K, Allison M, Vacca M, Kirk PDW, Frontini M. Transcriptional, epigenetic and metabolic signatures in cardiometabolic syndrome defined by extreme phenotypes. (doi: <https://doi.org/10.1101/2020.03.06.961805>)

Dedication

To my best friend and partner Yasmine.

Acknowledgments

First of all, I would like to express my deepest gratitude to my mentors Prof Julian Griffin and Dr Michele Vacca for the tremendous help and support given to me throughout my PhD journey. Their mentorship has been invaluable. I am grateful to Dr Zoe Hall, Dr Antonio Murgia, Dr Sonia Liggi and Dr Ben McNally for helping me run the LC-MS, with data processing and the training provided. In particular, I am very grateful to Dr Murgia for having provided me with an excellent training on the LC MS/MS system alongside the endless technical discussion and his support while he had already taken up a different job. I am thankful to Dr Albert Koulman and Dr Ben Jenkins for having let me use their lab space and mass spectrometers without any restrictions. Furthermore, I am also grateful to Dr Jenkins for his extensive training on the LC-MS Orbitrap system. I would also like to thank Dr Richard Kay for having run the LC-MS proteomic analysis. I am indebted with Stefanie Neun, Damon Parkington and his team for their great support in letting me use their plate readers for the measurement of enzyme activity and ELISA. I am also grateful to Dr Mattia Frontini and his team for the training provided and help with the recruitment of the healthy volunteers (BioNASH cohort). A particular thank goes to my colleague and friend Dr Luis Vicente Herrera-Marcos, whom thought me how to use the FPLC system and to whom I owe most of my technical knowledge regarding the lipoprotein separation. I am indebted to Dr Shivani Bhat for her help with English wording/editing of the introduction chapter. I would also like to thank Steven Murfitt for all the help on the day to day bench work at the Department of Biochemistry.

A special thanks go to my parents Carmelo and Giovanna, alongside my brother Roberto. Their support and love have proven essential in shaping the person I have become.

Contents

Chapter 1. Background and rationale	14
1.1 The Obesity Epidemic	14
1.2 The Metabolic Syndrome and Non-alcoholic fatty liver disease.....	14
1.2.1 Pathophysiology	17
1.2.2 Genetic factors of NAFLD.....	17
1.2.3 Adipose tissue dysfunction.....	18
1.2.4 Physiological role of insulin in lipid and glucose metabolism	19
1.2.5 Metabolic aspects of IR in MetS and NAFLD	20
1.2.6 DNL and its drivers in NAFLD – the role of SREBP 1c & ChREBP.....	21
1.2.7 Lipoprotein metabolism.....	24
1.2.7.1 The exogenous pathway.....	25
1.2.7.2 The endogenous pathway	26
1.2.7.3 Reverse cholesterol transport (RCT) – HDL metabolism and circulating lipoprotein remodelling enzymes	27
1.2.8 Dyslipidaemia in NAFLD and MetS	29
1.2.8.1 Impaired VLDL turnover	29
1.2.8.2 Increased atherogenic LDL particles – the role of sdLDL-C.....	30
1.2.8.3 Decreased levels of HDL-C	30
1.2.9 NAFLD: a tale of hepatic lipid fluxes	32
1.2.10 Lipotoxicity and NASH progression.....	32
1.2.11 Complications of the MetS and NAFLD	36
1.2.11.1 Type II diabetes mellitus (T2DM).....	36
1.2.11.2 Atherosclerotic cardiovascular disease (ASCVD).....	36
1.2.11.3 Chronic kidney disease	37
1.3 Lipidomics as a tool to study obesity and its metabolic-related disorders.....	38
1.3.1 Lipoprotein lipidomics	43
1.3.2 The use of liquid chromatography-mass spectrometry in lipidomics and metabolomics	44
Chapter 2. Materials and methods	47
2.1 Measurement of clinical biochemistry.....	47
2.2 Measurement of lipid levels by mass spectrometry	47
2.2.1 Lipid extraction	47
2.2.2 Lipid analysis by liquid chromatography-mass spectrometry	48
2.2.3 Esterified cholesterol analysis – LC-MS/MS	51

2.3 Measurement of apolipoprotein levels by mass spectrometry	51
2.3.1 Apolipoprotein extraction	51
2.3.2 Apolipoproteins analysis by liquid chromatography-mass spectrometry	52
2.4 Lipoprotein separation by Fast protein liquid chromatography.....	53
2.5 Statistical analyses	54
Chapter 3. Lipidomic indices reveal reduced LCAT activity in patients with metabolic syndrome.....	55
3.1 Abstract	55
3.2 Introduction	56
3.3 Methods.....	58
3.3.1 Ethics and the MetS study cohort	58
3.3.2 Sample collection and clinical biochemistry measurements.....	58
3.3.3 Measurement of lipid levels by mass spectrometry	58
3.3.4 Measurement of protein levels by mass spectrometry	59
3.3.5 Circulating lipoprotein remodelling enzyme activity - fluorimetric assay.....	59
3.3.5.1 Lp-PLA2.....	59
3.3.5.2 LCAT activity.....	59
3.3.5.3 PLTP activity.....	59
3.3.6 Statistics	60
3.4 Results.....	61
3.4.1 Clinical characteristics, serum lipidomic and apoprotein profile of healthy and MetS participants.....	61
3.4.2 LCAT, but not Lp-PLA2, activity is reduced in MetS thus justifying the changes in serum PC and LysoPC.....	65
3.4.3 LCAT activity and its lipidomic proxies show an inverse correlation with metabolic risk factors and positively correlate with HDL-C.....	66
3.4.4 Discussion	69
3.4.5 Limitations.....	71
3.4.6 Conclusion	72
Chapter 4. NAFLD is characterised by a reduced reverse polyunsaturated fatty acid transport from peripheral tissues to the liver.....	77
4.1 Abstract	77
4.2 Introduction	79
4.3 Methods.....	82
4.3.1 Ethics and the BioNASH study cohort.....	82
4.3.2 Sample collection and clinical biochemistry measurements.....	82

4.3.3 Measurement of lipid levels by mass spectrometry	82
4.3.4 Measurement of ApoA1	83
4.3.5 Measurement of ApoB	83
4.3.6 Statistics	83
4.4 Results.....	85
4.4.1 Clinical characteristics and whole serum lipidomic profile of healthy and NAFLD patients.....	85
4.4.2 HDL lipidomics of NAFLD patients suggest a reduced reverse PUFA transport from peripheral tissues to the liver	89
4.4.3 VLDL lipidomics of NAFLD patients shows an enhanced SFA export from the liver to peripheral tissues	94
4.4.4 Discussion.....	98
4.4.5 Limitations	102
Chapter 5. Conclusion.....	116
5.1 Summary and conclusion	116
5.2 Future directions	120

Abbreviations

ACC	Acetyl-CoA Carboxylate
ABCA1	ATP-Binding Cassette sub-family A member 1
ABCG1	ATP-binding cassette sub-family G member 1
ACL	ATP-citrate lyase
ACN	Acetonitrile
Akt	Protein kinase B
Apo	Apolipoprotein
AT	Adipose Tissue
ASCVD	Atherosclerotic Cardiovascular Disease
BMI	Body Mass Index
CE	Cholesterol Ester
CETP	Cholesteryl ester transfer protein
ChREBP	Carbohydrate response element binding protein
CKD	Chronic kidney disease
CM	Chylomicron
CVD	Cardiovascular Disease
DG	Diacylglycerol
DNL	<i>De Novo</i> Lipogenesis
ER	Endoplasmic reticulum
ESI	Electrospray ionisation
FA	Fatty Acid
FAS	Fatty acid synthase
FADS1	Fatty Acid Desaturase 1
FADS2	Fatty Acid Desaturase 2
FC	Free Cholesterol
FFA	Free Fatty Acid
GC-MS	Gas Chromatography-Mass Spectrometry
GLUT 4	Glucose transporter type 4
HDL	High-Density Lipoprotein
HSPGs	Heparan-Sulfate Proteoglycans

HOMA-IR	Homeostatic Model Assessment for Insulin Resistance
HSL	Hormone-Sensitive Lipase
IDL	Intermediate Density Lipoprotein
INSIG1	Insulin induced gene 1
IR	Insulin Resistance
LCAT	Lecithin–Cholesterol AcylTransferase
LC-MS	Liquid Chromatography-Mass Spectrometry
LDL	Low-Density Lipoprotein
LDLR	Low-Density Lipoprotein Receptor
LPL	Lipoprotein Lipase
LysoPC	Lysophosphatidylcholine
LysoPE	Lysophosphatidylethanolamine
MAFLD	Metabolic associated fatty liver disease
MetS	Metabolic Syndrome
MS	Mass Spectrometry
MUFA	Monounsaturated Fatty Acid
NAFLD	Non-Alcoholic Fatty Liver Disease
NASH	Non-Alcoholic Steatohepatitis
NCEP ATP-III	National Cholesterol Education Program Adult Treatment Panel III
OXPHOS	Oxidative Phosphorylation
PC	Phosphatidylcholine
PCA	Principal Component Analysis
PE	Phosphatidylethanolamine
PG	Phosphoacylglycerols
PGC-1 α	Peroxisome Proliferator-Activated Receptors γ Coactivator-1 α
PLA2	Phospholipase A2
PLTP	Phospholipid Transfer Protein
PNPLA3	Patatin-like Phospholipase domain-containing protein 3

PPAR α	Peroxisome Proliferator-Activated Receptors α
PPAR γ	Peroxisome Proliferator-Activated Receptors γ
PUFA	Polyunsaturated Fatty Acid
PyrC	Pyruvate Carboxylase
QqQ	Triple Quadrupole
RCT	Reverse Cholesterol Transport
SCD1	Stearoyl-CoA Desaturase-1
sdLDL	Small dense LDL cholesterol
SFA	Saturated Fatty Acid
SM	Sphingomyelin
SREBP1	sterol regulatory element-binding protein 1
T2DM	Type 2 Diabetes Mellitus
TG	Triacylglycerol
TM6SF2	Transmembrane 6 Superfamily Member 2
VIP	Variable Importance in the Projection
VLDL	Very Low-Density Lipoprotein
WAT	White Adipose Tissue
WHO	World Health Organization

Chapter 1. Background and rationale

1.1 The Obesity Epidemic

Overweight and obesity are defined as excessive fat accumulation that can adversely affect health. Body mass index (BMI), weight in kilograms per height in metres squared, is widely used as a marker of body fat in the clinic. The World Health Organisation (WHO) defines overweight as a BMI between 25 and 29.9 kg/m², and obesity as a BMI greater than 30 kg/m² (World Health Organization, 2018). Over the last three decades, the steady increase in obesity has become a major public health concern, which has now reached epidemic proportions (Ng et al, 2014). Worldwide, 1.9 billion adults are classified as overweight, of whom 650 million are obese (World Health Organization, 2018). In England, 62% of the population is classified as overweight and 24% as obese (Gov.UK national statistics, 2017). Obesity is strongly associated with a cluster of cardiovascular risk factors [referred to as Metabolic Syndrome (Eckel et al, 2005)] including hypertension, mixed dyslipidaemia, systemic insulin resistance (IR), and hyperglycaemia, and many other “travelling companions” like fatty liver, gout, and chronic-low-grade systemic inflammation. Obesity also promotes life-threatening comorbidities including type 2 diabetes mellitus (T2DM), cardiovascular disease (CVD), and cancers (e.g. liver, colon, breast, and prostate) ((Berrington de Gonzalez et al, 2010)).

1.2 The Metabolic Syndrome and Non-alcoholic fatty liver disease

The metabolic syndrome (MetS) and non-alcoholic fatty liver disease (NAFLD) are obesity-associated metabolic disorders. Although they are clinically defined as different diseases, several pathophysiological aspects overlap. Therefore, throughout the introduction of this thesis, the two conditions are described together, with the differences between them clearly specified.

The MetS is clinically defined by the co-existence of atherogenic dyslipidaemia, increased apolipoprotein B lipoproteins [very low density lipoprotein (VLDL), intermediate density lipoprotein (IDL), low density lipoprotein (LDL)], decreased high density lipoprotein (HDL), elevated blood pressure and fasting glucose, together with a pro-thrombotic state, and a pro-inflammatory state (chronic low-grade inflammation)

(Eckel et al, 2005). The real prevalence of MetS is difficult to estimate since differences in inclusion criteria have led to varied results worldwide (Eckel et al, 2005). However, in European countries, its prevalence is estimated to be between 10% and 30% (van Vliet-Ostaptchouk et al, 2014). Although the MetS was clinically identified nearly a century ago (Kylin, 1923), it was not until 1998 that a WHO panel proposed a set of criteria for the MetS (Alberti & Zimmet, 1998) to establish an international standard. Since then, different definitions have been proposed and among them, the most commonly adopted definition was proposed as a joint statement of the International Diabetes Federation Task Force on Epidemiology and Prevention; National Heart, Lung, and Blood Institute; American Heart Association; World Heart Federation; International Atherosclerosis Society; and International Association for the Study of Obesity (Alberti et al, 2009). The latter defined the MetS when 3 out of 5 cardiovascular risk factors [abdominal obesity, high blood glucose and triglycerides (TG), increased blood pressure, and reduced HDL-C] are present (Table 1).

Table 1. Clinical risk factors and defining levels for MetS according to NCEP ATP-III.

Risk factor	Defining level
Elevated waist circumference*	≥102 cm in males; ≥88 cm in female
Elevated triglycerides or under drug treatment for its reduction	≥1.7 mmol/L (150 mg/dL)
Reduced HDL-C or under drug treatment for reduced HDL-C	<1.0 mmol/L (40 mg/dL) in males; <1.3 mmol/L (50 mg/dL) in females
Elevated blood pressure or under antihypertensive drug treatment	Systolic ≥130 and/or diastolic ≥85 mm Hg
Elevated fasting glucose or under drug treatment of elevated glucose	≥ 5.6 mmol/L (100 mg/dL)

**Waist circumference cut-offs are population specific. Here, the values used for the European population are reported.*

NAFLD encompasses a spectrum of disorders ranging from simple steatosis, intrahepatic fat deposition (>5% fat content in the liver), to steatohepatitis (steatosis in the presence of inflammation) (NASH), fibrosis, and cirrhosis, which can ultimately evolve to hepatocellular carcinoma (HCC) (Vacca et al, 2015). The diagnosis of NAFLD is through the exclusion of all the secondary causes of fat accumulation in the liver (elevated alcohol consumption, presence of hepatitis B and/or C, drug abuse,

autoimmune liver disease, haemochromatosis or Wilson's disease) and liver biopsy, which is still considered the gold standard to differentiate fatty liver from NASH and to stage fibrosis (Buzzetti et al, 2016). NAFLD is one of the most common liver disorders worldwide with a global prevalence of 24% (Younossi et al, 2018). NASH related cirrhosis is predicted to become the leading cause of liver transplantation within the next two decades (Zezos & Renner, 2014).

Epidemiological studies have shown that despite the high prevalence of NAFLD, only a subset of patients develops more aggressive forms of this disease. Specifically, 5 to 10% of patients with NAFLD develop NASH, 30% of these develop cirrhosis, and 1-2% of these eventually develop HCC (Argo & Caldwell, 2009). The evolution of NAFLD to HCC is an area of active research. NAFLD is also considered as the hepatic manifestation of MetS, with a prevalence of 50% in patients with T2DM, 76% in obese subjects, and 100% in those morbidly obese with T2DM (Vacca et al, 2015). The close association with MetS is also represented by the fact that CVD is the leading cause of mortality for people with NAFLD (Younossi et al, 2018). Of note, despite the strong association of obesity with NAFLD, a subset of the population develops NAFLD in the absence of obesity (Younossi et al, 2018). This population is referred to as "Lean NAFLD". The latter term, firstly described in Asia, has a prevalence in Europe and the USA of up to 20% (Younossi et al, 2018). This condition is characterised by abdominal obesity, IR, and elevated triglycerides when compared to matched controls without NAFLD (Younossi et al, 2018).

Two recent position articles have proposed to re-define NAFLD into metabolic associated fatty liver disease (MAFLD) to strengthen the metabolic nature of this condition (Eslam et al, 2020a; Eslam et al, 2020b). This new definition highlights the inadequacy of a biopsy centric approach to classify the disease. For example, high variability in disease progression is well established. Specifically, some patients with hepatic steatosis can develop steatohepatitis and revert to steatosis over a short timeframe and although the progression to more severe forms of NAFLD spectrum is more likely in patients with NASH, not all NASH patients will progress towards the end stage of the disease (Eslam et al, 2020a). The new definition emphasises the crucial role of metabolic impairment in this condition. Specifically, MAFLD defining criteria include the presence of hepatic steatosis along with one of the three following cardiovascular risk factors: overweight or obesity, T2DM, or normal weight with

evidence of metabolic dysregulation (Eslam et al, 2020a). In sharp contrast to the NAFLD paradigm, MAFLD is no longer considered a disease of exclusion and elevated alcohol consumption and other concomitant liver diseases can coexist with this new definition (Eslam et al, 2020a).

1.2.1 Pathophysiology

Although the aetiology of the MetS is multifactorial, it is increasingly recognised that sedentary lifestyles along with overnutrition are key players (Cornier et al, 2008). The pathophysiological mechanism of the MetS has not been fully determined, yet abdominal obesity and insulin resistance are believed to be the main drivers of the MetS (Cornier et al, 2008). NAFLD is the result of the accumulation of hepatic fat. The sources of fats contributing to NAFLD can be summarised as follows: a) dietary fatty acids derived through the uptake of chylomicrons (CM), b) free fatty acids (FFA) derived thorough lipolysis of TG stored within white adipose tissue (WAT), and c) fatty acids (FA) newly synthesised within the liver through de novo lipogenesis (DNL) (Vacca et al, 2015). The raised FA levels in the liver can then be 1) stored as lipid droplets within hepatocytes, 2) secreted into the bloodstream as VLDL, or 3) oxidised via the β -oxidation pathway (Vacca et al, 2015). However, fat accumulation on its own is not sufficient to drive NAFLD progression towards its more aggressive forms. The multifactorial nature of NAFLD has been recognised over the last two decades and its pathophysiology is currently recapitulated by the multiple parallel hit hypothesis (Tilg & Moschen, 2010). Under this hypothesis, the onset and progression of NAFLD are driven by the synergistic action of multiple parallel factors including IR, lipotoxicity, endoplasmic reticulum (ER) stress, mitochondrial dysfunction, adipose tissue (AT) dysfunction, and genetic background. The following sections describe the role of different risk factors characterising MetS and NAFLD.

1.2.2 Genetic factors of NAFLD

Recent studies are increasingly revealing the genetic factors involved in the onset and progression of NAFLD towards more advanced forms of the disease (Brunt et al, 2015). Investigation of candidate gene analysis with a biologically plausible pathogenic role for NAFLD, have shown the involvement of mutations in genes

including mitochondrial superoxide dismutase 2 (SOD2) (Al-Serri et al, 2012) and fatty acid desaturase 1 (FADS1) (Wang et al, 2015). More recently, with the advent of a non-targeted approach based on genome-wide association studies (GWAS), novel genetic candidates have been associated with NAFLD specifically a) the Patatin-like phospholipase domain-containing protein 3 gene (PNPLA3) on chromosome 22 and b) the Transmembrane 6 superfamily member 2 gene (TM6SF2) on chromosome 19 (Brunt et al, 2015). PNPLA3 is involved in TG hydrolysis and acylglycerol transacylase activity within the liver (Kumari et al, 2012), and a missense mutation I148M in PNPLA3 (at SNP rs738409) leads to impaired hepatic triglyceride hydrolysis (He et al, 2010). Although this polymorphism has been extensively investigated, the mechanism by which a mutation in PNPLA3 increases hepatic TG is yet to be fully elucidated. Paradoxically, it has also been reported that carriers of this mutation have a reduced CVD events (Ruschenbaum et al, 2018). A non-synonymous mutation Glu167Lys in TM6SF2 (at SNP rs58542926) has been shown to influence hepatic TG content, with carriers of the variant having a 34% higher liver fat content compared to those without the variant (Zhou et al, 2019). Interestingly, none of the above mentioned SNPs are associated with IR (He et al, 2010; Zhou et al, 2019).

1.2.3 Adipose tissue dysfunction

The last two decades have highlighted the underappreciated and dynamic role of AT in obesity and its related disorders (i.e MetS and NAFLD) (Guerra et al, 2021). AT can be classified into three “main” categories: 1) WAT, > 95% of total fat mass, 2) brown AT (BAT), 1-2% of total fat mass, and 3) beige AT (BAT), located within WAT and with the capability of turning into brown-like adipocytes following exposure to cold temperatures or other stressors (Kahn et al, 2019). The anatomical localisation of excessive WAT plays a key role in the onset of the MetS and NAFLD, with visceral WAT surplus being more detrimental than subcutaneous WAT (Kahn et al, 2019). One hypothesis behind the mechanistic link between obesity and the MetS and NAFLD is the AT expandability hypothesis (Virtue & Vidal-Puig, 2010). The latter is based on the idea that adipose tissue has a defined limit of expansion for any given individual determined by genetic and environmental factors (Virtue & Vidal-Puig, 2010). At its maximum storage limit, AT can no longer store more lipid, thus any additional surplus is redirected into other tissues such as muscle, liver, and pancreas. This ectopic fat

deposition has detrimental effects leading to IR and apoptosis (Virtue & Vidal-Puig, 2010). Although the molecular basis regulating AT expansion capability is not fully understood, the continuous increase in AT mass leads to adipocyte hypertrophy and hyperplasia. These events lead to increased lipolysis as a means to counterbalance the expansion and release of pro-inflammatory cytokines as a stress response, which if protracted over time can lead to AT IR and adipocyte apoptosis (Virtue & Vidal-Puig, 2010).

1.2.4 Physiological role of insulin in lipid and glucose metabolism

Insulin plays a central role in glucose, lipid, and energy regulation, enabling the body to efficiently respond to changes in nutrient levels during fasting and feeding states (Boucher et al, 2014). In healthy subjects, the postprandial effect of insulin on insulin-sensitive tissues can be generalised as follows. In the liver, insulin promotes the formation of glycogen, through the activation of the enzyme glycogen synthase (GS) via the serine/threonine-protein kinases (Akt) pathway (Samuel & Shulman, 2016). It also suppresses glucose production through a) the reduction of gluconeogenic enzymes (Edgerton et al, 2017), and b) indirectly, through the inhibition of AT lipolysis (Figure 1). The latter is due to the inhibition of hormone-sensitive lipase (HSL), which normally releases free fatty acids (FFA) and glycerol into the bloodstream, as a source of energy for other organs. One of the mechanisms by which insulin inhibits HSL is through the promotion of the cyclic AMP (cAMP) phosphodiesterase activity which enhances cAMP hydrolysis with consequent reduction of cAMP depended PKA activity, that is required for the HSL activation (Lan et al, 2019). Reduced HSL activity results in a reduced FFA flux into the liver, normally taken up through the fatty acid translocase/cluster differentiation protein-36 (FAT/CD36), which leads to decreased hepatic acetyl-CoA levels, promoting the activation of pyruvate carboxylase (PyrC), and therefore reduced PyrC activity and gluconeogenesis (Perry et al, 2015). Furthermore, insulin suppresses the formation and export of VLDL into circulation through a reduced transcription of apo-B100 mRNA, as well as genes encoding MTP and APOC III via inhibition of the transcriptional factor forkhead box O1 (FoxO1) (Altomonte et al, 2004; Kamagate et al, 2008) (Figure 1). The postprandial decrease in VLDL export permits the preferential use of chylomicrons as a source of “fuel” from the peripheral tissues, therefore sparing the liver FA pool for fasting conditions.

Furthermore, insulin directly co-modulates DNL by the activation of the transcriptional factor sterol regulatory element-binding protein 1 (SREBP1) (Samuel & Shulman, 2016). SREBP1 regulates DNL through transcriptional upregulation of several key genes involved in FA synthesis, namely acetyl-CoA carboxylase, fatty acid synthase (FAS), and desaturation and elongation of FA through stearoyl-CoA desaturase 1 and long-chain elongase 6 (ELOVL6), respectively (Postic & Girard, 2008) (Figure 1). Insulin also promotes the TG-rich lipoprotein clearance through the activation of lipoprotein lipase (LPL) (Panarotto et al, 2002), a key enzyme in the metabolism of TG-rich lipoproteins. Moreover, insulin promotes glucose uptake in AT and skeletal muscles through the upregulation of the glucose transporter type 4 (GLUT4) (Figure 1).

1.2.5 Metabolic aspects of IR in MetS and NAFLD

IR, a key feature of the MetS and NAFLD, results when cells from insulin-sensitive tissues (liver, skeletal muscle, and AT) no longer adequately respond to insulin, negatively impacting glucose and lipid homeostasis (Boucher et al, 2014). The action of insulin on insulin-sensitive tissues in IR people can be generalised as follows. In AT, insulin fails to regulate HSL and LPL with subsequent continuous release of FFA (Lewis et al, 1995) and increased TG-rich lipoproteins (Brunt et al, 2015). The rise in plasma FFA and glycerol is partially redirected into the liver and skeletal muscle. The former primarily responds by a) increasing the synthesis of very-low-density lipoproteins (VLDL) (Lewis et al, 1995), and b) transient upregulation of mitochondrial β -oxidation which subsequently becomes dysfunctional with increased production of reactive oxygen species (ROS) (Koliaki et al, 2015), and increasing TG in the liver. Lastly, IR within the muscle results in defective uptake of glucose into cells, redirecting glucose to the liver, and consequently increases substrates for DNL.

1.2.6 DNL and its drivers in NAFLD – the role of SREBP 1c & ChREBP

DNL is an important metabolic pathway to redirect energetic surplus coming from non-lipid sources to a more energetically efficient form that can either be stored within the liver or exported as VLDL. In mammalian liver, the state of positive energy balance results in an accumulation of mitochondrial acetyl-CoA, which is at crossroads with many metabolic pathways (Shi & Tu, 2015). The mitochondrial acetyl-CoA surplus is transported into the cytosol, in the form of citrate and then converted back to acetyl-CoA by the ATP citrate lyase, to start the DNL process (Postic & Girard, 2008). In the cytosol, acetyl-CoA is carboxylated to malonyl-CoA by acetyl-CoA carboxylase, the rate-limiting, and first committed step in DNL (Harwood, 2005). Malonyl-CoA is subsequently transformed into palmitic acid by FAS and is then subject to various degrees of elongation and desaturation by ELOVL6 and SCD1 respectively (Mikkelsen et al, 1985). In healthy subjects, fasting hepatic DNL contributes to about 10% of the hepatic lipid pool (Sanders & Griffin, 2016), however, in IR/NAFLD patients, it is responsible for over 25% of the total liver fat (Sanders & Griffin, 2016).

DNL has been increasingly recognised as a key player in the pathophysiology of NAFLD, it is therefore crucial to understand the mechanisms behind its regulation in health and disease. DNL is influenced by both metabolic and hormonal stimuli, such as glucose and insulin, and finely controlled through transcriptional regulation of key fatty acids synthesis enzymes. The two main transcription factors regulating DNL are SREBP1c and carbohydrate response element-binding protein (ChREBP), which are activated by insulin and glucose, respectively (Vacca et al, 2015). SREBP1c can also be activated by SFA and the oxysterol sensor liver X receptor (LXR), whereas PUFA, glucagon, and 5' AMP-activated protein kinase (AMPK) signalling have inhibitory effects (Vacca et al, 2015). SREBP1c is mostly expressed in the liver and it is found as an inactive precursor bound to the ER membrane, where it is associated with the SREBP cleavage activating protein (SCAP) and the insulin-induced gene 1 (Insig1) acting as an inhibitor of SRBP (Eberle et al, 2004). Insulin activates SRBP1c through the Insulin/ phosphatidylinositol 3-kinases/protein kinase B (PI3K/Akt) pathway, which eventually leads to the separation of Insig1 from the SRBP-SCAP complex. The latter then relocates to the Golgi apparatus where it undergoes further maturation forming the active SRBP1c form (Eberle et al, 2004). SRBP1c then migrates to the nucleus where it binds to sterol regulatory element sequences of the DNL target genes

including ATP citrate lyase, ACC, and FAS. Of note, when SREBP1c is overexpressed, in an attempt to maintain cellular homeostasis, it exerts negative feedback on the insulin signalling pathway via the inhibition of insulin receptor substrate 2, with subsequent inhibiting the PI3K/Akt pathway (Engelking et al, 2004). The hyperinsulinemia observed in NAFLD therefore activates SREBP1c, which promotes DNL, negatively feedbacks insulin signalling (leading to decreased glycogen synthesis and increased gluconeogenesis) ultimately promoting hepatic fat accumulation (Vacca et al, 2015).

ChREBP is activated by the postprandial increase in glucose levels, with a mechanism not fully characterised (Denechaud et al, 2008). One proposed mechanism of activation involves the dephosphorylation at serine residue 196 or AMPK phosphorylation sites, which allows for its relocation to the nucleus and activation of target genes containing the carbohydrate response element (ChoRE) (Uyeda & Repa, 2006). This mechanism is also in line with the inhibitory effects exerted by glucagon during fasting, where increased levels of protein kinase A (PKA), promotes ChREBP phosphorylation at serine residue 196 (Iizuka & Horikawa, 2008). ChREBP also enhances the expression of liver pyruvate kinase (LPK), which converts phosphoenolpyruvate to pyruvate thus promoting glycolysis, and the expression of SCD1, favouring the conversion of newly generated SFA to MUFA (Benhamed et al, 2012).

The involvement of ChREBP in NAFLD has been reported in clinical and pre-clinical studies. In leptin-deficient mice, a well-established model of obesity, liver expression of ChREBP were remarkably increased, yet upon specific inhibition, the liver showed a striking reduction of DNL gene expression alongside decreased hepatic steatosis (Dentin et al, 2006). In a cohort of NASH patients, ChREBP expression was positively correlated with the degree of hepatic steatosis but it was inversely related to IR (Benhamed et al, 2012). The latter is attributable to the parallel upregulation of SCD1 by ChREBP, which avoids the accumulation of DNL products in the form of SFA but rather as MUFA. The latter has shown to have little impact on liver IR as compared to SFA (Musso et al, 2018).

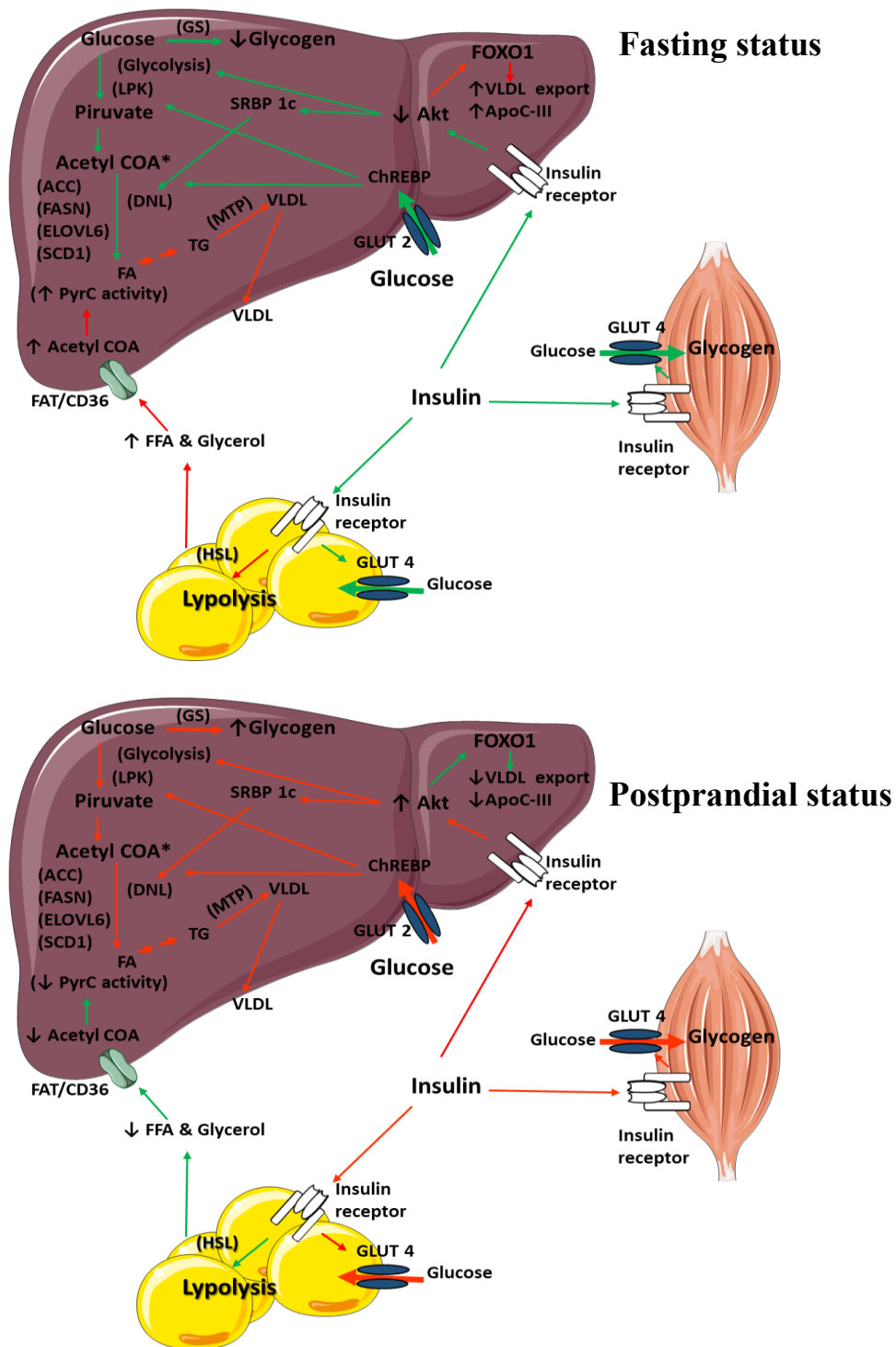


Figure 1. Simplified figure of lipid and carbohydrate metabolism, in fasting and postprandial status, in healthy subjects. Red lines = up-regulated pathway. Green arrows = down-regulated pathways. GS = glycogen synthase, DNL = de novo lipogenesis, ACC = Acetyl-CoA carboxylase, FAS = Fatty Acid Synthase, Elongation of very long chain fatty acids protein 6, Stearoyl-CoA desaturase 1, FA = fatty acid, PyrC = pyruvate carboxylase, FAT/CD36, fatty acid translocase/cluster differentiation protein-36, MTP = Microsomal triglyceride transfer protein, Akt = serine/threonine-protein kinases, SRBP1c = Sterol regulatory element-binding protein 1, ChREBP= carbohydrate response element-binding

protein, LPK= liver pyruvate kinase, FOXO1= forkhead box O1, GLUT 4 = Glucose transporter type 4, GLUT 2 = Glucose transporter type 2, HSL = Hormone-sensitive lipase. Figure based on (Samuel & Shulman, 2018), and done using the <http://smart.servier.com/> image resource.

1.2.7 Lipoprotein metabolism

Cholesterol is an essential component of cell membranes, the precursor for the synthesis of steroid hormones and bile acids, and the major sterol in animal tissues. Its structure includes four linked hydrocarbon rings (steroid core), a hydrocarbon tail linked to one end of the steroid, and a hydroxyl group linked to the other end (Tabas, 2002). Cholesterol is present in two forms, unesterified cholesterol (also known as free cholesterol, FC) and cholesteryl esters (CE). The latter, the most abundant form in blood plasma, is transported via lipoproteins due to their hydrophobic properties.

Lipoproteins are aggregates of lipids and proteins that allow the transport of hydrophobic lipids in the bloodstream, but also transport endogenous proteins, vitamins, hormones, and microRNA (Kuai et al, 2016). The outer part of the lipoprotein is composed of a monolayer of phospholipids (i.e PC, LPC, PE), unesterified sterols (i.e FC and oxysterols), and apolipoproteins, while the inner part is composed of non-polar lipids (such as TG and CE) (Figure 2). Apolipoproteins provide stability to circulating lipoproteins and play a crucial role in regulating metabolic processes via activation/inactivation of enzymes as well as acting as a receptor-ligand (Cohen & Fisher, 2013). Apart from apolipoprotein B (apo B), all the other apolipoproteins are exchangeable within the different particles, although their abundance in different fractions is relatively constant (Dominiczak & Caslake, 2011).

Lipoproteins show a great deal of heterogeneity, mostly based on their physicochemical properties alongside the methodology used for their separation (Scherer et al, 2011). Their size is widely spread ranging from 5 nm to over 100 nm. Based on their density, lipoproteins are classified into five main fractions: chylomicrons (CM), Very Low-Density Lipoprotein (VLDL), Intermediate Density Lipoprotein (IDL), HDL, and LDL. They can be further differentiated, for instance, using immunoaffinity isolation techniques. For example, Furtado et al., identified 16 HDL subspecies (Furtado et al, 2018), and the role of the different sub-fractions are currently being investigated in large cohorts.

Lipoprotein metabolism can be described through three pathways: a) the exogenous pathway that describes lipid transport from diet to internal organs, b) the endogenous

pathway that describes lipid transport from internal organs to peripheral tissues) and c) the reverse cholesterol transport (RCT)/HDL metabolism (endogenous pathway from peripheral tissues to internal organs).

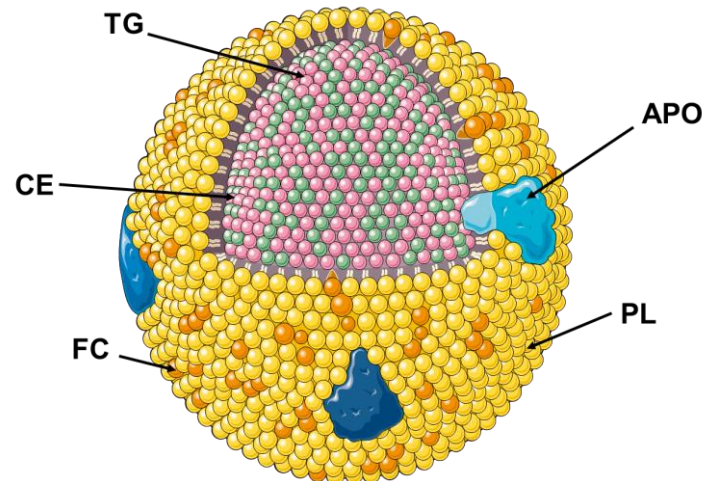


Figure 2. Simplified figure of a lipoprotein. TG = triglycerides, CE = cholesteryl esters, FC = Free cholesterol, PL = phospholipids, Apo = apolipoprotein. Figure done using the <http://smart.servier.com/> image resource.

1.2.7.1 The exogenous pathway

The exogenous pathway begins in the small intestine (jejunum) once dietary lipids have been hydrolysed, TG into FFA and monoacylglycerols (MAG), phospholipids (PL) into FFA and lysophospholipids, and CE into FFA and FC, which are then absorbed by the enterocytes via different mechanisms (Boren et al, 2012). Upon absorption, these lipids are assembled to TG, CE, and PL. Subsequently, in the ER, a large cell organelle acting as a major site of protein, lipid and steroid synthesis, carbohydrate metabolism and calcium storage (Schwarz & Blower, 2016), the enzyme microsomal triglyceride transport protein (MTP) lipidates the apolipoprotein B-48 (apo B-48) laying the basis for CM formation. This process is tightly regulated by the action of apo B-48 on MTP (Kindel et al, 2010). Besides TG, CM also contains smaller amounts of other lipids such as CE, FC, PL, and apolipoproteins such as Apo-AI, Apo-E, and Apo-Cs (Kindel et al, 2010). Once assembled, CM are released from the enterocytes into the intestinal lymphatic system, reaching the systemic blood circulation. Here, CM are subject to the hydrolysing action of the LPL, enzyme located in the capillary surfaces of peripheral tissues (i.e AT, skeletal muscle, heart), on CM TG. The released FA

relocates into tissues, leaving circulating CM with reduced TG, known as CM remnant. The latter undergo further delipidation by hepatic lipase (HL), an enzyme-bound onto heparan-sulfate proteoglycans (HSPGs) at the surface of hepatocytes and the sinusoid endothelial cells (Stow et al, 1985), rendering the particles smaller. These particles are then promptly taken up by the liver via a) the LDL receptor-related protein (LRP), and b) the HSPGs, which also function alone as a receptor (Mahley & Ji, 1999).

1.2.7.2 The endogenous pathway

VLDL particles are the carriers of endogenous lipids, mainly TG, to peripheral tissues as a source of “fuel”. These particles are assembled in the liver via a stepwise lipidation of its structural protein apolipoprotein B100 (apoB100). The lipidation is carried out by microsomal triglyceride transfer protein (MTP) in the ER (Adiels et al, 2008). This initial step leads to the formation of a pre-VLDL particle, which subsequently undergoes further lipidation, leading to the formation of a triglyceride-poor VLDL. The latter is then further enriched in lipids in the Golgi apparatus and exported in circulation as a TG rich VLDL (Adiels et al, 2008). VLDL particles, similarly to CM, are subject to TG depletion by LPL in peripheral tissues (Boren et al, 2012). VLDL TG-depleted transfer apoC-II and apoC-III to HDL, and in turn, accept apo-E. The presence of apo-E on VLDL permits these particles to bind to high-affinity hepatic receptors and with this mechanism, nearly 50% of apo-E VLDL are cleared from the circulation (Cohen & Fisher, 2013). VLDL-TG are also exchanged for HDL-CE by the circulating enzyme cholesteryl ester transfer protein (CETP) (Figure 2). These steps lead to a smaller and TG depleted VLDL particle defined as IDL. The latter can be further delipidated by HL, further reducing in size and forming LDL (Dominiczak & Caslake, 2011), or taken up by the liver by LRP or HSPGs (Hurt-Camejo & Camejo, 2018). LDL is also subject to CETP activity, leading to CE enriched LDL deriving from HDL (Shrestha et al, 2018) (Figure 2). Finally, LDL is directed to the liver and internalised through LDLR (van de Sluis et al, 2017).

1.2.7.3 Reverse cholesterol transport (RCT) – HDL metabolism and circulating lipoprotein remodelling enzymes

Reverse cholesterol transport (RCT) is the process by which HDL collects and transports cholesterol excess from peripheral tissues to the liver, where it is directly or indirectly (through transformation into bile acids) excreted into bile (Ouimet et al, 2019). RCT is a key player in cardiovascular protection since the accumulation of cholesterol in macrophages is a defining step in atherosclerosis (Boren et al, 2020). HDL is the smallest and densest of the lipoproteins, composed for nearly half of its mass of lipids and half proteins (Kontush et al, 2013). HDL biogenesis starts with the lipidation of the apolipoprotein AI (apoA-I), the most abundant apolipoprotein in HDL, produced mainly by the liver and, to a lesser extent, by the small intestine (Figure 2) (Kontush et al, 2013). ATP-binding cassette sub-family A member 1 (ABCA1), a ubiquitous transmembrane protein, is responsible for the transfer of PL and FC to apoA-1, which leads to the formation of a discoidal HDL or pre- β HDL (Ouimet et al, 2019). The latter is the preferential substrate of lecithin:cholesterol acyltransferase (LCAT), an enzyme synthesized mainly by the liver and to a lesser extent by the brain and testes (Jonas, 2000). LCAT circulates in plasma predominantly bound to HDL but also LDL. In humans, LCAT catalyses the transfer of polyunsaturated fatty acids (PUFA) from the sn-2 position of a PC to FC, generating a CE and LysoPC, with apoA-1 as the main activator (Jonas, 2000) (Figure 2). As CE are more hydrophobic than FC, they relocate to the core of HDL, thus reshaping the discoidal HDL into mature spherical HDL_(α) (Figure 2). Despite the crucial role of LCAT on HDL maturation, its role in atherosclerosis is still debated. For example, while Dullaart et al. reported increased activity of LCAT in MetS and positively correlated with carotid-intima media thickness (Dullaart et al, 2008), the opposite was reported in patients with NAFLD (Fadaei et al, 2018). Furthermore, while reduced levels of LCAT were found in patients with ischemic heart disease independently of HDL levels (Sethi et al, 2010), a large population study showed that LCAT mass was not associated with increased atherosclerosis (Holleboom et al, 2010). Lack of association between LCAT mass and CVD were also reported by Calabresi et al. (Calabresi et al, 2011), in a multicenter, observational study including 540 participants. Studies on patients carrying genetic LCAT deficiency and preclinical models have also yielded conflicting results (Ossoli et al, 2016b), thus leaving its role in disease still debated.

Spherical mature HDL are further enriched in FC and PL by the ATP-binding cassette sub-family G member 1 (ABCG1), which specifically acts on mature HDL (Gelissen et al, 2006). Another important circulating enzyme, involved in lipoprotein remodelling, is the phospholipid transfer protein (PLTP), ubiquitously expressed in human tissues (i.e lung, thymus, and AT), but mainly synthesized by the liver (Huuskonen et al, 2001). PLTP mediates the net transfer of PL from VLDL, IDL, and LDL, into HDL particle during lipolysis to generate smaller HDL (HDL₂) and can also convert larger HDL (HDL₃) particles to HDL₂ and pre β -HDL (Zannis et al, 2015), as well as promote HDL particle fusion creating HDL₂ (Rye & Barter, 2014). Furthermore, PLTP is also capable of transferring several lipids such as diacylglycerol, phosphatidic acid, sphingomyelin, cerebroside and phosphatidylethanolamine, and α -tocopherol (Albers et al, 2012), thus rendering it a non-specific transporter.

While the role of PLTP in lipoprotein remodelling and its relevance to CVD have been investigated in murine models, the physiological role in humans is yet to be fully understood.

HDL is also remodelled by CETP, which mediates the transfer of cholesteryl esters from HDL to VLDL, IDL, and LDL in exchange for triglycerides (Shrestha et al, 2018). Because of its ability to decrease HDL CE and increase VLDL CE, CETP has been studied as a target for CVD prevention (Shrestha et al, 2018). Results from different randomised clinical trials have failed to show any significant benefit on major coronary events by CETP inhibition except for the Randomized Evaluation of the Effects of Anacetrapib through Lipid Modification (REVEAL) trial (Group et al, 2017). Whether inhibition of CETP activity is a viable option for CVD reduction is still debated.

In humans, HDL half-life is 2 to 4 days (Zannis et al, 2015), and its catabolism is mediated through 1) liver uptake of HDL through the SR-BI; 2) liver uptake of cholesterol coming from HDL and transported to the liver via apo-B lipoproteins (CETP mediated exchange) by LDLR; 3) kidney uptake of lipid poor apoA-I, where it can be filtered at the level of the glomerulus and then catabolized by proximal renal tubular epithelial cells (Rader, 2006).

1.2.8 Dyslipidaemia in NAFLD and MetS

NAFLD and MetS are characterised by increased VLDL levels, decreased HDL-C (Speliotes et al, 2010) along with increased concentrations of atherogenic small sdLDL particles, despite total LDL-C not necessarily being increased (DeFilippis et al, 2013; Sugino et al, 2011; Toledo et al, 2006). Some of the mechanisms leading to the dyslipidaemia observed in NAFLD and MetS are discussed below.

1.2.8.1 Impaired VLDL turnover

The increased plasma VLDL-TG levels observed in the early phases of NAFLD and MetS are attributable to several factors. As already described, in the context of IR and hyperglycaemia, the increased delivery of FFA from AT to the liver, coupled with increased DNL (driven by SREBP1c and ChREBP activation), results in a net increase of FA within the liver thus providing a surplus of substrate for VLDL synthesis. Besides the increased VLDL-TG, IR also leads to qualitative changes in these particles. Specifically, VLDL are particularly enriched in SFA TG and reduced in PUFA, this being in line with increased liver DNL which ultimately leads to the production of the SFA palmitic acid (Kotronen et al, 2009b; Roumans et al, 2020). Furthermore, in IR, insulin no longer suppresses VLDL assembly and export, therefore leading to a continuous release in the circulation of large VLDL₁ (Sparks et al, 2012). Interestingly, Borén et al., recently reported that in MetS nearly 46% of hypertriglyceridemia was attributable to delayed catabolism and only 20% was explained by increased VLDL₁ secretion (Boren et al, 2015). The putative mechanism by which MetS causes delayed VLDL₁ catabolism was attributed to elevated levels of apoC-III in these particles. ApoC-III exerts a powerful inhibitory effect on LPL which normally renders VLDL and its delipidated forms, IDL, and LDL, more susceptible to clearance by the liver. Large epidemiological studies also showed that elevated levels of apoC-III in other lipoprotein fractions had a major role in modulating hypertriglyceridemia and CVD risk (Jensen et al, 2018; Sacks, 2015). Furthermore, apoC-III inhibitors have been tested in clinical trials showing promising results in reducing plasma TG levels in hypertriglycaemic patients (Taskinen et al, 2019). Additionally, delayed TG turnover can potentially be caused by the AT IR since LPL in AT is transcriptionally upregulated by insulin (Wang & Eckel, 2009).

1.2.8.2 Increased atherogenic LDL particles – the role of sdLDL-C

Increased levels of sdLDL-C are a characteristic feature of NAFLD and MetS. The main driver of this feature is attributed to elevated VLDL levels (Boren et al, 2020). In this context, CETP is considered a key player exchanging TG from VLDL to LDL particles in exchange for CE (Chapman et al, 2010). TG enriched LDL are then delipidated by HL, which leads to smaller and denser particles (Diffenderfer & Schaefer, 2014). Several lines of evidence have shown that sdLDL-C levels are a stronger determinant of CVD risk than total LDL-C (Boren et al, 2020). Some of the mechanism by which sdLDL-C are more atherogenic than larger LDL-C fractions include greater propensity to penetrate the arterial wall due to smaller size (Berneis & Krauss, 2002), delayed removal from circulation due to reduced LDL receptor affinity (Taskinen & Boren, 2015), higher binding capacity for arterial wall proteoglycan (Flood et al, 2004), susceptibility to glycation (Younis et al, 2009) and higher susceptibility of PL and CE components to oxidation (Ivanova et al, 2017). The development of automated enzymatic method assay for sdLDL is allowing the screening of these particles in large population studies (Ivanova et al, 2017), rendering its use in the clinical settings more feasible.

1.2.8.3 Decreased levels of HDL-C

Low levels of HDL-C are a hallmark of MetS and NAFLD. One of the mechanisms by which these conditions are associated with low HDL-C has been attributed to hypertriglyceridemia. Specifically, elevated circulating VLDL levels facilitate the CETP activity with the consequent net transfer of TG from VLDL to HDL along with CE transfer in the opposite direction. CETP enhanced activity promotes reduced HDL-C because of the CE removal per se, and increased HDL catabolic rate (Rashid et al, 2003). The latter is possible because increased HDL-TG content reduces its stability and consequently facilitating the dissociation of apoA-I from HDL, which then leads to faster apoA-I catabolism by the kidney (Rashid et al, 2003). Reduced TG hydrolysis in VLDL decreases the formation of IDL and LDL which contribute to the maturation of HDL (Rashid et al, 2003). The effect of NAFLD and MetS on the biogenesis and maturation of HDL is still under investigation. In human liver cells, insulin promotes the gene expression of apoA-I (Muraio et al, 1998), thus raising the possibility that IR could

also drive a reduced production of HDL. Preclinical models show that hyperinsulinemia decreases HDL-C biosynthesis through the reduction of hepatic ABCA1 functionality (21402379). Taken together, these data strongly support the role of IR and hypertriglyceridemia as drivers of the low HDL-C levels observed in NAFLD and MetS. Besides low HDL-C levels, aspects of HDL functionality such as the cholesterol efflux capacity (CEC), a measure of the capacity of HDL to accept cholesterol from macrophages, is significantly reduced in MetS (Annema et al, 2016; D'Amore et al, 2018; Paavola et al, 2017) and NAFLD (Fadaei et al, 2018; van den Berg et al, 2018).

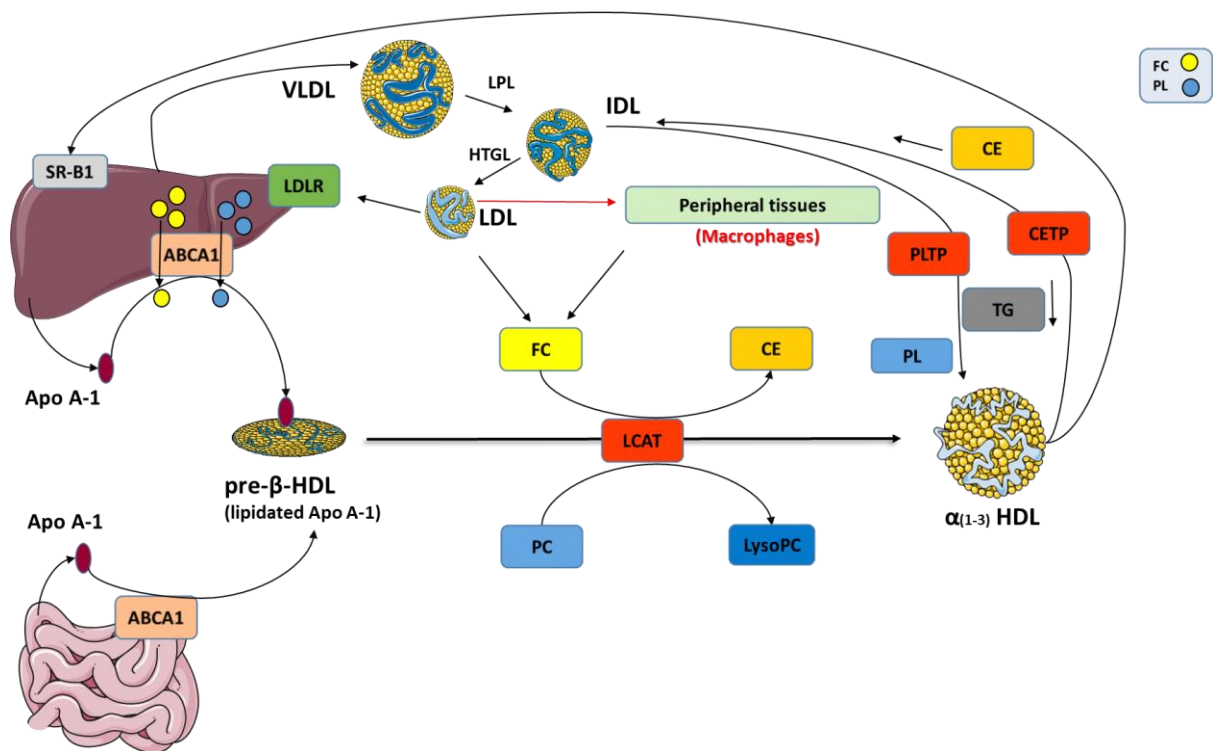


Figure 2. Simplified summary of key lipoprotein remodelling steps, with a focus on HDL reverse cholesterol transport. SR-B1= Scavenger receptor class B type 1, ABCA1 = ATP-binding cassette sub-family A member 1, LDLR = low density lipoprotein receptor, Apo A-1 = apolipoprotein A1, LPL = lipoprotein lipase, HTGL = hepatic triglyceride lipase, FC = unesterified cholesterol, PC = phosphatidylcholine, CE = cholesteryl esters, LysoPC = lysophosphatidylcholine, PL = phospholipids, TG = Triglyceride, PLTP = Phospholipid transfer protein, CETP = cholesteryl ester transfer protein. Figure based on (Rye & Barter, 2014), and done using the <http://smart.servier.com/>.

1.2.9 NAFLD: a tale of hepatic lipid fluxes

Recently Azzu et al. described NAFLD in terms of derangement of the hepatic fat fluxes equation (Azzu et al, 2020). In their equation, the pool of hepatic fat, [P], is described by the following formula: $[P] = k_{\text{syn}}/k_{\text{deg}}$. k_{syn} is defined as the rate of fat synthesis, expressed as the units of mass, including DNL, hepatic FFA uptake, and lipoprotein uptake, whereas k_{deg} is the rate of fat degradation, expressed as fractional removal over time, comprising hepatic fatty acid oxidation and export (Azzu et al, 2020). This equation frame describes the complexity and dynamic nature of NAFLD, explaining for instance how even in absence of energy surplus, an increased k_{syn} , if not paralleled by equally increased k_{deg} , will result in hepatic fat accumulation and vice-versa. The flux model is supported by experimental studies showing that both FFA fluxes to the liver and intrahepatic TG levels correlate with VLDL secretion in healthy people (Mittendorfer et al, 2016), whereas in NAFLD this correlation does not hold true anymore (Adiels et al, 2006; Mittendorfer et al, 2016), likely pointing out to a reduced k_{deg} . This model has also been used to interpret the role of genetic polymorphisms (i.e PNPLA3 polymorphism I148M) that predispose to NAFLD (Azzu et al, 2020).

1.2.10 Lipotoxicity and NASH progression

Lipotoxicity refers to an abnormal ectopic fat accumulation in peripheral tissues, leading to toxic lipid formation paralleled with cellular dysfunction and apoptosis (Musso et al, 2018). The understanding of how lipotoxicity drives hepatic IR and NAFLD progression has greatly benefited from studies of skeletal muscle physiology and the pathophysiology of lipodystrophy. Lipodystrophy encompasses a heterogeneous group of conditions characterized by a lack of and/or dysfunctional WAT with consequent IR, NAFLD, and mixed dyslipidemia (Semple et al, 2011). Skeletal muscle ectopic lipid accumulation is associated with muscle IR in healthy young subjects (Krssak et al, 1999) and people with IR but otherwise healthy (Perseghin et al, 1999). Animal models also support the role of skeletal muscle ectopic fat as a driver of IR, with a mechanism involving DAG accumulation, lipids with signalling functions, and precursor of glycerophospholipids, which inhibits the GLUT4 translocation to the plasma membrane upon insulin stimulation (Samuel & Shulman, 2012). To elucidate the role of ectopic hepatic fat on liver IR, while ruling out other fat

depots, studies in patients with severe lipodystrophy (Petersen et al, 2002) coupled with murine models of lipodystrophy (Kim et al, 2000) have coherently shown the presence of NAFLD in absence of excess visceral fat. The mechanism by which ectopic hepatic fat promotes IR and NAFLD progression is still debated, but it likely involves different pathways and multiple lipid species (Figure3) (Samuel & Shulman, 2018). A mechanism that has been coherently reported in both murine and human studies involves DAG accumulation, which activates the intracellular enzyme protein kinase C (PKC) isoform ϵ . Once activated, PKC ϵ phosphorylates the hepatic insulin receptor-1 at the inhibitory site serine with consequent inhibition to the insulin action on its receptor (Mack et al, 2008). Rats placed on a 3 days high-fat diet show a significant increase in liver DAG and PKC ϵ activity, while knockdown of PKC ϵ in the liver was protected against lipid-induced IR (Samuel et al, 2007). Furthermore, obese patients display increased hepatic levels of DAG (Magkos et al, 2012) as well as increased activation of hepatic PKC ϵ (Kumashiro et al, 2011). Ceramides, lipids with a structural role in cell membranes, and bioactive properties have also been investigated as putative mediators of lipid-induced hepatic IR and NAFLD progression (Samuel & Shulman, 2019). The causative role of ceramides in skeletal muscle IR has been widely reported, whereas in hepatic IR is still debated (Petersen & Shulman, 2017). Some human studies have reported increased levels of hepatic ceramides across the IR-NAFLD spectrum (Chiappini et al, 2017; Gorden et al, 2015; Luukkonen et al, 2016), while others did not (Kumashiro et al, 2011; Magkos et al, 2012; Ter Horst et al, 2017). The mechanisms by which ceramides could lead to hepatic IR are not fully characterised, yet two different pathways have been proposed, both acting through inhibition of Akt, a key player in the insulin signalling pathway (Chavez & Summers, 2012).

In the first model, increased hepatic ceramides activate the intracellular enzyme PKA isoform zeta (ζ), which phosphorylates Akt (Powell et al, 2003) and this prevents the recruitment of Akt to the plasma membrane upon insulin receptor activation (Stratford et al, 2001). In the second model, ceramides activate the enzyme protein phosphatase 2A (PP2A), which leads to dephosphorylation and inactivation of Akt (Chavez et al, 2003). Furthermore, ceramides have also been implicated in the progression of NAFLD, through the promotion of mitochondrial dysfunction and inflammatory pathways (Pagadala et al, 2012). Despite the debate on the role of ceramides in

hepatic IR, its association with CVD (Hilvo et al, 2020), T2DM (Hilvo et al, 2018), and its role in skeletal muscle IR, they remain at the centre of intensive research.

The type of FFA plays also a crucial role in promoting IR and NAFLD progression (Musso et al, 2018). Different studies have shown that NAFLD is characterised by an increased level of SFA, especially palmitic (C16:0) and stearic (C18:0) acids, and decreased MUFA and PUFA FA (Chiappini et al, 2017; Puri et al, 2007; Sanders et al, 2018). SFA can exert hepatic lipotoxicity through different pathways. For instance, SFA activates c-Jun N-terminal kinase (JNK), a member of the mitogen-activated protein kinase (MAPK) family (Musso et al, 2018), and a key mediator of hepatic SFA lipotoxicity (Solinas & Becattini, 2017). JNK promotes IR via the inactivation of insulin receptor substrate-1 and its phosphorylation at the inhibitory site Ser-307 (Solinas et al, 2006). JNK also impairs oxidative phosphorylation (OXPHOS) while promoting the production of reactive oxygen species formation through the interaction with the outer membrane mitochondrial protein SH3 domain-binding protein 5 (Sab). JNK also promotes apoptosis through the activation of the pro-apoptotic protein p53 (Musso et al, 2018).

Another mechanism by which SFA promotes lipotoxicity is through the promotion of ER stress, a process by which ER homeostasis is perturbed leading to aberrant accumulation of unfolded or misfolded proteins in the ER lumen (Han & Kaufman, 2016). Specifically, palmitic acid induces ER stress in hepatocytes by activating protein kinase RNA-like endoplasmic reticulum kinase (PERK)/ Activating Transcription Factor 4 (ATF4)/ C/EBP-homologous protein (CHOP) pathway (Wei et al, 2006). Palmitic acid activates PERK, which leads to increased levels of eIF2 α . The latter promotes a pro-adaptive signalling pathway by the inhibition of global protein synthesis and selective translation of ATF4, which upregulates the pro-apoptotic transcription factor CHOP that subsequently induces apoptosis (Cao et al, 2012; Salvado et al, 2015). Rodent studies have also shown that palmitic acid promotes NAFLD progression enhancing inflammation through the activation of the toll-like receptor (TLR) 2 (Miura et al, 2013). TLR 2 belongs to a family of plasma membrane receptors that recognise bacteria and virus, and once activated induce pro-inflammatory cytokines triggering an inflammatory response (Kawai & Akira, 2007). The discussion above highlights the crucial role of different lipids in IR and NAFLD progression which is being increasingly appreciated due to the advancement in the field of lipidomics.

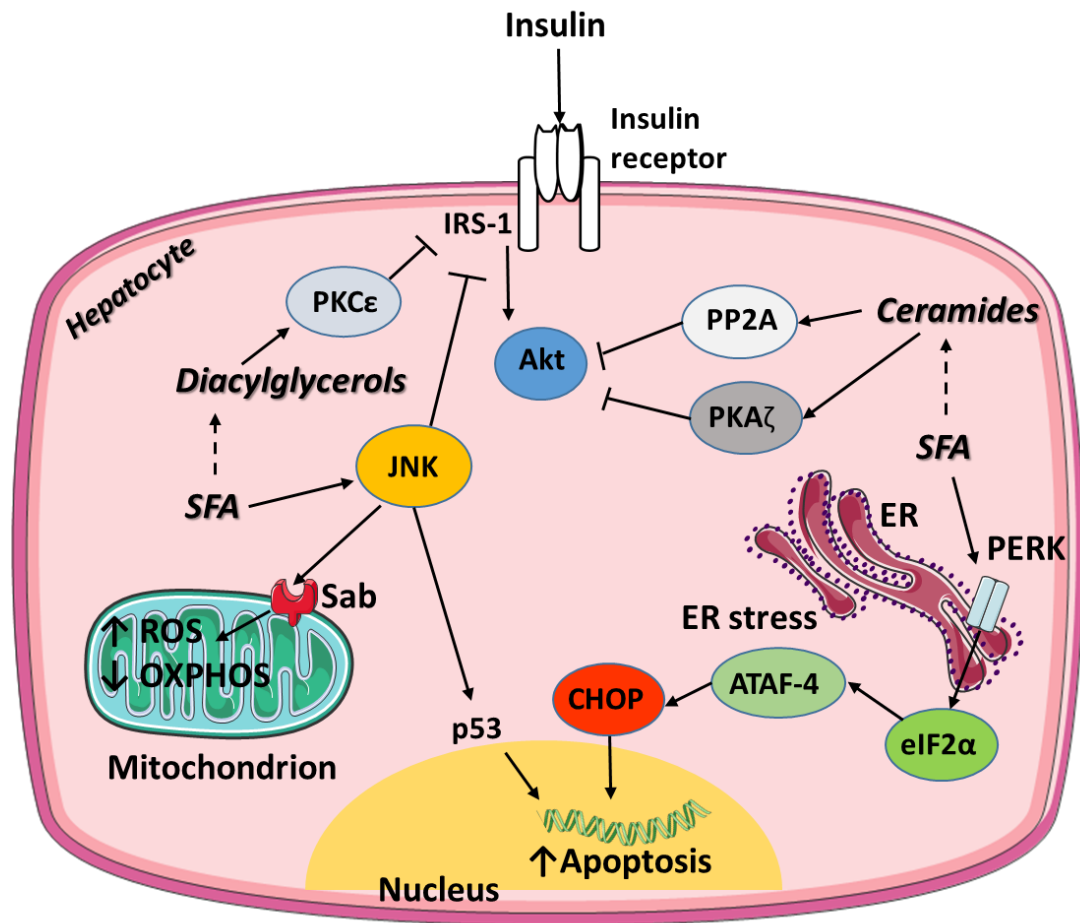


Figure 3. Simplified figure of key pathways of lipotoxicity in hepatocytes. IRS-1 = insulin receptor-1, PKC ϵ = protein kinase C ϵ , Akt = serine/threonine-protein kinases, SFA = saturated fatty acids, JNK = c-Jun N-terminal kinase, Sab = SH3 domain-binding protein 5, ROS = reactive oxygen species, OXPHOS = oxidative phosphorylation, PP2A = protein phosphatase 2A, PKA ζ = protein kinase A ζ , ER = endoplasmic reticulum, PERK = transmembrane protein kinase RNA-like endoplasmic reticulum kinase, ATF4 = activating transcription factor 4, CHOP = C/EBP-homologous protein. Dotted lines indicate possible but not mandatory steps. Figure done using the <http://smart.servier.com/> image resource.

1.2.11 Complications of the MetS and NAFLD

1.2.11.1 Type II diabetes mellitus (T2DM)

T2DM is a multifactorial metabolic disorder characterised by dysregulation of glucose and lipid metabolism caused by IR, impaired insulin secretion (pancreatic β -cell dysfunction), or the coexistence of both (DeFronzo et al, 2015). T2DM is clinically marked by increased fasting blood glucose, an increased presence of glucose in the urine, or abnormal response to a glucose load. T2DM has reached pandemic proportions, affecting 8.5% of adults worldwide, becoming a major public health burden (Emerging Risk Factors et al, 2010). MetS and NAFLD are closely related to T2DM since IR is a key feature of both conditions. Large prospective studies have shown that people with MetS and NAFLD have a 5- and 3-fold increased risk for incident T2DM, respectively (Cornier et al, 2008; Gastaldelli & Cusi, 2019). Similar to the mixed dyslipidaemia described in the MetS and NAFLD, T2DM is also characterised by increased circulating levels of large VLDL and decreased HDL-C (Adiels et al, 2008). Furthermore, both conditions are well-established risk factors for cardiovascular diseases (CVDs).

1.2.11.2 Atherosclerotic cardiovascular disease (ASCVD)

Cardiovascular disease (CVD) is the leading cause of death worldwide, with atherosclerotic cardiovascular disease (ASCVD) being the most prevalent form of CVD (Roth et al, 2017). Atherosclerosis is the process by which the tunica intima (the innermost layer of arteries), accumulates fat with a simultaneous reduction of arterial wall elasticity (Lusis, 2000). Epidemiological studies have shown that people with MetS and NAFLD have a 2 and 3-fold increased risk of CVD, respectively (Mottillo et al, 2010; Targher et al, 2016).

ASCVD is a multifactorial disease that begins early in life (Berenson et al, 1998). Although some pathophysiological aspects of ASCVD are not fully understood, evidence from genetic, epidemiological, and randomized studies of LDL-lowering therapies, have shown that LDL-C has a causative role in this process (Ference et al, 2017). Besides LDL-C concentration, a mounting body of evidence is showing that the LDL composition is crucial in determining its atherogenicity (Boren et al, 2020).

Atherosclerosis is hypothesised to result from the adhesion of LDL particles to the tunica intima via proteoglycans (Boren et al, 2020). The retained lipoproteins show an increased predisposition to oxidation by arterial-wall enzymes and oxidants. Oxidised LDL exhibit pro-inflammatory activity which attracts monocytes and other immune-competent cells and acts on the smooth muscle that further attracts other monocytes (Boren et al, 2020). These monocytes then differentiate into macrophages and in an attempt to clear up the LDL surplus, can give rise to foam cells, further triggering a complex inflammatory process that develops atherosclerotic plaques. Recently, it has been increasingly appreciated the role of hypertriglyceridemia and ApoC-III in the onset and progression of ASCVD and CVD in general (Ginsberg et al, 2021). In a prospective population-based study with a 10-year follow-up, Pechlaner et al. found that ApoC-III was significantly and positively associated (hazard ratio/standard deviation 1.38; 95% confidence interval [CI]: 1.17 to 1.63) with CVD, independently of traditional risk factors such as HDL-C and non-HDL cholesterol (Pechlaner et al, 2017). Furthermore, in a multicentre, randomised, double-blind, placebo-controlled trial involving more than 8,000 statin-treated adults with hypertriglyceridemia and established cardiovascular disease or with diabetes, the use of a polyunsaturated fatty acid (ethyl eicosapentaenoic acid (EPA), Icosapent Ethyl)) after a median follow-up of 4.9 year significantly reduced the cardiovascular risk in the icosapent ethyl group, as compared with the patients in the placebo arm (Bhatt et al, 2019), thus further supporting the importance of monitoring TG and ApoC-III as therapeutic targets in CVD prevention.

1.2.11.3 Chronic kidney disease

Chronic kidney disease (CKD) is defined as persistent alterations in kidney structure, function, or both, which impair health (Romagnani et al, 2017). The Kidney Disease Improving Global Outcomes initiative classifies CKD based on glomerular filtration rate and albuminuria (https://kdigo.org/wp-content/uploads/2017/02/KDIGO_2012_CKD_GL.pdf). The global prevalence of CKD varies between 7–12% (Hill et al, 2016). Several factors can contribute to the pathogenesis of CKD, amongst them MetS and NAFLD and their components, especially high blood pressure and hyperglycaemia, play a central role. Indeed, T2DM is the leading cause of CKD, and subjects with MetS and NAFLD have a 2.5- and 2-

fold higher risk of developing CKD, respectively (Byrne & Targher, 2020; Singh & Kari, 2013).

There are several mechanisms by which T2DM and MetS increase the risk of CKD. Hyperglycaemia promotes the reabsorption of sodium in kidneys via activation of the sodium/glucose cotransporter 2, which after a cascade of events eventually activates the renin-angiotensin system which causes dilatation of the afferent arteriole and vasoconstriction of the efferent arteriole, ultimately increasing GFR (van Bommel et al, 2017).

Prolonged and uncontrolled hypertension is also a well-established risk factor for CKD (Romagnani et al, 2017). While the kidney can normally cope with transitional increased blood pressure (i.e during physical activity), persistently elevated blood pressure leads to mechanical damage of kidneys' glomeruli, a network of capillaries that transport circulating blood within the kidney functional unit, nephrons, thus impairing their function. Epidemiological studies have shown that obesity is associated with CKD, with a mechanism that can be direct or indirect (i.e obesity-associated hypertension) (Rhee et al, 2016). Some of the direct mechanisms include reduced production of adiponectin and increased production of resistin and leptin promoting a state of systemic inflammation, oxidative stress, and IR, all of which have a detrimental effect on kidney structure and function (Camara et al, 2017).

1.3 Lipidomics as a tool to study obesity and its metabolic-related disorders

The characterisation of the main lipid species and pathways involved in IR and NAFLD has dramatically increased in the past decade due to progress in lipidomics, a well-established but still expanding field, that aims to dissect the role of lipids and their metabolic pathways on a large scale (Yang & Han, 2016). Before the advent of lipidomics, researchers were limited to the study of major lipid classes, such as PL, CE, FC, TG using thin layer chromatography, and total fatty acid composition by gas chromatography mass spectrometry (GC-MS). The lipidomic field takes advantage of several analytical techniques, most importantly chromatography coupled with mass spectrometry (MS) and nuclear magnetic resonance (NMR) spectroscopy (Griffin et al, 2011).

Lipidomic studies are shedding light on the “lipidomic signature” of IR, MetS, and NAFLD in blood plasma and tissues (i.e liver) (Chiappini et al, 2017; Kotronen et al, 2009b; Monnerie et al, 2020; Sanders et al, 2018). For example, while elevated plasma TG levels partially mediate the increased risk of CVDs in MetS and NAFLD (Zhang & Lu, 2015), lipidomic studies have shown that the composition of TG can help better stratify the CVD risk (Sanders & Griffin, 2016). In a prospective population-based study with a 10-year follow-up, Stegemann et al. found that TG (54:2) in combination with cholesteryl ester (16:1), and phosphatidylethanolamine (36:5), and traditional risk factors resulted in improved CVD risk prediction (Stegemann et al, 2014). Furthermore, Kotronen et al., examined the lipidomic composition of lipoproteins showing that in healthy subjects with a wide range of insulin sensitivity, serum TG from VLDL, with a lower carbon number and a double bond content associated with IR, whereas those containing essential fatty acids were negatively associated with IR (Kotronen et al, 2009b). Also, with a translational approach using both pre-clinical models and human cohorts (interventional and observational), Sanders et al., demonstrated the relevance of DNL in NAFLD which is partially driven by a high refined carbohydrate diet (Sanders et al, 2018). More recently, Charidemou et al., also demonstrated that a high protein meal can promote hepatic DNL in healthy adults which poses a question on the safety of high protein diets for the treatment of obesity (Charidemou et al, 2019). Other authors have also proposed lipidomic based non-invasive biomarkers of NAFLD, but further studies are warranted to validate these results (Guerra et al, 2021). Table 2, adapted from (Guerra et al, 2021), summarise some of the key lipidomic findings in NAFLD. Taken together, these data clearly show the clinical relevance of lipidomics is obesity and its related disorders, but also the need for further studies to validate these results in people with different age, health status and genetic background.

Table 2. Summary of key lipidomic studies in NAFLD

Study	Number of participants	Diagnosis	Tissue	Main findings
Puri et al 2007 (Puri et al, 2007)	9 CT 9 NAFLD 9 NASH	Liver biopsy	Liver	TAG, DAG, total cholesterol, SFA, n6: n3 ratio ↑ NAFLD and NASH TAG, FA 20:4n-6, TAG FA 22:6n-3 ↓ NAFLD and NASH PC, PE ↓ NAFLD FC, LysoPC ↑ NASH
Puri et al 2009 (Puri et al, 2009)	50 CT 25 NAFLD 50 NASH	Liver biopsy	Plasma	TAG, DAG, FFA and CE MUFA, CE, DAG, PC, PE with 18:3 or 20:3 FA ↑ NAFLD and NASH DAG, PC, PE, TAG SFA ↓ NAFLD 22:6n-3/22:5n-3 ratio in PC, PE ↓ NASH
Barr et al 2010 (Barr et al, 2010)	9 CT 24 NAFLD 9NASH	Liver biopsy	Serum	FFA 16:0, SM 18:0/16:0, 18:1/18:0, PC 28:0, LysoPC 20:2, 20:1, LPE P-16:0 ↑ NAFLD and NASH FFA 18:3, 20:2n6, SM 18:1/12:0, 18:2/14:0, 18:2/16:0, 36:3, PC 18:0/22:6 ↓ NAFLD and NASH PC 14:0/20:4, 16:0/20:3, P-18:0/20:4, LysoPC 18:1 ↑ NASH FFA 20:4, LysoPC P-24:0, P-22:0, O-20:0 ↓ NASH
Anjani et al 2015 (Anjani et al, 2015)	24 CT 22 NASH	Liver biopsy	Serum	PC, PE, and PG, CER d18:0/22:0, d18:1/16:0, d18:1/18:0, d18:1/20:0, d18:1/22:0, d18:1/23:0, d18:2/20:0, d18:2/18:0, d18:2/20:0, d18:2/21:0, d18:2/22:0, d18:2/23:0; SM 36:1, PC 32:0, 32:1, 34:1, 34:3.36:1, 36:3, 36:4, 36:5, 38:3, 38:4, 38:5, 38:6, 40:4, 40:5, 40:6, PE 34:1, 34:3, 36:1, 36:2, 36:4, 36:5, 38:3, 38:4, 38:5, 38:6, 40:4, 40:5, 40:6, 40:7, LysoPC 16:0, 16:1, 20:3, 22:5, PG 36:1, 36:2, 36:3, 38:3, 38:4, PI 32:1, 34:1, 36:4, 38:4, 40:4, 40:5 ↑ NASH CER d18:1/24:0, SM 42:3 ↓ NASH

Gorden et al 2015 (Gorden et al, 2015)	31 CT 17 NAFLD 20 NASH 20 Cirrhosis	Liver biopsy	Plasma	<p>TAG, CE, CER, DAG 36:2, HexCER d18:1/24:1, GlucCER d18:1/24:1, d18:1/26:1, PC 36:4, 38:4, PE 38:5, 38:4, 40:6, 40:5, LysoPC 16:0, PI 36:1, 38:4, 38:3 ↑ NAFLD and NASH</p> <p>HexCER d18:1/24:1, d18:1/26:1, CER m18:1/16:0, m18:1/26:1, GlucCer d18:1/26:1, 18:1/26:0, PC 32:0, PI 36:1 ↑ Cirrhosis</p> <p>Total cholesterol, CE 18:2, 20:4, 20:3, TAG 52:4, 52:3, DAG 36:2, CER d18:1/18:0, 18:1/20:0, d18:1/22:0, d18:1/24:1, d18:1/24:0, d18:0/18:0, d180/24:1, m18:1/16:0, m18:1/26:1, m18:0/18:0, m18:0/20:0, m18:0/22:0, m18:0/24:0, HexCER d18:1/24:1, d18:1/26:1, GlucCer d18:1/24:1, d18:1/26:1, 18:1/26:0, SM d18:1/18:1, d18:1/18:0, d18:1/20:0, d18:1/22:0, d18:1/24:0, PC 32:0, 34:3, 36:4, 38:6, 38:5, 38:4, 38:3, 40:6, PE 36:4, 38:6, 38:5, 38:4, 40:6, 40:5, LysoPC 16:0, PI 36:1, 38:4, 38:3 ↓ Cirrhosis</p>
Chiappini et al 2017 (Chiappini et al, 2017)	7 CT 39 NAFLD 15 NASH	Liver biopsy	Liver	<p>SFA (14:0, 16:0, 18:0) ↑ NASH</p> <p>PC, PE, PI, PS PC/PE, SM ↓ NASH</p>
Apostolopoulou et al 2018 (Apostolopoulou et al, 2018)	7 CT 7 NAFLD 7 NASH	Liver biopsy	Liver	Total CER, LactCER 24:1, HexCER 22:0, 24:0, 24:1; dhCER 16:0, 22:0, 24:1 ↑ NASH
			Serum	dhCER 20:0 ↑ NAFLD Total dhCER, dhCER 16:0, 22:0, 24:1 ↑ NASH
Tiwari-Heckler et al 2018 (Tiwari-Heckler et al, 2018)	28 CT 25 NAFLD 42 NASH	Liver biopsy	Plasma	<p>TAG, SM, PC ↑ NAFLD and NASH</p> <p>LysoPE ↓ NAFLD and NASH</p>
Sanders et al 2018 (Sanders et al, 2018)	663 CT 233 NAFLD	Ultrasound	Plasma	<p>TAG 54:2, 48:1, 48:2, 50:1, 50:2 ↑ NAFLD</p> <p>TAG 52:3, 52:4, 56:7, 56:6, 54:4, 56:8 ↓ NAFLD</p>

Ooi et al 2021 (Ooi et al, 2021)	50 CT 110 NAFLD 16 NASH	Liver biopsy	Plasma	CER d18:0/16:0, d18:0/18:0, d18:0/20:0, d18:0/22:0, d18:0/24:0, d18:0/24:1, DAG SFA (16:0, 18:0), MUFA (18:1), PUFA (18:2), TAG SFA (16:0, 17:0, 18:0), MUFA (18:1), PUFA (18:2, 20:3, 20:4) ↑ NAFLD
			Liver	Total dhCER, TAG, DAG, CER d18:0/18:0, d18:0/20:0, d18:0/22:0, d18:0/24:0, d18:0/24:1, LPC 26:0, PI 18:0/22:5, CE 18:0, > 20 DAG, > 40 TAG ↑ NAFLD and NASH PC 15-MHDA/18:2, PC 15-MHDA/22:6, PC 17:1/18:2, 18:1/22:6, CE 22:5 ↓ NAFLD and NASH Total CER, CE, THC, CER d18:1/16:0, d18:1/18:0, d18:1/20:0, d18:1/22:0, d18:1/24:0, GM3 d18:1/20:0, PC 28:0, 31:0, PC O-40:7, PS 38:4, CE 18:3, FC ↑ NAFLD SM 37:2, d18:2/20:0, PC 17:0/18:2, 18:1/18:2, 39:5, 17:0/22:6, PC P-38:5, PE 18:1/22:6, PE P-18:1/22:4, 20:1/22:6 ↓ NAFLD Total DHC, DHC d18:1/18:0, d18:1/22:0, d18:1/24:0, SM d18:0/16:0, PC 36:0, ↑ NASH PC 16:1/20:4, 38:6, PC 15-MHDA/20:4, PE 16:0/20:4, 38:5, PI 38:5, ↓ NASH

CT, control; NAFLD, non-alcoholic fatty liver disease; NASH, nonalcoholic steatohepatitis; DAG: diacylglycerol; TAG: triacylglycerol; SFA: saturated fatty acids; MUFA: monounsaturated fatty acid; PUFA: polyunsaturated fatty acids; FC: free cholesterol; CE, cholesteryl esters; FFA: free fatty acids; SM: sphingomyelin; PC: phosphatidylcholine; LysoPC, lysophosphatidylcholine; PI: phosphatidylinositol; PS: phosphatidylserine; PE: phosphatidylethanolamine; LysoPE, lyso phosphatidylethanolamine; CER: Ceramides; dhCER, dihydroceramides; DHC/Hex2Cer, dihexosylceramide; THC, trihexosylceramide; GM3; GM3 ganglioside; LactCER, lactosylceramide; GlucCER, glucosylceramide. Table adapted from (Guerra et al, 2021)

1.3.1 Lipoprotein lipidomics

Although several studies show the whole plasma “lipidomic signature” under different conditions (Fernandes Messias et al, 2017; Kulkarni et al, 2013a; Puri et al, 2009), the changes reported do not provide information on the origin of each lipid species. For example, for CVD risk it is more relevant knowing which compartment circulating cholesterol is partitioned to among the lipoproteins (HDL-C vs. LDL-C) rather than the total amount. This is likely to happen to other lipid species, and therefore to have a better understanding of the biological function of circulating lipid species, it is important to study the lipoproteins fractions in isolation.

Lipoproteins are commonly separated according to their density through ultracentrifugation (UTC). UTC is one of the first methods described to separate lipoprotein and it is still considered the gold standard in the lipoprotein field. UTC can be performed with a sequential floatation, separating CM, VLDL, IDL, LDL, and HDL (Havel et al, 1955), or with a single step density gradient centrifugation, allowing further speciation (HDL₂ and HDL₃) (Chapman et al, 1981). There are several limitations with this method including the technical expertise required, the amount of time needed, the large volumes of sample (1 mL) required, possible loss of apolipoprotein from fractions, and the lack of parameters specifying the density cut-off between lipoproteins. Besides UTC, several other separation methods have been described, including electrophoretic mobility (Noble, 1968), fraction precipitation (Warnick et al, 1982), immunoaffinity for apolipoproteins (Cheung & Albers, 1984) and particle size, achievable through size exclusion chromatography (SEC) (Innis-Whitehouse et al, 1998). Each method has its drawbacks; it is therefore important to decide which separation technique adopts based on the question the investigator aims to answer.

SEC has been used in this work because of a) the low sample volume required, and b) it has been validated against UTC (Han et al, 2012; Innis-Whitehouse et al, 1998) while having a higher throughput. On the other hand, SEC does not allow to separate chylomicron from VLDL, thus being not recommended for post prandial lipidomic studies. IDL are distributed between the VLDL and LDL fractions, and albumin co-elutes with HDL, thus contributing to the lysophosphatidylcholine pool found in these fractions. Because my project does not investigate the meal impact on lipoprotein metabolism and I did not study the LDL remodelling, the impact of albumin on HDL

lipidome might affect only a single lipid class (LPC) (Wiesner et al, 2009), and thus considered an acceptable drawback.

Here, it is briefly reported the principle of separation for the SEC only as it is the method adopted for this work, but the detail of the different methods can be found in comprehensive reviews (Hafiane & Genest, 2015; Krauss, 2010).

SEC separation is based on the capacity of the column, packed with fine, porous beads made of agarose, to retain the smaller particles due to their ability to diffuse into the pores and let elute first the larger particles, which are bigger than the pores so do not diffuse through them (Osei et al, 2015). The technical details are reported in the method section (Chapter Two).

1.3.2 The use of liquid chromatography-mass spectrometry in lipidomics and metabolomics

Liquid chromatography (LC) is an analytical technique that allows the separation of different compounds based on their affinity with two phases, one stationary (solid) and one eluent (liquid) while passing through a chromatographic column. The LC system consists of a series of pumps (from 1 to 4) which lead a solution of a mixture of solvents (mobile phase) through a chromatographic capillary column (stationary phase). Before entering the column, the mobile phase will be mixed with the sample solution through a valve system. Once inside the columns, compounds are separated due to their affinity with the stationary phase. The affinity is affected by different factors such as flow rate, mobile phase composition, and column temperature as well as the chemical composition of the analytical mixture. The time required by a compound to elute from a column is defined as its retention time (RT), and that is the parameter used to identify the various compounds (Griffin et al, 2011). Based on the affinity between compounds and the stationary phase, there are two major classes of chromatographic techniques:

- normal-phase liquid chromatography
- reverse-phase liquid chromatography.

Normal-phase LC uses a polar stationary phase and a non-polar mobile phase, whereas the reverse-phase LC, uses a polar mobile phase and a non-polar stationary phase. Besides the different approaches available, the extraordinary variety of columns available permits the separation of a huge range of compounds, thus

rendering LC a very popular separation method in metabolomics. A key limitation of LC is the overlapping RT of many compounds. To overcome this issue, the separated metabolite can be further analysed by MS.

MS is a powerful analytical technique which enables direct identification of molecules based on the mass-to-charge ratios (m/z) as well as fragmentation pattern (Urban, 2016). In its most basic form, a mass spectrometer is composed of an ionising source, an analyser, and a detector. The ionisation of a metabolite is a mandatory step for its separation and detection while one of the most common is the electrospray ionization (ESI) or soft ionisation due to the small fragmentation generated during the ionising process (2019). The ESI can be used in combination with a variety of analyser, which, despite the different approaches used, ultimately rely on the use of the m/z as a discriminant of separation (Kofeler et al, 2012). Two very common analysers include the triple quadrupole (QqQ), and the orbitrap MS analyser. The former is used for targeted assays, which refer to the measurement of a specific set of metabolites, whereas the orbitrap is mostly used for open profile studies, which refer to the measure of as many metabolites as possible without pre-defined mass transitions as used in QqQ MS. Once a compound has been separated, it is finally directed towards the detector, which generates an electrical signal that is proportional to the abundance of the compound.

The QqQ MS employs two quadrupoles, acting as mass analysers, and one quadrupole for fragmentation (collision cell), located between them. Quadrupoles consist of four parallel charged metal rods arranged through a central axis. Static potential (DC voltages) and alternative potentials (RF voltages) are applied to the quadrupole rods with the two pairs of rods having opposite polarity. These voltages generate an oscillating field that allows only specific ions with determined m/z to move towards the detector, while other compounds will be deflected away. In the QqQ, the first quadrupole filters the ion of interest (parent ion) according to its m/z and then fragments it in the collision cell using collision-induced dissociation (CID). Specifically, fragmentation is obtained through the collision of the ion with an inert gas (i.e helium, nitrogen or argon), eventually generating a fragment ion. The latter is further separated in the third analyser and then quantified by a detector. The use of tandem LC-MS/MS is among the most common approaches in metabolomics, providing excellent sensitivity but a relatively low mass accuracy as compared to other methods (Mann & Kelleher, 2008).

A more recent analyser is the orbitrap MS. The latter is composed of two outer electrodes and a central spindle electrode. Ions are injected into space between the central and outer electrodes where they are trapped by an electrostatic field. Here, ions oscillate around the central electrode and along its axis. Ions with different m/z oscillate at different frequencies, thus allowing their separation. The oscillating frequencies generate an image current which is detected by the outer electrodes and quantified according to its size, which represents the ion abundance. The image current is then processed by a Fourier transformation. The orbitrap MS is characterised by a high resolution and high mass accuracy (2-5ppm) (Hu et al, 2005), which are of crucial relevance for untargeted approaches.

Chapter 2. Materials and methods

This chapter provides a general description of the materials and methods used throughout this thesis. Methods specific for each study are reported in their respective chapters.

2.1 Measurement of clinical biochemistry

Clinical biochemistry for the different studies, including full lipid profile, glucose, insulin, circulating liver enzymes, and total free fatty acids, was performed by The Pathology Partnership (Addenbrooke's Hospital, Cambridge, UK). HOMA2 values were obtained by the program HOMA Calculator v2.2.3 available at <https://www.dtu.ox.ac.uk/homacalculator/>.

2.2 Measurement of lipid levels by mass spectrometry

2.2.1 Lipid extraction

Lipids were extracted from blood serum, previously stored at -80 °C, using an adaptation of the Folch method (Folch et al, 1957). Briefly, 10 µL of blood serum was mixed with chloroform/methanol (2:1, 1 mL) and then 10 µL of internal standard mix including the following: N-palmitoyl-d31-D-erythro-sphingosine (16:0-d31 Ceramide, 12.2 µM), heptadecanoic-d33 acid (17:0-d33 FFA, 40.0 µM), , 1-palmitoyl(D31)-2-oleyl-sn-glycero-3-phosphatidylcholine (16:0-d31-18:1 PC, 40.1 µM), 1-palmitoyl(d31)-2-oleyl-sn-glycero-3-phosphoethanolamine (16:0-d31-18:1 PE, 38.0 µM), 1-palmitoyl-d31-2-oleyl-sn-glycero-3-[phospho-rac-(1-glycerol)] (16:0-d31-18:1 PG, 12.5 µM), N-palmitoyl(d31)-d-erythro-sphingosylphosphorylcholine (16:0-d31 SM, 47.4 µM), glyceryl tri(pentadecanoate-d29) (45:0-d87 TAG, 40.3 µM) (Avanti Polar Lipids Inc, USA) was added. Samples were sonicated for 10 min and subsequently, deionised water was added (400 µL). Samples were then centrifuged (17,000 × rpm, 10 min). 500 µL of the organic fraction was transferred into a new vial and dried under a stream of nitrogen, whereas 500 µL of the aqueous part was placed in a new vial and dried in a CentriVap Centrifugal Concentrator with attached cold trap (78100

series, Labconco Co, Kansas City, USA). Dried samples were then stored into a - 80 C until analysis.

2.2.2 Lipid analysis by liquid chromatography-mass spectrometry

Before analysis, dried samples were reconstituted in 20 μL of 1:1 chloroform/methanol, sonicated for 10 minutes, and then diluted in isopropyl alcohol/acetonitrile/water (2:1:1, 100 μL). The analysis of intact lipids was performed through LC-MS using a Dionex Ultimate 3000 ultra-high performance liquid chromatography system (UHPLC; Thermo Scientific) coupled to an LTQ Orbitrap Elite Mass Spectrometer (Thermo Scientific, Hemel Hempstead, UK). 10 μL of sample was injected onto a C18 CSH column, 1.7 μM pore size, 2.1 mm x 50 mm, (Waters Ltd, Manchester, UK) maintained at 55 °C. A gradient of solvent A, 10 mM ammonium formate in acetonitrile/water 6:4, and solvent B, 10 mM ammonium formate in isopropanol/acetonitrile 9:1, was used for the positive mode acquisition. For the negative mode, mobile phase remained the same except the use a 10 mM ammonium acetate instead of ammonium formate. The HPLC was coupled to a heated electrospray source optimised at 50:50 mobile phase A to mobile phase B for spray stability (capillary temperature; 300 C, source heater temperature; 420 C, sheath gas flow; 40 (arbitrary), auxiliary gas flow; 15 (arbitrary), spare gas; 3 (arbitrary), source voltage; 4 kV. The mass spectrometer scan rate set at 4 Hz, giving a resolution of 25,000 (at 200 m/z) with a full-scan range of m/z 100 to 1800 m/z collected in positive and negative ion mode. Two representative MS spectra (one positive and one negative) highlighting the major lipid classes are reported in Figure 1. Peak identification and mass spectra processing were carried out with Xcalibur Software (Thermo Scientific). Peak areas were normalised to their class-specific internal standard, leading to a semi-quantitative data, here referred to as normalised intensity. Lipids with missing values higher than 40% were removed from the dataset, whereas the others were imputed with the half minimum value method (Hinz et al, 2019). The area ratios were then blank corrected (a blank was a sample that followed the entire extraction procedure as done with the regular samples but without serum, thus blank, and injected after each 10 regular samples). Specifically, normalised intensities with a value less than three times the blank samples were set to zero and removed from the dataset. As a quality control I used a cohort specific pooled sample (serum combined from each participant and extracted as described above) injected every 10 regular

samples. Pooled samples were used to assess the coefficient of variation (CV) across the LCMS run. Samples with a CV <25% were retained whilst higher CV led to the exclusion of the specific lipid.

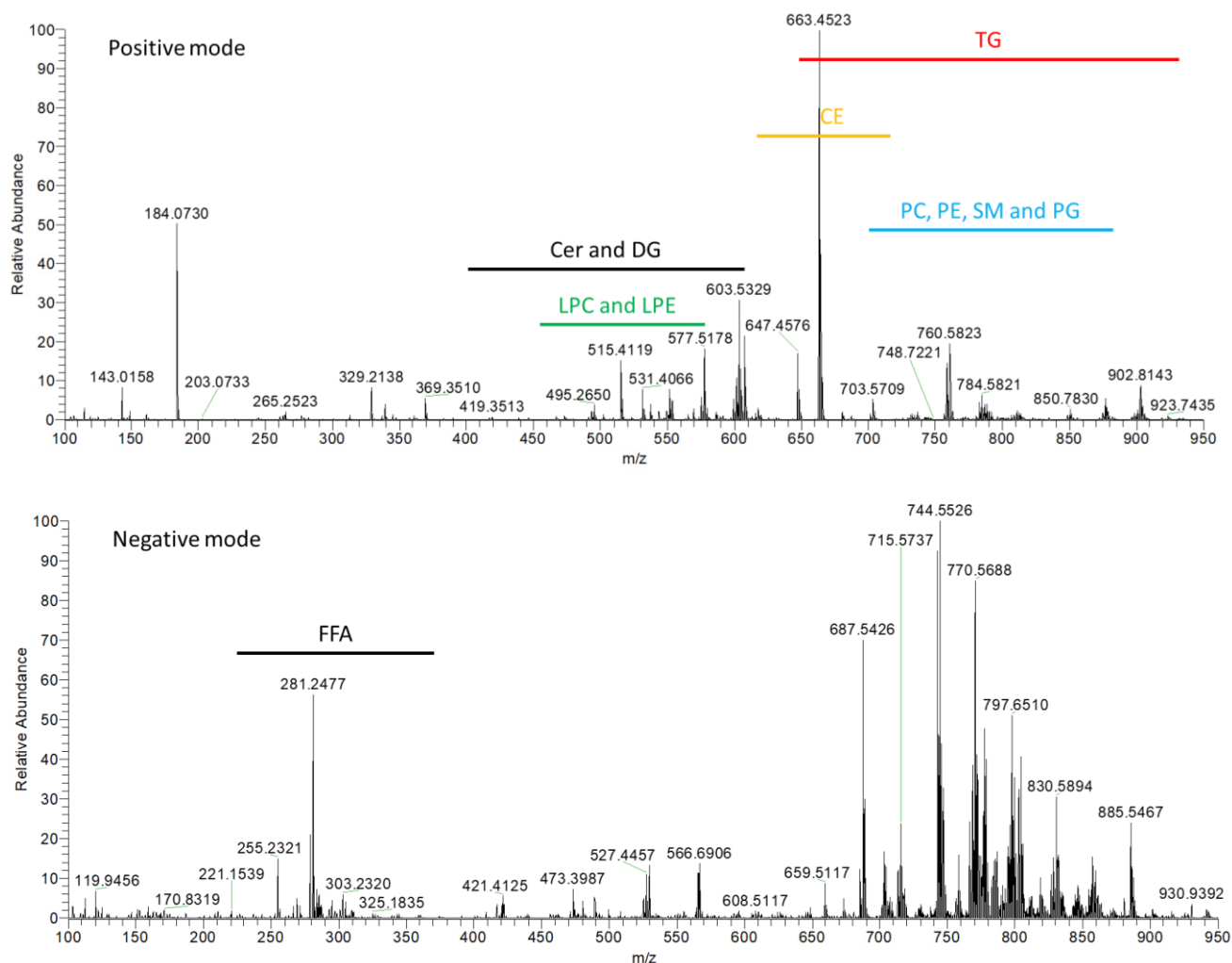


Figure 1. Representative mass spectrometry (positive and negative modes) of total lipid extract of untargeted whole serum lipidome. Cer, ceramide; DG, diacylglycerol; LPC, lysophosphatidylcholine; LPE, lysophosphatidylethanolamine; CE, cholesteryl ester; TG, triacylglycerides; PC, phosphatidylcholine; PE, phosphatidylethanolamine; SM, sphingomyelin; PG phosphatidylglycerol; FFA, free fatty acids.

To assess the linearity and range covered within our lipidomic platform, by employing calibration lines (lipid standards), we identified that our lipidomic data are in the range between 5 nM and 25 μ M with a linear response, while the calibration curve turns quadratic after 25 μ M. A representative calibration curve (duplicate) for a PC (PC 28:1) is reported in Figure 2. This work, however, did not use calibration lines to obtain a

fully quantitative data but a semi-quantitative result was obtained by using a single specific internal standard, as above detailed.

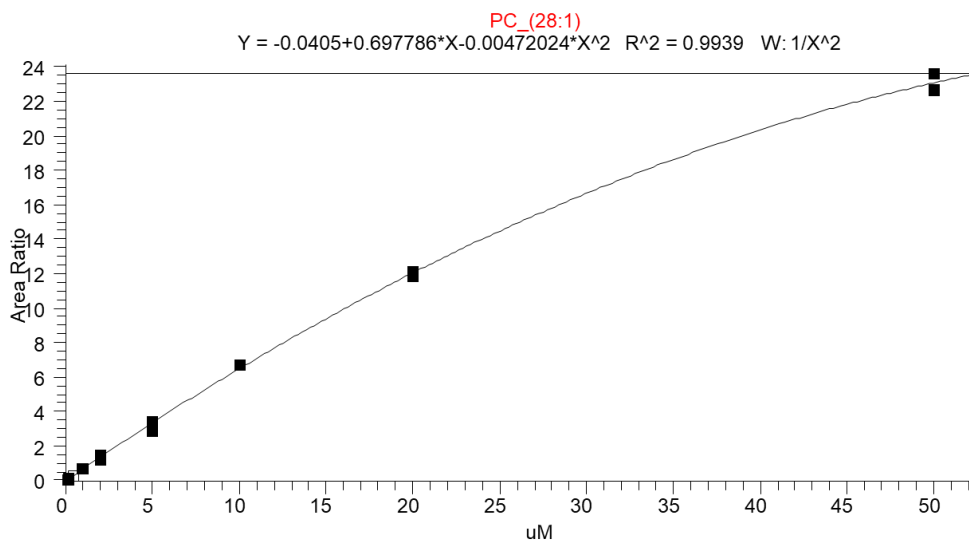


Figure 2. Representative calibration curve showing the linearity of a standard lipid (phosphatidylcholine 28:0, (PC 28:0)). In the y axes is reported the normalised intensity referred to as Area_ratio (peak intensity divided to a labelled internal standard), while the x axes report the concentration expresses to as μM .

With regards to the reproducibility of our platform, below is reported the coefficient of variation for the intraday variability and intraday variability (3 weeks) of several IS at 5 μM concentrations (Table 1).

Table 1. Inter and intraday variability of the LCMS lipidomic platform.

Internal standard	LPC_(C14:0)-d42	SM_(C16:0)-d31	PG_(C16:0)-d31/C18:1	PC_(C16:0)-d31/C18:1	C16-d31 Ceramide	PE_(C16:0)-d31/C18:1	TG_(45:0)-d29	
Internal standard (shorthand notation)	IS_LPC	IS_SM	IS_PG	IS_PC	IS_Cer	IS_PE	IS_TG	
AREA Inter-	Timing	Duplicate at 3 weeks between the two analysis						
	Mean	48730606	320042416	198765580	509610817	146002237	170457773	396978106
	Std Dev.	3817879	44769467	22146204	40744358	18335448	20393972	85852911
	CV (%)	8	14	11	8	13	12	22
AREA Intra-	Timing	Duplicate within the same day						
	Mean	50190859	329665328	213955398	527044342	138818410	176313186	412649285
	Std Dev.	3527761	32840732	25850804	40151990	26724945	15694049	68439178
	CV (%)	7	10	12	8	19	9	17

LPC, lysophosphatidylcholine; SM, sphingomyelin; PG phosphatidylglycerol; PC, phosphatidylcholine; Cer, ceramide; PE, phosphatidylethanolamine; TG, triacylglycerides; IS, internal standard; CV, coefficient of variation.

2.2.3 Esterified cholesterol analysis – LC-MS/MS

The organic lipid-containing layer from the Folch extraction was analysed by targeted LC-MS/MS using a UHPLC⁺ series coupled to a TSQ Quantiva mass spectrometer (Thermo fisher scientific, Waltham, MA, US). Ten microlitres of sample containing isotopically labelled cholesteryl-d7 pentadecanoate at the concentration of 42.5 μ M (Avanti Polar Lipids Inc, USA) was injected onto an Acquity C18 CSH column (Waters Ltd., Warrington, UK; 100 \times 2.1 mm, 1.7 μ m) with a column temperature of 55 °C. A gradient separation was used as described for the lipidomics experiments. A heated electrospray ionisation source was operated in positive ion mode; desolvation temperature and gas flow were 270 °C and 45 arbitrary units, respectively. Selected reaction monitoring transitions used are included in Table 2. Xcalibur software (Thermo Fisher Scientific) was used for peak integration. Peak areas were normalised to the internal standard. Post-acquisition processing (blank correction, imputation and QC analysis) was the same as above described.

Table 2. Targeted (LC MS/MS) parameters for the measurements of circulating cholesteryl esters (CE).

Metabolite	HMDB ID	Column	Retention Time (RT)	Mode	Precursor	Product	Collision Energy (CE)	Lens
			(min)		<i>m/z</i>	<i>m/z</i>	(V)	(V)
CE15:0 d7		18 CSH	7.6	Positive	640.58	376.387	24.713	155
CE16:0	HMDB0000885	18 CSH	7.7	Positive	647.815	369.333	24.511	140
CE18:1	HMDB0005189	18 CSH	7.6	Positive	673.537	369.333	27.242	152
CE18:2	HMDB0000610	18 CSH	7.5	Positive	671.53	369.333	28.86	151
CE18:3	HMDB0010369	18 CSH	7.2	Positive	669.56	369.333	21	151
CE 20:4	HMDB0006726	18 CSH	7.4	Positive	695.567	369.333	30.124	148

CE, cholesteryl esters; HMDB, Human Metabolome Database; CSH, Charged Surface Hybrid.

2.3 Measurement of apolipoprotein levels by mass spectrometry

2.3.1 Apolipoprotein extraction

Apolipoprotein were extracted from blood serum as previously reported (Kay et al, 2007). As compared to the original method, we focused on a subset of apolipoprotein found relevant to the circulating lipoprotein lipid remodelling based on a literature search I performed at the beginning of my project. Briefly, 10 μ L of serum was diluted by a factor of 10 with 50 mM ammonium bicarbonate in water. Diluted serum (10 μ L) then was transferred to 490 μ L of 10 mM dithiothreitol in 50 mM ammonium

bicarbonate, with 0.5 mg/mL bovine serum albumin (BSA) as an internal standard. Samples were incubated at 60°C for 1 hour, allowed to cool to room temperature and 100 µL of 100 mM iodoacetamide in 50 mM ammonium bicarbonate was added and samples incubated at room temperature in the dark for 30 min. Trypsin (10 µL at 100 µg/ml) was added to a 100 µL aliquot of each sample and incubated for 16 hours at 37 °C. After incubation, 20 µL 1% formic acid (aq) was added to halt digestion prior to analysis by LC-MS/MS.

2.3.2 Apolipoproteins analysis by liquid chromatography-mass spectrometry

LC-MS/MS analysis was performed on an M-Class liquid chromatography system coupled to a TQ-XS (Waters, Milford, MA, USA). A gradient of solvent A, 0.1% formic acid in water, and solvent B, 0.1% formic acid in acetonitrile was used to separate digested proteins. Sample (2 µL) was injected onto an HSS T3 50 x 1.0 mm column (Waters) at 25 µL per minute at 15% B, rising to 50% B over 5 minutes. The column was washed at 85% B for 2.5 minutes before returning to initial conditions for a total run time of 10 minutes. Positive electrospray ionisation was performed with a needle voltage of 3 kV, source and desolvation temperature of 450 °C and 150 °C respectively, and a cone voltage of 30V. Selected reaction monitoring transitions used are included in Table 3. Peptide peaks were integrated using TargetLynxXS (Waters) and expressed a ratio of the average peak area to the mean peak area value of two typically digested BSA peptides.

Table 3. Targeted (LC MS/MS) parameters for the measurements of circulating apolipoproteins.

Protein	Peptide sequence	Q1 m/z	Q3 m/z	Collision Energy (CE)
APOA-I	DYVSQFEGSALGK	700.8	808.4	20
APOA-IV	LGEVNTYAGDLQK	675.7	540.2	20
		675.7	575.6	20
APOB-100	TEVIPPLIENR	640.8	838.4	20
APOC-I	TPDVSSALDK	516.8	620.3	20
		516.8	719.4	20
APOC-II	TYLPAVDEK	518.2	658.2	15
		518.2	771.2	15
APOC-III	GWVTDGFSSLK	598.7	854.2	20
		598.7	953.3	20
APOD	NILTSNNIDVK	615.8	890.4	20
		615.8	1003.5	20
APOE	LGPLVEQGR	484.7	399.7	15
		484.7	588.2	20
APOM	EFPEVHLGQWYFIAGAAPT	754.4	615.8	30
BSA 1	LVNELTEFAK	582.3	951.29	20
BSA 2	LGEYGFQNALIVR	740.5	1017.4	25

2.4 Lipoprotein separation by Fast protein liquid chromatography

The serum lipoprotein profile was performed by size exclusion chromatography (SEC) using a previously described method (Innis-Whitehouse et al, 1998). Briefly, fractions were determined in 50 μ L of serum samples diluted with 50 μ l of a PBS solution via SEC, using a Superose 6 increase column, (10/300GL, 10 \times 300, 24 ml). SEC was carried out using an ÄKTA purifier 10 (GE Healthcare; Uppsala, Sweden), equipped with a fraction collector Frac-950. The system was controlled by a UNICORN control system version 4.10 (GE Healthcare). SEC flow rate was set at 450 μ l/min at 10°C. A representative chromatogram of the total cholesterol FPLC eluate profiling in a healthy and a NAFLD participant is reported in Figure 3. Eluting fractions were collected in 96 glass-coated well-plates (Eppendorf Protein Low- Bind; Hamburg, Germany). After fractionation, samples were dried down under a gentle steam of nitrogen and stored at - 80°C before further processing. Selected fractions obtained by Superose-6 SEC were further investigated by MS as detailed above.

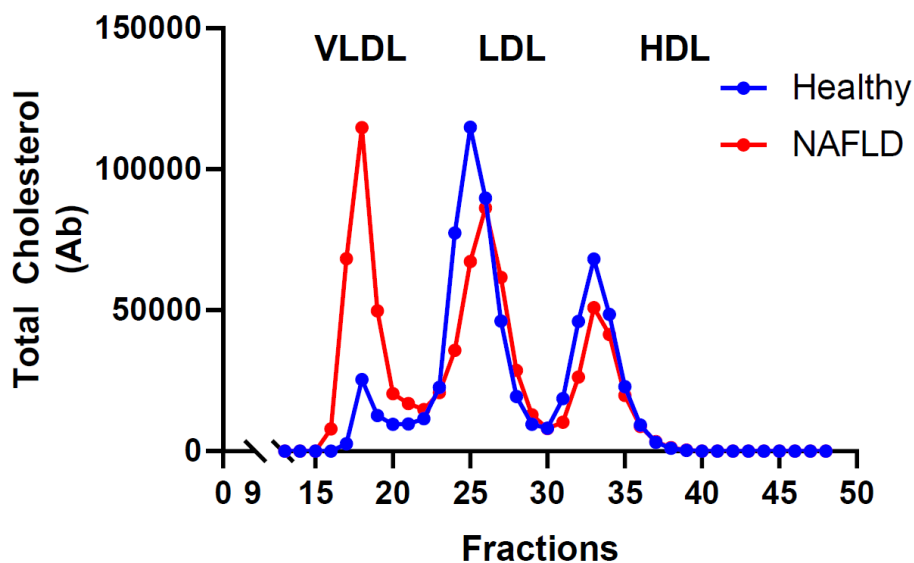


Figure 3. Representative lipoprotein cholesterol profiles (colorimetric assay) of a fasting blood serum of a healthy volunteer and a NAFLD patient. The fraction numbers, are represented on the x-axis and the absorbance units in arbitrary units (ab), measured at 570 nm, are represented by the y-axis.

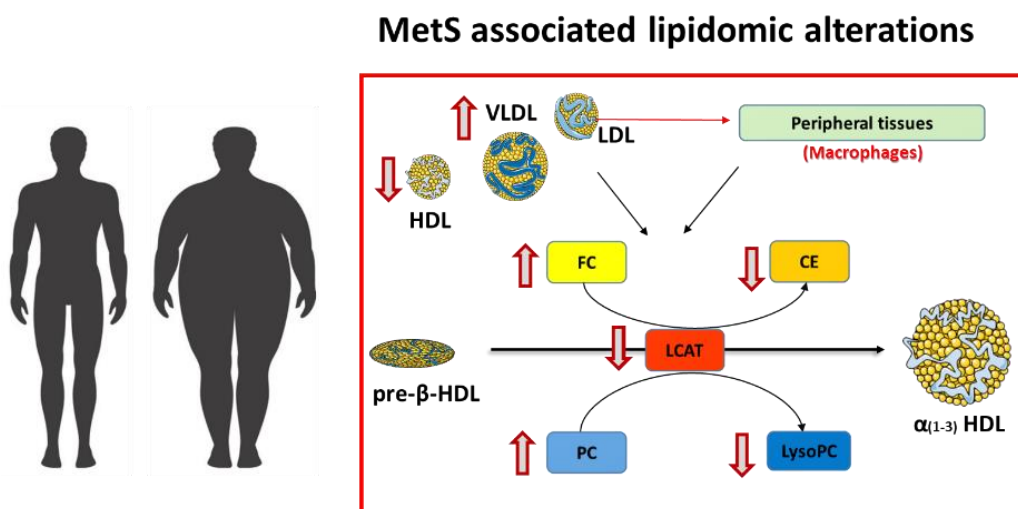
2.5 Statistical analyses

Data are shown as mean \pm standard deviation unless otherwise specified. Normality was visually assessed from plots of the data (skewness/kurtosis) obtained with the `lm` function in R, and logarithmic transformations were applied to non-normally distributed data. In Chapter 3, lipids are grouped into their major lipid classes by summing any lipid species belonging to a specific class, while in Chapter 4 lipids are grouped as in Chapter 3 (total lipids) in addition to a further classification based on their number of double bonds within each lipid class as saturated, lipids with no double bonds, monounsaturated, lipids with a maximum of 1 double bond per chain, polyunsaturated, lipids with 2 or more double bonds per chain (further details are provided in the respective chapters). Comparisons of clinical and omics data between healthy and MetS/NAFLD were assessed using two-way or three-way ANOVA with “sex” and “disease state” or “sex”, “T2DM” and disease state as covariates, respectively. Overall, a P-value <0.05 was considered significant, yet multiple testing correction (Benjamini-Hochberg procedure to control the False Discovery Rate (FDR)) were applied when lipids were investigated as independent hits as specified in the method section of Chapter 3 and 4. Correlation matrices between omics layers along with clinical variables, were performed with Pearson correlation coefficient, with P-value <0.05 considered significant, or multiple regression (`lm` function, in R) with “sex” as a covariate, when relevant; a P-value <0.05 was considered significant. Statistical analysis was performed with R version 4.0.0 and Microsoft Excel 2016. Graphs were obtained using R version 4.0.0 and Graph Pad (Graph Pad Prism 7.0).

Chapter 3. Lipidomic indices reveal reduced LCAT activity in patients with metabolic syndrome

3.1 Abstract

The Metabolic Syndrome, a cluster of cardiovascular risk factors, has been associated with changes in circulating lipidome, but underlying mechanisms remain unclear. The present study aimed to define the fasting lipidomic differences between MetS (n=14) and healthy people (n=11), and the contribution of circulating lipoprotein remodelling enzymes in the observed changes. Compared to healthy people, MetS patients showed increased: triglycerides, diglycerides, free fatty acids, and phosphatidylcholines in their blood, whereas lysophosphatidylcholine alongside cholesteryl ester to free cholesterol ratio were decreased. Employing lipidomic ratios, used as an indirect proxy of enzymatic activity, along with direct measurements of the circulating lipoprotein remodelling enzymes, we demonstrated that the lipidomic changes seen in the MetS were attributable, in part, to reduced activity of the enzyme lecithin cholesterol acyltransferase (LCAT). Both direct and indirect proxies of LCAT activity showed a positive correlation with HDL-C and a negative correlation with obesity and insulin resistance, thus suggesting a close link between LCAT activity and the MetS. Taken together, these results provide, for the first time, a mechanistic attempt to decipher the lipidomic profile associated with the MetS.



Simplified representation of the hypothesised mechanistic pathway involved in the lipidomic remodelling occurring in MetS.

3.2 Introduction

The majority of lipidomic studies conducted to date have been performed in a fasting status. When compared to healthy people, MetS patients display a plethora of lipid changes that have only recently begun to be characterised. For instance, in line with the hypertriglyceridemic nature of the MetS, lipidomic studies have shown that MetS is characterised by elevated levels of circulating triglycerides (TG) and diglycerides (DG) irrespective of their fatty acid composition (Capel et al, 2020; Surowiec et al, 2019). Interestingly, the same studies also reported discordant results for the phosphatidylcholine (PC) levels. Specifically, when compared to healthy participants, Capel et al., reported elevated levels of PC in MetS patients (Capel et al, 2020), while Surowiec et al, reported reduced levels in MetS (Surowiec et al, 2019). In line with the former study, Kulkarni et al, found that MetS patients showed a general increase in plasma PC when compared to healthy subjects (Kulkarni et al, 2013b) whereas a smaller study reported that only PC34:2, the most abundant circulating PC, was increased in MetS when compared to healthy people, and is positively correlated with the MetS defining criteria (Ramakrishanan et al, 2018). A lipidomic analysis of the Framingham Heart Study, involving 658 participants, reported that PC and lysophosphatidylcholine (LysoPC) were inversely associated, while sphingomyelin (SM), TAG, and DAG were directly correlated with obesity (Yin et al, 2020). The same study also reported that LysoPC were inversely associated, while specific SM were positively associated with hyperglycaemia. Moreover, several TG and DG showed a positive correlation with dyslipidaemia, while different PC and LysoPC were inversely correlated with the latter (Yin et al, 2020). As pointed out in a recent systematic review of the literature, the paucity of studies investigating the lipidomic signature of MetS, along with differences in the study design, and lack of replication cohorts, except for the Framingham Heart Study, make the interpretation of the different studies very difficult (Monnerie et al, 2020). Most importantly, however, the lack of follow-up experiments that would provide mechanistic insight into the observed changes is also a major issue in the field.

This chapter aims to investigate the fasting lipidomic changes occurring in patients with MetS and to provide a mechanistic explanation. For this purpose, I employed state-of-the-art mass spectrometry lipidomics and targeted proteomics, along with commercially available enzymatic assays which pointed out to an impaired

phospholipid remodelling in MetS, partly driven by a reduced activity of the enzyme lecithin–cholesterol acyltransferase.

3.3 Methods

3.3.1 Ethics and the MetS study cohort

11 healthy volunteers and 14 patients at the first diagnosis of MetS were included in this study. Briefly, the presence of MetS was defined when 3 out of 5 criteria for MetS were present according to the NCEP: ATP III (Alberti et al, 2009). Exclusion criteria were: the presence of diseases that could have influenced participants' metabolism (i.e. autoimmune disease, cancer, thyroid, and adrenal disorders, endocrine disorders, and acute and chronic kidney failure), alcohol intake over 25 g/day, and pharmacological treatment except for hypertension drugs in MetS patients. Moreover, only patients with no evidence of organ damage (kidney function and interventricular septum thickness within normal range) or atherosclerosis (carotid intima-media thickness (CIMT) < 0.9 mm, no atherosclerotic plaques at the carotid doppler ultrasound) were included in this study

The clinical characteristics of the study population are summarised in Supplementary Table 1. The study protocol was approved by the Ethical Committee of the Azienda Ospedaliero-Universitaria Policlinico di Bari, Italy, following the Declaration of Helsinki. Participants were recruited at the University Hospital of Bari, Italy. All patients gave written informed consent.

3.3.2 Sample collection and clinical biochemistry measurements

After overnight fasting, serum was collected in healthy and MetS participants for the assessment of standard clinical biochemistry tests. Serum was separated by centrifugation and stored at -80 °C. Details of the clinical measurements are described in Chapter 2 Materials and Methods (section 2.1).

3.3.3 Measurement of lipid levels by mass spectrometry

Lipid extraction and their measurements through liquid chromatography coupled with mass spectrometry are reported in Chapter 2 Materials and Methods (section 2.2).

3.3.4 Measurement of protein levels by mass spectrometry

Protein extraction and their measurements through liquid chromatography coupled with mass spectrometry are reported in Chapter 2 Materials and Methods (section 2.3).

3.3.5 Circulating lipoprotein remodelling enzyme activity - fluorimetric assay

3.3.5.1 Lp-PLA2

Lp-PLA2 activity of serum was measured in duplicates using a commercially available kit (Cayman, Europe), following manufacturer's instructions. Specifically, samples were incubated for 30 minutes with Ellman's reagent at room temperature with the subsequent addition of 2-thio PAF, used as a substrate for Lp-PLA2 activity. The reaction causes an increase in colorimetric absorbance measured once every minute at 405-414 nm. Measurements were obtained using a plate reader Tecan Infinite 200 PRO (Tecan, Mannedorf, Switzerland).

3.3.5.2 LCAT activity

LCAT activity of serum was measured in duplicates using a commercially available kit (Merck, St Louis, USA) following the manufacturer's instructions. Specifically, samples were incubated with LCAT substrate for 4 h at 37 °C. The fluorescent substrate emits fluorescence at 470 nm. When the substrate is hydrolysed by LCAT, a monomer is released that emits fluorescence at 390 nm. The LCAT activity is expressed as a change of 470/390-nm emission intensity and thus providing a semi-quantitative analyses. Measurements were obtained using a plate reader Tecan Infinite 200 PRO (Tecan, Mannedorf, Switzerland).

3.3.5.3 PLTP activity

PLTP activity of serum was measured in duplicates using a commercially available kit (Merck, St Louis, USA) following the manufacturer's instructions. Specifically, the assay uses a proprietary substrate to detect PLTP mediated transfer of the fluorescent substrate. The transfer activity results in an increase in fluorescence intensity ($(\lambda_{ex} = 465 \text{ nm})/(\lambda_{em} = 535 \text{ nm})$). Measurements were obtained using a plate reader Tecan Infinite 200 PRO (Tecan, Mannedorf, Switzerland).

3.3.6 Statistics

Data are shown as mean \pm standard deviation unless otherwise specified. Normality was visually assessed from plots of the data (skewness/kurtosis) obtained with the `lm` function in R, and logarithmic transformations were applied to non-normally distributed data. Lipids are grouped into their major lipid classes by summing any lipid species belonging to a specific class. Comparisons of clinical and omics data between healthy and MetS were assessed using two-way ANOVA (with “sex” and “disease state” as covariates), and P-value <0.05 considered significant. Correlation matrices between omics layers along with clinical variables, were performed with Pearson correlation coefficient, with P-value <0.05 considered significant, or multiple regression (`lm` function, in R) with “sex” as a covariate, when relevant; a P-value <0.05 was considered significant. Data of the whole serum lipidome, single lipid species, was analysed by student two-sided T-Test reporting the unadjusted alongside the adjusted P-value (Benjamini-Hochberg procedure to control the False Discovery Rate (FDR)). Statistical analysis was performed with R version 4.0.0 and Microsoft Excel 2016. Graphs were obtained using R version 4.0.0 and Graph Pad (Graph Pad Prism 7.0).

3.4 Results

3.4.1 Clinical characteristics, serum lipidomic and apoprotein profile of healthy and MetS participants

Compared to controls, MetS patients were significantly older, with higher BMI and abdominal obesity, and insulin resistant (Supplementary Table 1). They also displayed the classical features of mixed dyslipidaemia: remarkably elevated TG and reduced HDL-C, with an expected significant sex effect on these parameters, while they did not show significant differences in total cholesterol, LDL-C, and blood pressure (Supplementary Table 1).

The serum lipidome analyses included 8 major lipid species measured through ESI LC-MS (TG, DG, FFA, PC, LysoPC, and SM), colorimetric assay (CE and FC) (Figures 1 a-h), and ESI LC-MS/MS (CE) (Supplementary Table 2). We also profiled the main apoproteins involved in the serum lipidomic remodelling through ESI LC-MS/MS (Figure 2).

In keeping with the definition of MetS and some studies pointing to AT-IR as a driver of MetS (Azzu et al, 2020; Karpe et al, 2011), patients with MetS showed increased levels of total TG, DG, and FFA (Figures 1a-c) compared to controls. Interestingly, MetS patients displayed significantly increased levels of total PC along with reduced LysoPC when compared to controls (Figures 1d-e), while total SM, CE, and FC (Figures 1f-h) did not show significant changes.

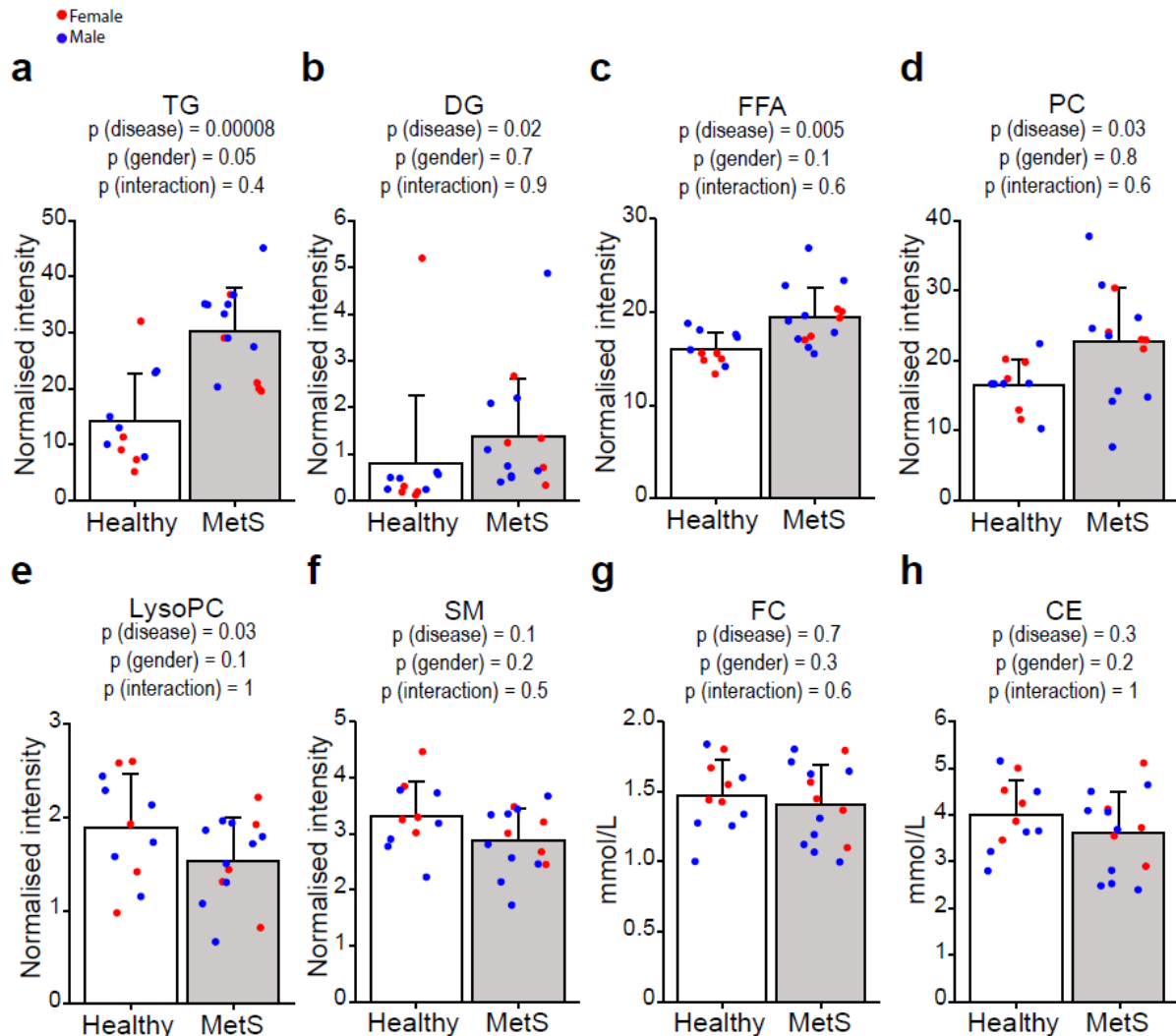


Figure 1. Serum levels of major lipidomic classes from healthy and MetS participants. (a) TG, (b) DG, (c) FFA, (d) PC were increased in MetS ($n=14$) whereas (e) LysoPC were reduced as compared to controls ($n=11$). SM, FC, and CE (f-h) were not significantly changed. All lipid species were analysed by LC-MS except for FC and CE analysed calorimetrically as reported in the method section. Statistical significance was assessed using two-way ANOVA controlling for sex and interaction between MetS and sex, with a P-value <0.05 considered significant. Data are mean \pm standard deviation.

With regards to the apoprotein profile, compared to healthy participants, MetS patients displayed a significant reduction in ApoA-I and ApoD (Figures 2a-b), this being in agreement with the low levels of HDL-C in the MetS group. ApoA-IV, ApoM, ApoE, ApoC-I, and ApoB-100, did not show a significant difference between the two groups (Figures 2c-g), while Apo-CII and ApoC-III were remarkably increased in the MetS group in comparison to controls (Figures 2h-i). Increased levels of ApoC-III contribute to hypertriglyceridemia via the inhibition of a) the activity of lipoprotein lipases (LPL) and b) the uptake of TG by the liver (Santos-Baez & Ginsberg, 2020), thus resulting in an increased half-life of TG-rich lipoproteins. ApoC-II, however, is a cofactor of LPL

and promotes its activity (Wolska et al, 2017). Interestingly, elevated levels of ApoC-II have been reported in patients with T2DM and obesity (Beliard et al, 2009; Ooi et al, 2016) and their levels were strongly associated with TG levels.

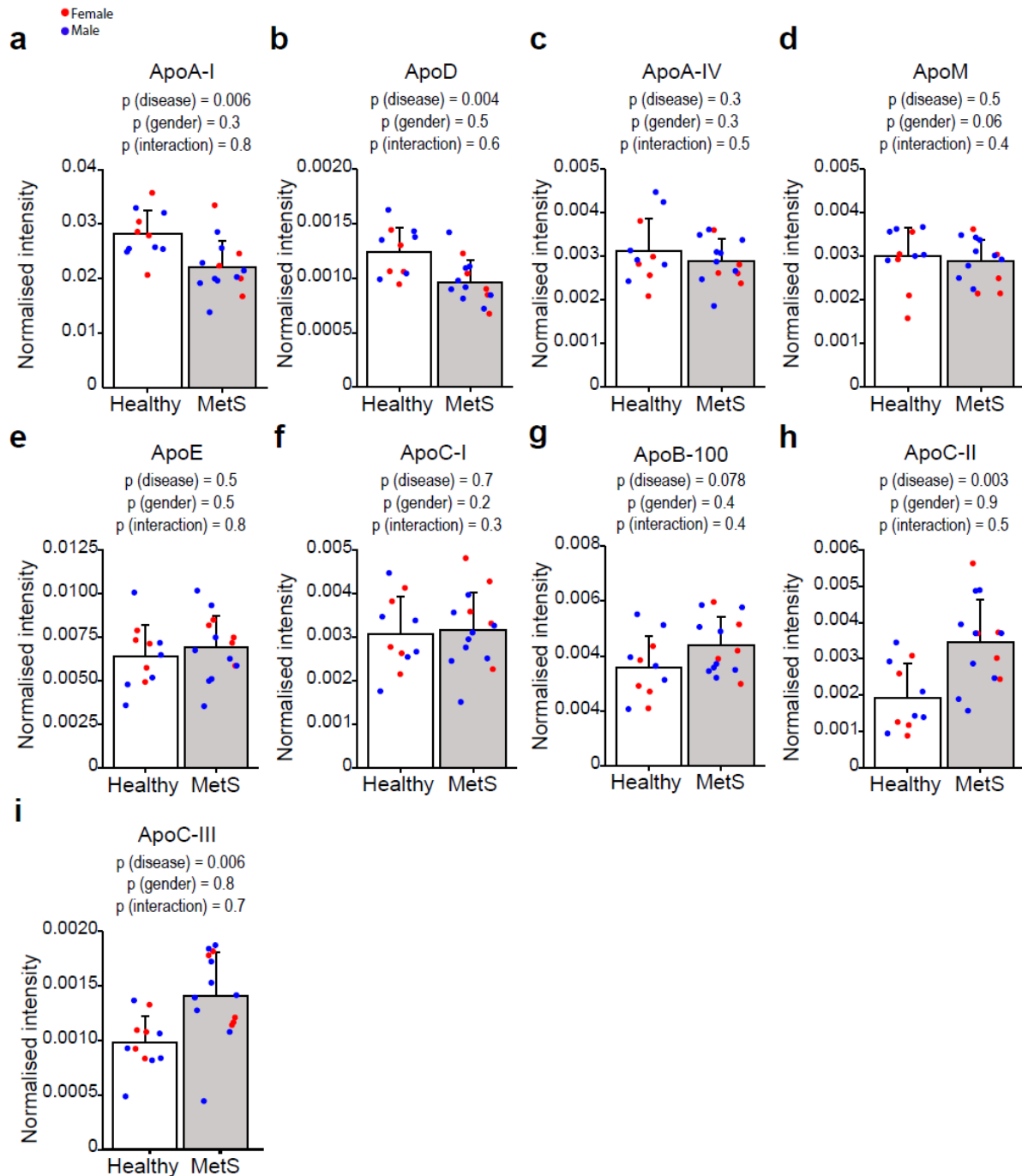


Figure 2. Serum levels of major apolipoproteins involved lipoprotein remodelling.

ApoA-I (a) and ApoD (b) were decreased in MetS (n=14), ApoA-IV, ApoM, ApoE, ApoC-I and ApoB-100 (c-g), were not significantly different, whereas ApoC-II (h) and ApoC-III (i) were increased as compared with controls (n=11). All apolipoproteins were analysed by LC-MS/MS as reported in the method section. Statistical significance was assessed using two-way ANOVA using the disease state and Sex as covariates; a P-value <0.05 was considered significant. Data are mean \pm standard deviation.

To further assess the association between the lipidomic and targeted proteomic changes, I correlated the significant features of both omics as shown in Figure 3. The latter showed that apart from the expected positive correlations of TG, DG, and FFA with ApoC-II and ApoC-III, PC and LysoPC reported the highest correlations with ApoA-I and to a lesser extent to ApoD, thus suggesting a possible lipidomic remodelling of the HDL fractions.

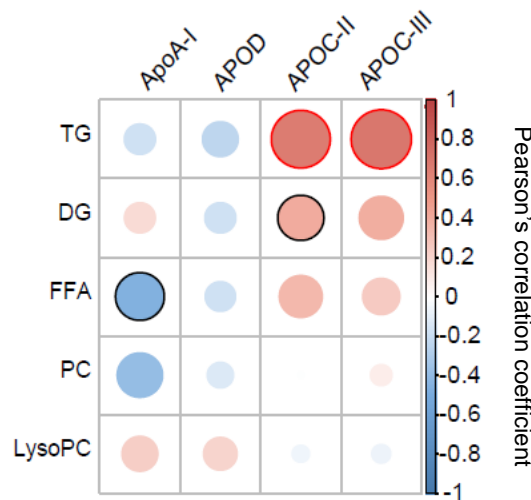


Figure 3. Heatmap of correlation matrix, Pearson's correlation coefficient, among significantly changed lipidomic and apoprotein species in MetS and healthy controls. Data are plotted based on whether they are positively (red) or negatively (blue) correlated with red bold borders highlighting correlations with a $p < 0.01$ and black bold borders highlighting correlations with a $p < 0.05$.

Apart from the anticipated lipidomic and apoprotein features of the MetS, these results suggest an alteration of circulating lipoprotein remodelling enzymes. PC and LysoPC are biochemically interconvertible species, and their metabolism can be modulated both intracellularly (e.g. in the liver, intestine, adipose tissue, or macrophages), and extracellularly (Law et al, 2019). In circulating blood, PC can be remodelled into LysoPC by two enzymes: a) lecithin–cholesterol acyltransferase (LCAT), a key player in the formation of large and mature HDL (Ossoli et al, 2016b) that transfers 18:1 or 18:2 fatty acids from PC to FC, thus generating CE and LysoPC (Rousset et al, 2009); and b) lipoprotein-associated phospholipase A2 (Lp-PLA 2), an enzyme with pro- and anti-inflammatory capabilities (Marathe et al, 2014) that catalyses the hydrolysis of fatty acids at the sn-2 position of oxidised phospholipids ultimately generating a fatty acid and a LysoPC.

I therefore decided to further investigate the changes in serum phospholipid remodelling enzymes.

3.4.2 LCAT, but not Lp-PLA2, activity is reduced in MetS thus justifying the changes in serum PC and LysoPC

To gain insight into the biology of lipoprotein remodelling, employing commercially available kits, I determined the activity levels of circulating lipoprotein remodelling enzymes. Specifically, I studied Lp-PLA 2, phospholipid transfer protein (PLTP), and LCAT activity in serum. Lp-PLA2 showed no significant changes between the groups, although there was a significant effect of sex, with the activity being increased in males with MetS as compared to controls (Supplementary Figure 2a), while in agreement with previous studies (Qin et al, 2014), PLTP was significantly increased in the MetS group when compared with controls (Supplementary Figure 2b). Although PLTP mediates the net transfer of PL from TG-rich lipoproteins into HDL particles, it is also capable of transferring several lipids such as diacylglycerol, phosphatidic acid, sphingomyelin, cerebroside and phosphatidylethanolamine, and α -tocopherol (Albers et al, 2012), thus rendering this enzyme a non-specific transporter. The extent to which the increased PLTP levels have impacted the PC and LysoPC in our study are of challenging interpretation, but it is nonetheless an important enzyme to take into account when characterising lipoprotein remodelling. LCAT activity was significantly reduced in the MetS group when compared with controls (Figure 4a). I further confirmed this observation assessing different product/substrate ratios that have been proposed as indirect proxies of LCAT activity (Angelini et al, 2014; Gerl et al, 2018; Ossoli et al, 2019); while LysoPC/PC ratio can be affected by both LCAT and Lp-PLA2 activity, the conversion of FC to CE in plasma can only be catalysed by LCAT (Ossoli et al, 2016a). As shown in Figure 4b-c, both CE/FC and LysoPC/PC ratios were significantly reduced in MetS patients. This was even more evident (Figure 4d) when combining the information from cholesterol and phospholipids using a recently proposed formula, called “non-equilibrium reaction quotient” (Q’; formula: $(CE \cdot LysoPC)/(FC \cdot PC)$) (Gerl et al, 2018). Furthermore, in support of the notion that these product/substrate ratios can be used as indirect proxies of LCAT activity, I found significant correlations among these variables (Figure 5a-c). Taken together, these data suggested that the changes in the whole serum lipidomics previously described most likely reflect the suppressed LCAT activity seen in my cohort.

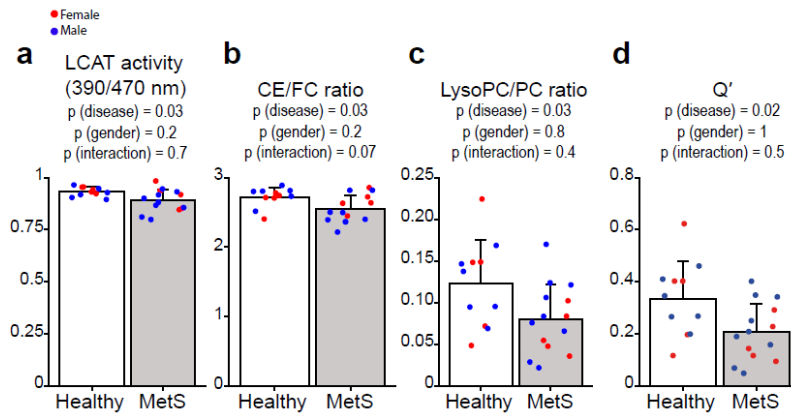


Figure 4. Direct and indirect measurements of LCAT activity. The direct measurement of LCAT activity (a) and its lipidomic predictors (b-d) were significantly reduced in MetS (n=14) when compared with controls (n=11). All lipid species were analysed by ESI LC-MS except for FC and CE analysed colorimetrically as reported in the method section. LCAT activity was measured with a fluorometric assay. Statistical significance was assessed using two-way ANOVA controlling for sex and interaction between MetS and sex, with a P-value <0.05 considered significant. Data are mean \pm standard deviation

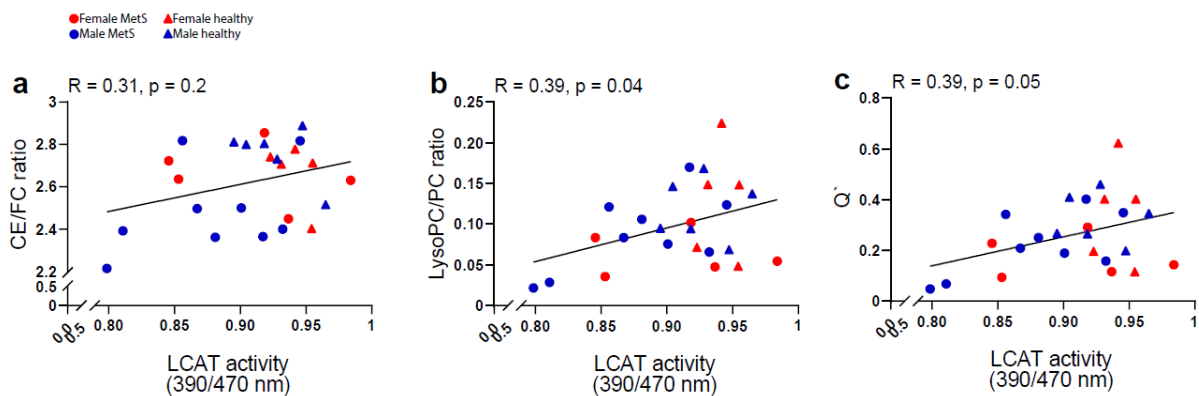


Figure 5. Correlation between direct and indirect measurements of LCAT activity. Lipidomic predictors of LCAT activity (a-c) positively correlated with LCAT activity, with LysoPC/PC and Q' having the highest correlations. All the measurements were performed on MetS (n=14) and controls (n=11). Lipid species were analysed by ESI LC-MS except for FC and CE analysed calorimetrically as reported in the method section. The correlation between variables was assessed with Pearson's correlation coefficient. P-values < 0.05 were considered statistically significant

3.4.3 LCAT activity and its lipidomic proxies show an inverse correlation with metabolic risk factors and positively correlate with HDL-C

The role of LCAT in the pathophysiology of CVD is still debated, with conflicting results coming from preclinical and clinical studies (Ossoli et al, 2016a). Contradictory findings have also been reported in patients with metabolic risk factors (Dullaart et al, 2008;

Lucero et al, 2015; Magkos et al, 2009; Nakhjavani et al, 2011), further highlighting the intricate nature of LCAT function. Because of the coherent reduction of LCAT activity and its product to substrate ratios in MetS, I sought to understand the extent to which these parameters correlated with characteristic metabolic risk factors linked to the MetS, such as obesity (BMI), insulin resistance (HOMA2-IR), and HDL-C. LCAT activity and all of the lipidomic indices investigated showed a remarkable and significant negative correlation with BMI (figure 6a,d,g,j). The ratios were also negatively correlated with HOMA2-IR (Figure 6b,e,h,k), but only the direct measurement of LCAT (figure 5b) reached a significant correlation. Lastly, the LCAT activity and relative ratios investigated showed a positive correlation with HDL-C (figure 5c,f,i,l), with the Q` showing the highest association ($R = 0.57$) and significance ($p=0.0008$). Taken together, these data suggest that LCAT and its proxies display a strong relationship with metabolic risk factors, this being partially attributable to reduced HDL-C levels in the MetS group compared to controls.

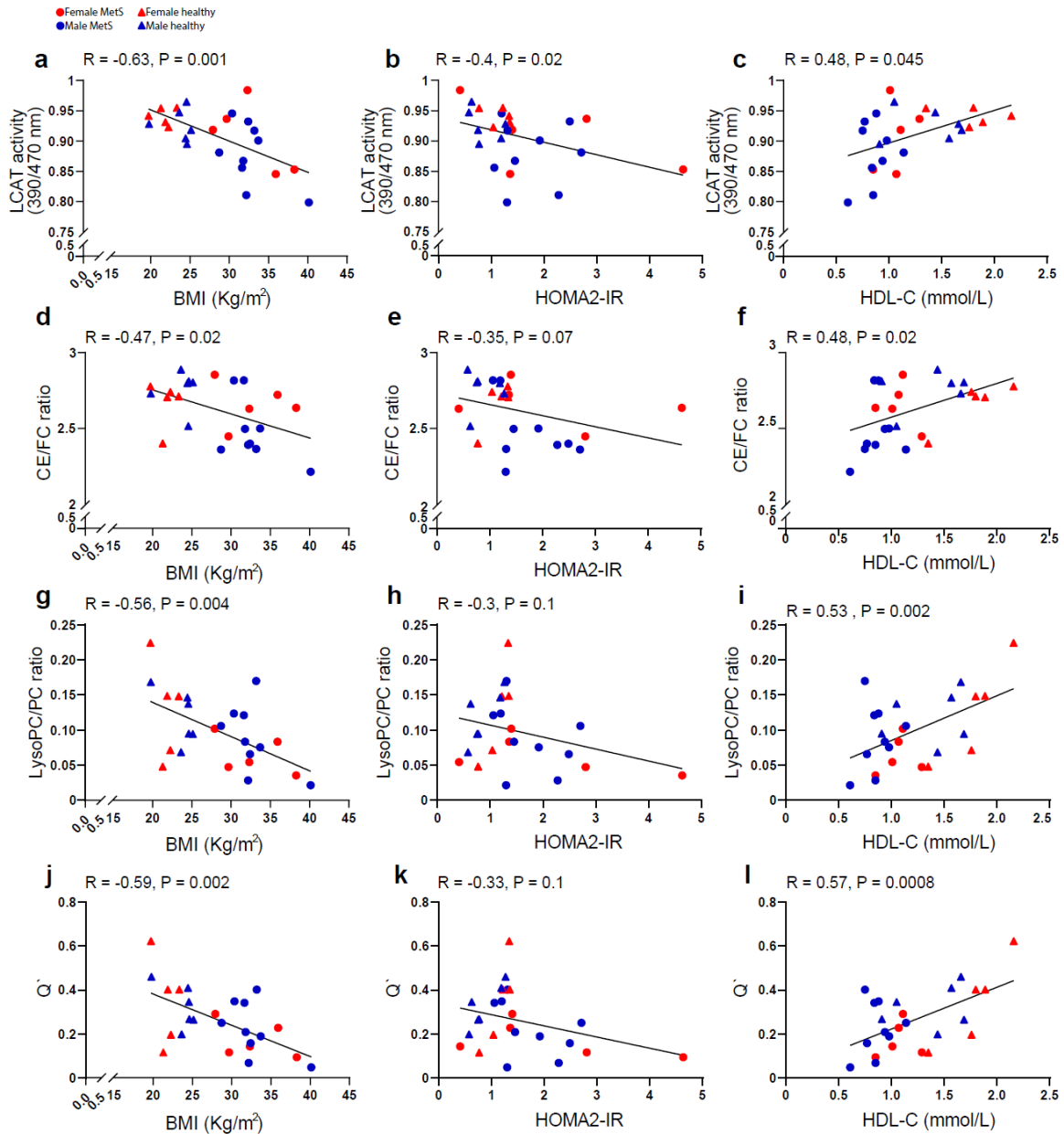


Figure 6. Correlation between indirect measurements of LCAT activity with metabolic risk factors. Lipidomic predictors and direct measurement of LCAT activity (a-l) were negatively correlated with BMI and HOMA2-IR and positively correlated with HDL. All the measurements were performed on MetS (n=14) and controls (n=11). Lipid species were analysed by ESI LC-MS except for FC and CE analysed colorimetrically as reported in the method section. The correlation between variables was assessed with Pearson's correlation coefficient. P-values < 0.05 were considered statistically significant after adjusting for sex.

3.4.4 Discussion

The MetS, a cluster of CVD risk factors, is characterised by mixed dyslipidaemia (elevated VLDL-TG and reduced HDL-C), and its treatment is a cornerstone of CVD primary and secondary prevention. Beyond the traditional lipid markers (i.e HDL-C and TG), several studies have started to characterise the lipidomic signature of the MetS (Monnerie et al, 2020), but underlying mechanisms are lacking. In this chapter, besides the expected MetS-associated lipidomic changes (elevated TG, DG, and FFA), I observed a phospholipid remodelling which was due, at least in part, to a reduced LCAT activity. The latter, along with lipidomic ratios used as proxies of LCAT activity, showed a strong correlation with some defining features of the MetS, thus suggesting a close link between LCAT activity and metabolic risk factors. Changes in circulating PC and LysoPC in MetS patients have been reported by several authors (Monnerie et al, 2020), however, results are inconsistent and this has partially been attributable to differences in study design. Elevated PC levels in MetS have been reported by some authors (Capel et al, 2020; Kulkarni et al, 2013b; Ramakrishanan et al, 2018) but not from others (Surowiec et al, 2019; Yin et al, 2020). Because PC, in healthy people, are predominantly associated with HDL particles, and reduced HDL-C is one of the inclusion criteria of the MetS, increased PC in MetS is somehow unexpected. However, different studies have found elevated levels of PC in MetS and this suggests a probable enrichment of these lipids in fractions other than HDL. Indeed, PC constitute about 8% of the VLDL lipidome (Christinat & Masoodi, 2017), therefore, it is tempting to speculate that the increased VLDL-TG fraction observed in the MetS, can be paralleled by an increase in PC, thus leading to an overall PC level in the whole plasma. The use of lipidomic ratios, as opposed to single lipid investigation, might be a more informative approach in describing biological processes. In this chapter, I used the Q' ratio as a proxy of LCAT activity. Q' is defined as the products to substrates of the LCAT reaction: $(CE*LysoPC)/(FC*PC)$, and was recently proposed by Gerl and colleagues (Gerl et al, 2018). Q' was used as a proxy of the LCAT activity in a cohort of patients with CVD, where they showed a reduction of this index in patients when compared to controls. However, the authors did not report a direct validation of their proxy against the LCAT activity or the enzyme mass (Gerl et al, 2018). My findings are in line with their work suggesting that Q' is also altered in patients at high CVD risk but without organ damage. Furthermore, my study

confirmed, for the first time, the positive correlation between Q' with a direct measurement of the LCAT activity. Although it was beyond the scope of this work to characterise the mechanisms by which LCAT was reduced in MetS, the targeted proteomics data further supported the notion of a reduced LCAT activity in MetS. Indeed, as compared to healthy people, MetS participants were characterised by lower levels of ApoA-I, which is the main activator of LCAT activity although the mechanism has not been fully characterised. Furthermore, MetS participants also displayed elevated ApoC-III levels, which have been shown to dose-dependently inhibit the LCAT activity in reconstituted HDL (Cho, 2009). Taken together, these data coherently point towards a reduced LCAT activity in the MetS. It is, however, important to underline that despite the crucial role of LCAT in the maturation of HDL, and its intensive investigation over the last 50 years, the role of LCAT in cardiovascular health is still debated with studies showing conflicting results in both pre-clinical and clinical settings (Norum et al, 2020). Despite the controversies in the field, my data support the notion of LCAT being suppressed in a cohort of patients at high of CVD risk.

3.4.5 Limitations

The findings in this chapter are subject to at least two limitations. First, the present study involved a secondary analysis of a previously published study, so I utilised data from the highest number of available participants and no formal sample size calculation was performed. This implies that results must be interpreted with caution, although two layers of evidence, enzyme activity, and lipidomic ratios, support my findings. Second, The MetS group was significantly older than the healthy controls, and after adjustment for ageing, the significant differences in the lipidomic ratios between the two groups were no longer present. Linear regression indicated the increased age in the MetS group explained 22% of the variance in the Q' ($p=0.02$) while for the LCAT activity it only explained 11% of the variance ($p=0.1$). This further weakens my results as I cannot rule out the role of ageing as a driver for the observed lipidomic changes. However, because the direct measurement of LCAT is not influenced by age, along with a previous study that reported no association between Q' and age (Gerl et al, 2018), I still find relevant the suppression of LCAT in MetS. To address this issue it is important to further investigate these indices in age-matched studies.

3.4.6 Conclusion

The purpose of the current study was to characterise the circulating lipidomic changes associated with the MetS and to provide a mechanistic explanation. The lipidomic data showed that compared to healthy controls, MetS patients were characterised by elevated PC and reduced LysoPC levels, along with the expected increased TG and DG. Correlation between targeted proteomics and lipidomics data suggested a remodelling of the HDL fractions in MetS. Lipidomic ratios, along with fluorimetric enzymatic assays, pointed to a reduction of LCAT activity while ruling out the involvement of Lp-PLPA2 in MetS when compared to healthy people. Direct measurements and indirect proxies of LCAT activity were also positively correlated with HDL-C and inversely correlated with BMI and HOMA2-IR. Taken together, these data suggest that LCAT activity might be a key modulator of the circulating lipidome in patients with MetS and that LCAT is strongly related with the metabolic derangement observed in this condition. These results warrant confirmation in larger study populations.

Supplementary materials

Supplementary Table 1. Clinical characteristics of the study cohort.

	Healthy	MetS	P-value	
			Sex	MetS
N (M/F)	6/5	9/5		0.6
Age (years)	29 ± 2	42 ± 10	0.4	0.0004
Body mass index (Kg/m ²)	22.8 ± 1.9	32.7 ± 3.4	0.1	0.00000003
Waist circumference (cm)	86 ± 8	111 ± 7	0.08	0.00000004
Systolic blood pressure (mm/Hg)	116 ± 8	122 ± 12	0.02	0.2
Diastolic blood pressure (mmHg)	78 ± 6	80 ± 7	0.3	0.6
Creatinine (mg/dl)	0.7 ± 0.17	0.9 ± 0.18	0.00003	0.008
Microalbuminuria (mg/l)	11.7 ± 1.6	15 ± 3.2	0.9	0.7
Total cholesterol (mmol/L)	5.5 ± 1	5 ± 1.1	0.2	0.4
HDL (mmol/L)	1.6 ± 0.4	0.9 ± 0.2	0.001	0.000002
LDL (mmol/L)	3.5 ± 0.9	3.4 ± 1.1	0.4	0.8
Triglycerides (mmol/L)	0.8 ± 0.3	1.5 ± 0.3	0.003	0.00006
Glucose (mmol/L)	5 ± 0.4	5.7 ± 0.7	0.7	0.006
Insulin (pmol/L)	53 ± 17	101 ± 61	0.4	0.002
HOMA2-IR	1 ± 0.3	1.9 ± 1.1	0.5	0.01

Data are mean ± SD. Differences between the two groups were analysed with 2-way ANOVA, and significance accepted at $p < 0.05$. M = Male, F = Female, BMI = Body Mass Index, TC = total cholesterol, HDL-C = high-density lipoprotein cholesterol, LDL-C = low-density lipoprotein cholesterol, TG = triglycerides, HOMA2-IR = Homeostasis Model Assessment 2 of Insulin Resistance.

Supplementary Table 2. Average value for lipid species in the whole serum of Healthy and MetS participants.

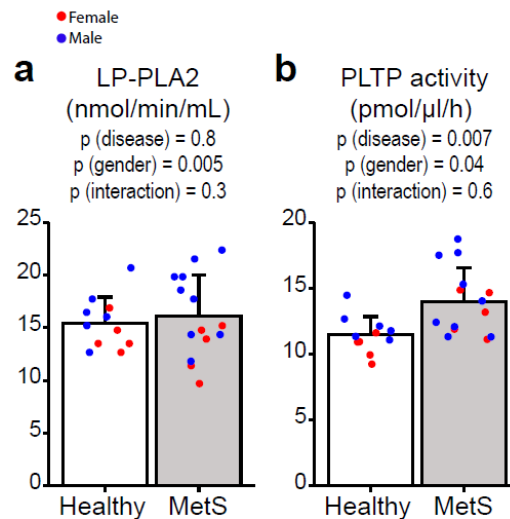
Whole serum lipidome	Average normalised peak intensity - Healthy	Average normalised peak intensity - MetS	P-value	FDR
CE 16 0	0.411	0.402	0.884534653	0.930604166
CE 18 0	0.325	0.373	0.380575892	0.463110422
CE 18 1	39.352	39.596	0.832339241	0.884908035
CE 18 2	51.843	35.758	0.0196652	0.043010482
CE 20 4	24.528	19.485	0.115112903	0.189336767
DG 32 0	0.159321086	0.092046459	0.243699636	0.33261707
DG 34 1	0.108778231	0.102718975	0.012856743	0.031837802
DG 37 0	0.084824089	0.069177777	0.11622653	0.189336767
DG 38 8	0.349389706	0.940988321	0.020014779	0.043010482
DG 41 5	0.082156665	0.177741432	2.46519E-06	4.81E-05
LysoPC 15 0	0.010360738	0.007563991	0.319470554	0.403331574
LysoPC 16 0	0.692126414	0.693633619	0.909608664	0.937363362
LysoPC 16 1	0.014687905	0.015281642	0.918801711	0.937363362
LysoPC 17 0	0.012790905	0.011126363	0.580806068	0.690134268
LysoPC 18 0	0.325172269	0.252231062	0.170994451	0.257767755
LysoPC 18 1	0.269313457	0.156068212	0.002245602	0.00986112
LysoPC 18 2	0.268527176	0.154704396	0.003621153	0.013592192
LysoPC 18 3	0.140838234	0.149435702	0.720441127	0.823681686
LysoPC 20 3	0.063191507	0.046477716	0.104020014	0.178068159
LysoPC 20 4	0.043007377	0.026013381	0.000801808	0.005061411
LysoPC 20 5	0.052824818	0.024530703	0.000186948	0.001452442
PC 30 0	0.080767222	0.085586673	0.898560647	0.935614694
PC 32 0	0.281899667	0.313913895	0.242038273	0.33261707
PC 32 1	0.228358318	0.323204525	0.035343376	0.071393619
PC 32 2	0.062821669	0.083520648	0.068165627	0.122941577
PC 34 1	3.535585472	4.929156768	0.331956372	0.413920908
PC 34 2	6.568506053	9.593782425	0.067592892	0.122941577
PC 34 4	0.025174981	0.026685511	0.737229718	0.823681686
PC 35 2	0.138002281	0.142590461	0.590082186	0.693003497
PC 36 4	3.98809162	4.884301395	0.261416843	0.352041349
PC 36 5	0.308982022	0.388173434	0.314094329	0.401563635
PC 36 6	0.039237277	0.082340383	0.06977506	0.12363651
PC 38 7	0.57729321	0.774130529	0.241262138	0.33261707
PC 38 8	0.059159191	0.07102255	0.740415753	0.823681686
PC 40 0	0.08085624	0.155468724	0.124382921	0.196291797
PC 40 5	0.093837589	0.160207878	0.094168001	0.163982209
PC 40 9	0.271965242	0.409207094	0.013470016	0.032392181
PC 42 8	0.026458309	0.032343396	0.239925001	0.33261707
PC 42 9a	0.064336461	0.108317521	0.006892067	0.019888537
PC 42 9b	0.064336461	0.108317521	0.006892067	0.019888537
SM 26 1	0.038403762	0.07439313	0.138833026	0.215725163
SM 32 1	0.093972905	0.092958474	0.816508278	0.884908035
SM 33 1	0.31081373	0.040715321	8.61905E-05	0.000818946
SM 34 0	0.044982104	0.03273963	0.00446445	0.015030316

SM 34 2	0.128144362	0.114845383	0.304990085	0.397366428
SM 34 4	0.060446233	0.026742823	0.217432725	0.318271091
SM 35 3	0.02886031	0.015415948	0.000113006	0.000951138
SM 35 4	0.054145167	0.018189352	0.065268148	0.122075611
SM 36 2	0.080053791	0.080049914	0.742129044	0.823681686
SM 36 4	0.359171212	0.36641058	0.947735205	0.957212557
SM 39 1	0.046499889	0.042180325	0.343569225	0.423176728
SM 40 1	0.45293963	0.630525155	0.057244268	0.111185981
SM 41 1	0.162961689	0.144313469	0.302269104	0.397366428
SM 41 2	0.076223142	0.080969042	0.976977997	0.976977997
SM 42 2	0.702713625	0.615523888	0.185853935	0.276047757
SM 42 4	0.157507504	0.143491559	0.111666428	0.18797182
SM 43 5	0.034128588	0.025486603	0.032657117	0.06731365
SM 44 4	0.114987985	0.099041189	0.119949413	0.192299852
SM 44 5	0.367182916	0.235831394	0.019932648	0.043010482
TG 39 1	0.278069549	1.300649016	0.005025656	0.016373912
TG 46 1	0.119341106	0.13000335	0.234485553	0.33261707
TG 48 1	0.394532932	0.610449585	0.017553444	0.040293133
TG 48 2	0.286131151	0.369823345	0.047246376	0.093566353
TG 50 1	0.836468903	1.815968634	6.45962E-05	0.000724912
TG 50 2	1.248247296	1.905620078	0.003902709	0.013592192
TG 50 3	0.495514687	0.794676077	0.005346223	0.016874017
TG 51 2	0.129254553	0.207446742	0.001014893	0.006029658
TG 51 3	0.076587605	0.123505963	0.003224022	0.01356776
TG 52 1	0.61358433	1.421168547	3.04712E-08	3.08E-06
TG 52 2	2.600571787	6.08536918	1.82628E-06	4.61E-05
TG 52 3	2.075300893	5.046089209	8.26253E-06	0.000119217
TG 52 4	0.950946332	1.782204882	0.003397666	0.013592192
TG 53 2 a	0.075540129	0.155602421	1.46336E-07	7.39E-06
TG 53 2 b	0.075760345	0.137174887	0.001333268	0.007481114
TG 53 3	0.081434785	0.508221769	8.91922E-05	0.000818946
TG 54 1	0.114106124	0.244500483	2.85585E-06	4.81E-05
TG 54 2	0.346611382	0.69036496	1.31754E-06	4.44E-05
TG 54 3	1.105323274	1.805550841	0.001989238	0.009132412
TG 54 4	0.898778359	1.602380526	0.00193844	0.009132412
TG 54 5	0.398020176	0.678646158	0.012924256	0.031837802
TG 54 6	0.143875205	0.217944487	0.011898269	0.030813465
TG 55 2	0.171100972	0.412848174	1.19937E-05	0.000151421
TG 56 6	0.219177678	0.286022492	0.014695336	0.034516952
TG 56 7	0.135282204	0.212061272	0.010284861	0.027336077
TG 56 9	0.261915077	1.481717308	0.00385904	0.013592192
TG 57 3	0.054153722	0.106533008	0.000447025	0.003009969
TG 57 4	0.048980741	0.091410204	0.001743356	0.009110976
TG 57 9	0.034622606	0.054390902	0.010198682	0.027336077
FFA 14 0	0.302	0.389	0.000351032	0.002532448
FFA 15 0	0.035	0.040	0.064928655	0.122075611
FFA 16 0	7.142106257	8.600472092	0.00797862	0.022384463
FFA 17 0	0.074683697	0.095778543	0.003683136	0.013592192

FFA 17 1	0.035861929	0.035933378	0.795237938	0.873032954
FFA 18 0	6.853645383	8.433201254	0.006469691	0.019801175
FFA 18 1	1.06005879	1.331500654	0.159480253	0.244053115
FFA 18 2	0.270751664	0.30841671	0.306877044	0.397366428
FFA 18 3	0.07722938	0.059335179	0.529180317	0.636276333
FFA 20 4	0.092097111	0.086052748	0.827656182	0.884908035
FFA 21 0	0.012456402	0.018018219	0.001804154	0.009110976
FFA 22 0	0.012527612	0.018430634	0.027877688	0.058659302
FFA 22 6	0.026136606	0.025782511	0.691882355	0.803219745

Statistical significance was calculated using two-tailed Student-T test on log2-transformed lipids; adjusted P-value < 0.05 was considered significant; the adjusted P-value was calculated using the false discovery rate (FDR) as described in the methods.

Supplementary Table 3. Unadjusted and adjusted for multiple testing, false discovery rate (FDR), P-values related to Figure 1.

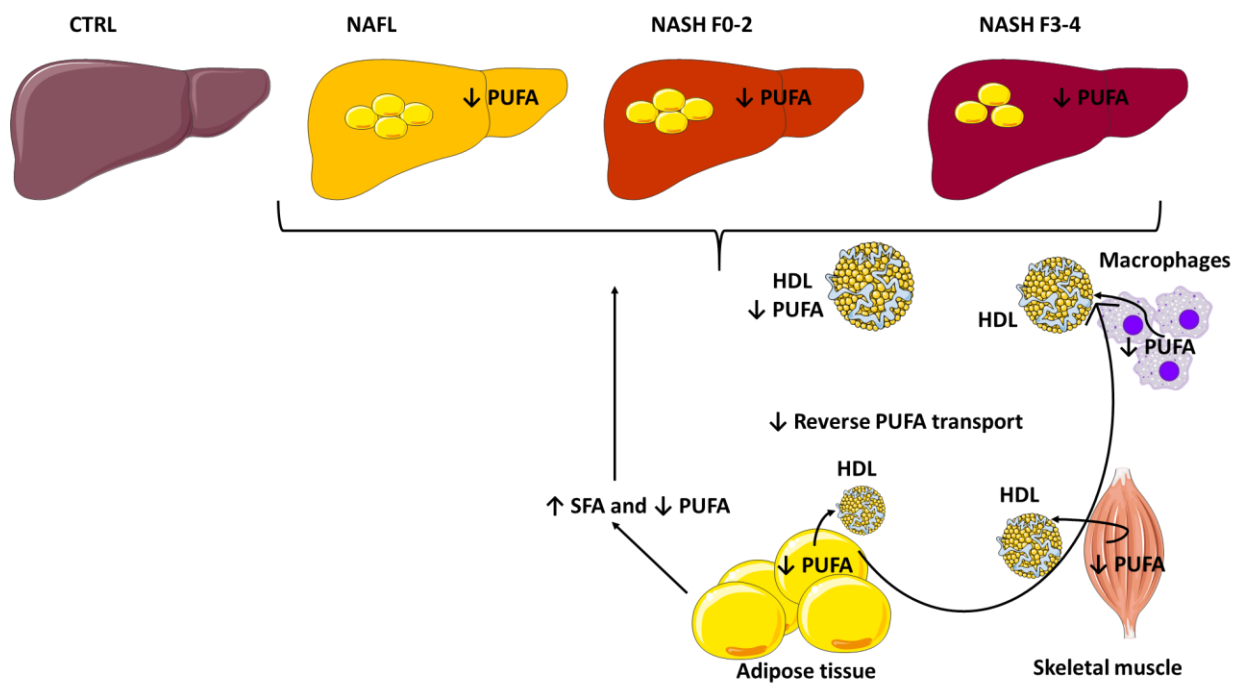


Supplementary Figure 2. Lipoprotein remodelling enzymes. While LP-PLA2 (a) did not show significant changes between MetS and the control group, PLTP activity (b) was increased in the MetS group. LP-PLA2 and PLTP assays (a-b) were performed on serum from healthy (n=11) and MetS (n=14) participants. Enzyme activities were measured with a fluorometric assay. Statistical significance was assessed using two-way ANOVA controlling for sex and interaction between MetS and sex, with a P-value <0.05 considered significant. Data are mean ± standard deviation.

Chapter 4. NAFLD is characterised by a reduced reverse polyunsaturated fatty acid transport from peripheral tissues to the liver

4.1 Abstract

Non-alcoholic fatty liver disease (NAFLD) is a cluster of liver diseases, ranging from simple steatosis to more aggressive forms, which can ultimately lead to liver failure, hepatocellular carcinoma, and death. While hepatic lipidomic studies have coherently reported a “signature” of lipid changes characterising the NAFLD spectrum, studies using whole serum have reported conflicting results. The latter is in part due to the fact that circulating lipidome is influenced by the nutritional status/habits of the subjects but also due to the fact that the whole serum lipidome is a mixture of multiple pathophysiological events that can be better studied looking into the composition of specific lipoprotein fractions. Here, I aimed to define the whole serum lipidomic profile, alongside its HDL and VLDL fractions, to study the inter-organ cross-talk between liver and peripheral tissues (and vice versa) in NAFLD. In the whole serum the most important changes occurring in NAFLD were related to a depletion in the absolute values of phospholipids (PL) and free fatty acids (FFA), particularly the polyunsaturated fatty acids (PUFA) components of these lipid classes. A deeper look into the composition of the HDL fraction, confirmed that they were the main contributors of the observed serum PUFA/PL depletion. On the contrary, the lipidome of the VLDL fraction demonstrated a generalised increase in PL, which was driven by their saturated and monounsaturated fatty acid fraction, but unchanged PUFA, likely reflecting the well described enhanced hepatic de novo lipogenesis (DNL) occurring in NAFLD. Taken together, these data show that NAFLD is characterised by a reduced absolute content of PUFA and PL within HDL, and allows us to speculate that an impaired PUFA transport from peripheral tissues to the liver (via FFA and HDL) might probably be a contributing factor in the pathophysiology of NAFLD.



Simplified representation of the hypothesised mechanistic pathway by which reduced PUFA HDL might contribute to the established depletion of hepatic PUFA observed in the NAFLD spectrum.

4.2 Introduction

NAFLD is a continuum of diseases ranging from simple steatosis (intrahepatic fat deposition), to steatohepatitis (steatosis in the presence of inflammation) (NASH), fibrosis, and cirrhosis, which can ultimately evolve to hepatocellular carcinoma (HCC) (Vacca et al, 2015). NAFLD has reached pandemic proportions with a global prevalence of 24%, thus being a public health priority (Younossi et al, 2016). Of note, the leading cause of death in these patients is CVD, with a mechanism not entirely understood (Targher et al, 2020). NAFLD is often associated with mixed dyslipidaemia (low HDL-C, and increased VLDL-TG), which partly explain the elevated CVD risk (Targher et al, 2020). A deeper understanding of the lipid derangements observed in this condition is being revealed by lipidomic studies (Musso et al, 2018). Specifically, hepatic lipidomic studies have coherently reported a lipid remodelling alongside the NAFLD spectrum, which is characterised by elevated levels of saturated fatty acids (SFA) and reduced levels of polyunsaturated fatty acids (PUFA). For example, Araya et al. first reported a depletion in PUFA within the liver (total lipids alongside the TG fraction) in NAFLD compared to non-NAFLD subjects (Araya et al, 2004). Chiappini et al. also reported reduced total hepatic PUFA in NASH patients when compared to controls. Additionally, they reported a decrease in phospholipids (PL) [(i.e phosphatidylcholines (PC) and phosphatidylethanolamines (PE)], sphingomyelins (SM) but not ceramides (Cer) in NASH compared to controls (Chiappini et al, 2017). Moreover, Allard et al. found a depletion of total hepatic PUFA in NASH patients compared to controls, despite a similar dietary intake among the groups (Allard et al, 2008). The latter study suggested that the PUFA depletion observed in NASH patients was attributable to a dysfunctional FA metabolism rather than a nutritional deficiency per se. AT, the major provider of FA to the liver (Donnelly et al, 2005), might be partly responsible for these changes. However, AT FA pool is mostly derived from the FA released by the lipolysis of VLDL and chylomicron TG. These events render thus difficult to trace the flux of lipids among organs and the extent to which AT influences the liver and vice versa. Moreover, in humans, DNL in AT is quantitatively less responsive than liver DNL after glucose infusion (Diraison et al, 2003). Overall, in human AT, DNL contributes for a minimal part of the total AT TG pool (Morigny et al, 2021). It should be noted that the in vivo study of AT in humans has been hampered

by the complexity of directly labelling pathway precursors in AT coupled with the slow AT turnover (years) (Arner et al, 2011).

A mechanism by which hepatic PUFA are depleted in NAFLD has been partly attributed to a decreased activity of the enzyme fatty acid desaturase 1 (Araya et al, 2004; Chiappini et al, 2017). However, others have found no changes (Allard et al, 2008) or increased activity of FADS1 in NAFLD (Lopez-Vicario et al, 2014). This pathway is thus still debated.

Because of the risks and cost associated with liver biopsy procedures, the search for non-invasive alternatives such as blood samples (serum/plasma) to study lipid metabolism in NAFLD has been increasingly investigated. Compared to healthy controls, NAFLD patients display increased level of SFA and MUFA and reduced PUFA in the TG fraction of the whole plasma (Mayo et al, 2018; Sanders et al, 2018; Yang et al, 2017; Zhou et al, 2016), which has been explained by the enhanced DNL characterising this condition. However, apart from these findings, whole plasma lipidomic studies have reported conflicting results regarding the other lipid classes (Capel et al, 2020; Tiwari-Heckler et al, 2018; Zhou et al, 2016). Because these lipids are found in HDL and LDL, they are consequently less directly related to the hepatic metabolism and thus more challenging to interpret (if not studied as isolated fractions).

Several factors might contribute to the discrepancies observed in the circulating lipidome of NAFLD patients. Some of them include the differences in inclusion criteria such as presence of dyslipidaemia, elevated blood pressure, sex, different ethnicity, and lack of studies investigating isolated lipoproteins (lipoprotein lipidomics). Among these factors, I believe that the information obtained by the study of lipoprotein lipidomics could be more informative as compared to whole serum lipidomics, and thus helping us to better understand the lipid remodelling which occurs in NAFLD.

This chapter aims to investigate the quantitative and qualitative lipidomic changes occurring in patients across the NAFLD spectrum, and whether these changes can be explained by changes in lipoprotein abundance and composition. Specifically, the aim of this chapter is to understand whether lipidomics of specific lipoprotein fractions can provide a better biological matrix to investigate the lipid remodelling occurring in the liver of NAFLD subjects. For this purpose, I employed state-of-the-art mass spectrometry lipidomics to profile whole serum and the lipoprotein fractions (HDL and

VLDL) obtained through fast protein liquid chromatography in healthy and biopsy-confirmed NAFLD participants.

4.3 Methods

4.3.1 Ethics and the BioNASH study cohort

89 patients with a biopsy-proven NAFLD (patients with alternate diagnoses and aetiologies and kidney dysfunction were excluded), and 20 healthy volunteers were involved in this study. Patients were recruited at the NASH Service at the Cambridge University Hospital, whereas healthy volunteers were recruited amongst members of the NIHR Cambridge BioResource (<http://www.cambridgebioresource.org.uk>), at the NHS Blood and Transplant Unit, Cambridge, UK. The recruitment of NAFLD patients was approved by the local Ethics Committee, whereas healthy volunteers' recruitment was approved by the NHS Research Ethics Committees (REC 12/EE/0040). The biopsy was scored by an experienced liver pathologist for steatosis (0-3), ballooning (0-2), inflammation (0-2), and fibrosis (0-4) and were classified according to the SAF system (Bedossa et al, 2012), whereas the healthy controls were selected according to the non-invasive score proposed by Kotronen et al. (Kotronen et al, 2009a) since liver biopsy can only be performed when clinically required. The study protocols followed the principles of the Declaration of Helsinki and all participants gave written informed consent.

4.3.2 Sample collection and clinical biochemistry measurements

Serum was collected in healthy and NAFLD participants for the assessment of standard clinical biochemistry tests. Serum was separated by centrifugation and stored at -80 °C. Details of the clinical measurements are described in Chapter 2 Materials and Methods (section 2.1).

4.3.3 Measurement of lipid levels by mass spectrometry

Lipid extraction and their measurements through liquid chromatography coupled with mass spectrometry are reported in Chapter 2 Materials and Methods (section 2.2).

4.3.4 Measurement of ApoA1

ApoA1 of HDL fractions was measured by liquid chromatography coupled with mass spectrometry and details are reported in Chapter 2 Materials and Methods (section 2.3). In addition to the use of a specific internal standard per lipid class, ApoA1 was used to normalise the lipidomic data of HDL.

4.3.5 Measurement of ApoB

ApoB of VLDL fractions was measured in duplicates using a commercially available ELISA kit (Abcam, Cambridge, UK) following the manufacturer's instructions. Measurements were obtained using a plate reader Tecan Infinite 200 PRO (Tecan, Mannedorf, Switzerland). In addition to the use of a specific internal standard per lipid class, ApoB was used to normalise the lipidomic data of VLDL.

4.3.6 Statistics

Data are shown as mean \pm standard deviation unless otherwise specified. Normality was visually assessed from plots of the data (skewness/kurtosis) obtained with the `lm` function in R, and logarithmic transformations were applied to non-normally distributed data. Comparisons of clinical data between healthy and NAFLD patients were assessed using ANOVA. Regarding categorical variables, a chi-square test was adopted. Whole serum lipidomic data were analysed using three-way ANOVA controlling for sex, presence of diabetes mellitus (T2DM) and interaction between sex, T2DM and disease state, with a P-value <0.05 considered significant. However, when lipids were investigated as independent hits, multiple testing correction (Benjamini-Hochberg procedure to control the False Discovery Rate (FDR)) was applied as specified in the legend to tables. Lipoprotein lipidomics data, where participants were only males, were analysed using two-way ANOVA controlling for presence of T2DM and the interaction between disease state and T2DM, with a P-value <0.05 considered significant. As with whole serum, when lipids were considered as an independent unit, FDR was reported along with the raw P-value. To assess the power of the of this study, whole serum and lipoprotein lipidomics, I performed a PostHoc power analyses by assessing first the effect size with the following freely available tool: <https://webpower.psychstat.org/models/means03/effectsize.php>, while the power was

assessed with G*power software (<https://www.psychologie.hhu.de/arbeitsgruppen/allgemeine-psychologie-und-arbeitspsychologie/gpower>). Variables with an effect size (f) below 0.3 (whole serum) and 0.5 (lipoproteins) fell below an acceptable power level of 0.7, therefore being potentially exposed to type 2 error. All the significant variables had a power above the optimal power of 0.8. Univariate correlations were carried out using the Pearson correlation coefficient, with P-value <0.01 considered significant. Statistical analysis was performed with R version 4.0.0 and Microsoft Excel 2016. Graphs were obtained using R version 4.0.0 and Graph Pad (Graph Pad Prism 7.0).

4.4 Results

4.4.1 Clinical characteristics and whole serum lipidomic profile of healthy and NAFLD patients

This study involved 109 participants, including 20 healthy volunteers (age and sex-matched), 36 patients with NAFL, 31 patients with mild NASH, and 22 patients with NASH with moderate/advanced fibrosis (Supplementary Table 1). As expected, the patients in the NAFLD spectrum displayed a significantly higher BMI, impaired glucose metabolism (HOMA2-IR, insulin, and glucose), and mixed dyslipidaemia (elevated TG and decreased HDL-C), along with elevated liver enzymes (ALT, AST), while LDL and total cholesterol were not significantly different across the groups (Supplementary Table 1).

Lipids were analysed as total lipid class (sum of each lipid measured), and according to their acyl chain saturation levels (saturated, monounsaturated and polyunsaturated), as imbalances in the FA saturation levels have been involved in the pathophysiology of NAFLD.

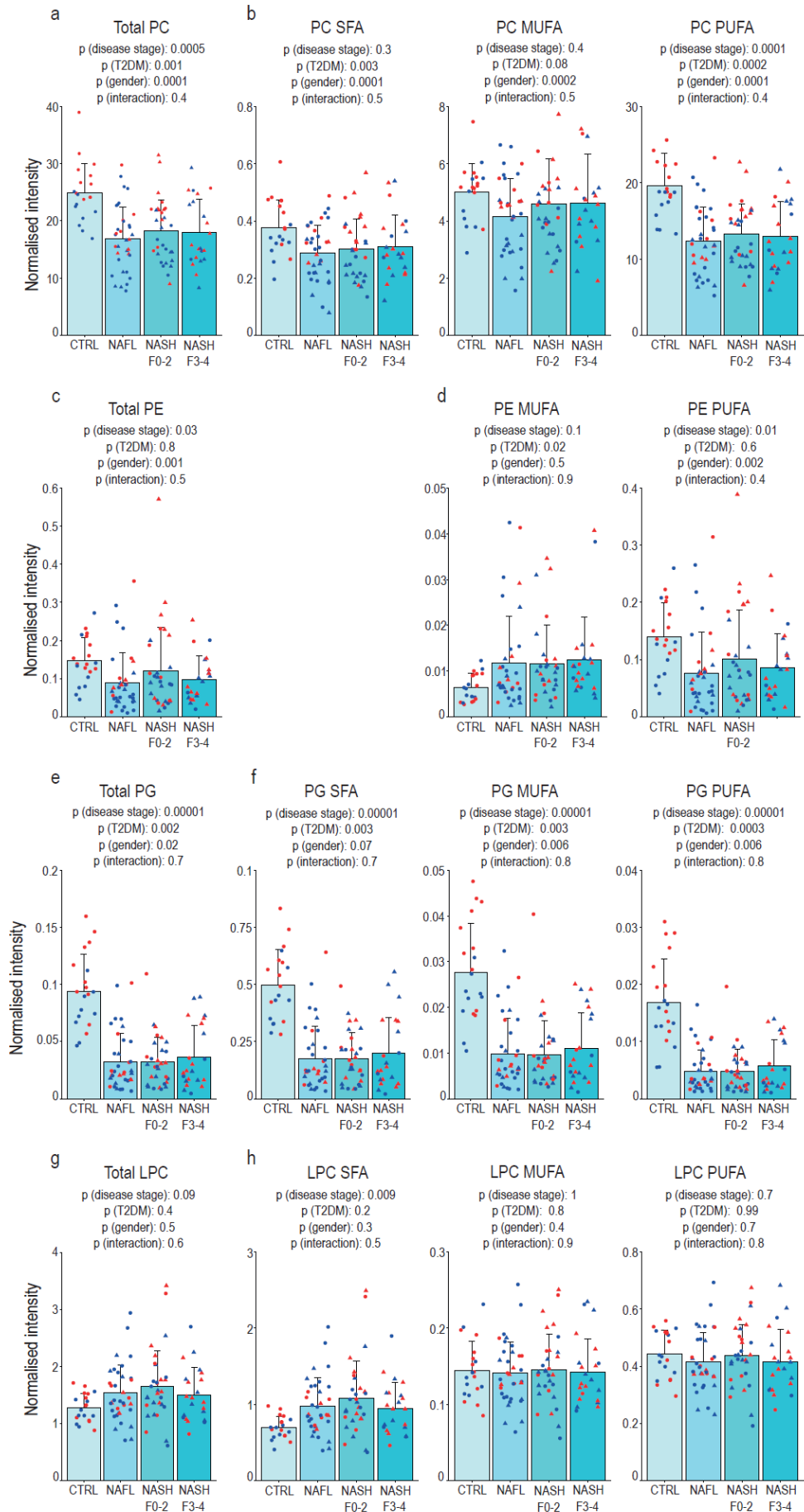
The whole serum lipidomic analysis revealed a quantitative and qualitative depletion of several phospholipid classes [phosphatidylcholines (PC), phosphatidylethanolamines (PE), phosphatidylglycerols (PG)] in the NAFLD group as compared to the controls (Figure 1a-e). The total reduction of PC and PE were mainly driven by the depletion of their PUFA component, while PG were markedly reduced irrespectively of their acyl chain saturation levels (Figure 1b,d,f). Furthermore, I observed a significant sex and T2DM effect on most of the PL measured (Figure 1), this being in line with the differences in the lipoprotein metabolism among men and women alongside the presence of diabetes. Within the lysophosphatidylcholines (LPC), the only significant change observed was in the saturated fraction, which increased in NAFLD compared to controls (Figure 1 g,h), whereas within the lysophosphatidylethanolamines (LPE), only the MUFA content was significantly changed, which was reduced in NAFLD compared to controls (Figure 1i,j). The sphingolipids sphingomyelins (SM) and ceramides (Cer) did not show significant differences between NAFLD and controls (Figure 1 k-n). Of note both lipids were characterised by a significant sex effect. Several observational studies have reported sex differences in circulating ceramides, with females showing higher ceramide levels

than males (Bui et al, 2012; Hammad et al, 2010; Mielke et al, 2015). Difference in sex but lack of interaction is in line with a previous human study assessing the mid- to late-life trajectories of plasma ceramide levels (Mielke et al, 2015). While the mechanism of these differences have not been fully elucidated, differences in sex hormones have been suggested as putative mediators of sphingolipid metabolism in rodent studies (Muralidharan et al, 2021; Norheim et al, 2018).

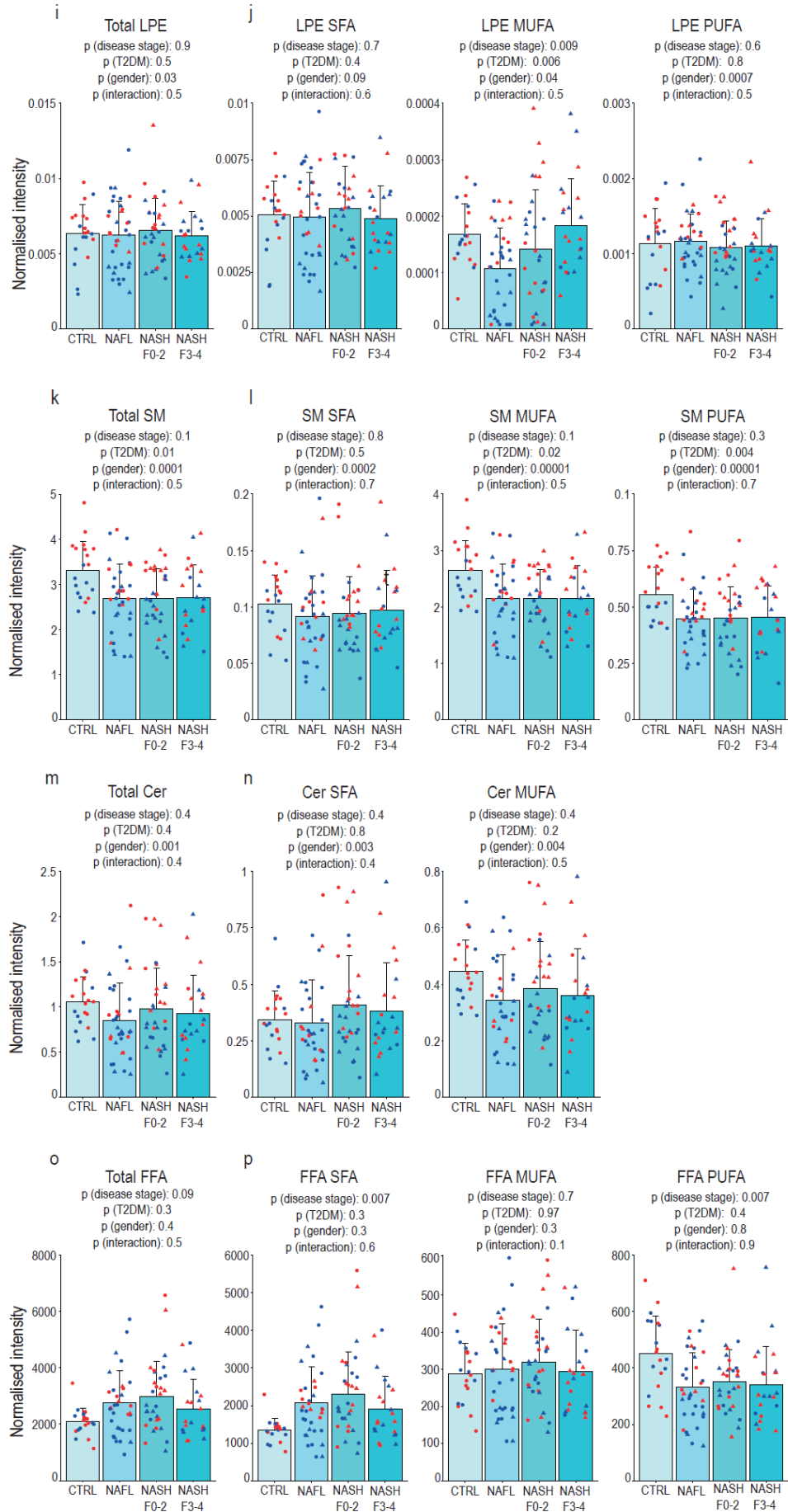
While between NAFLD and controls total free fatty acids (FFA) and LC-MS measured total triglycerides (TG) were not significantly different, when compared to controls, NAFLD subjects showed a marked increase in saturated FFA and TG, coupled with a depletion in polyunsaturated FFA and TG (Figure 1 o,p, q,r). Lastly, to better understand the extent to which lipidomic data related to metabolic parameters, I correlated the significantly changed lipids with key clinical data (Figure 2). Pearson correlation analysis showed that PG (total, SFA, MUFA, PUFA) had the strongest inverse correlation with obesity and insulin resistance, whereas SFA from LPC and FFA were positively correlated with HOMA-IR (Figure 2). Moreover, most of the lipids significantly reduced in the NAFLD groups were also positively correlated with HDL-C (Figure 2).

Taken together, these data show that in NAFLD, the whole serum lipidome is depleted of PL, predominantly PUFA containing PL, in keeping with previous hepatic lipidomic studies, and suggest that there might be a close relationship between IR, HDL-C, and the circulating lipidome. However, this type of whole serum lipidomic studies leave unresolved which is the main lipoprotein acting as a driver of the observed changes: these results can be justified either by a reduced liver export of PUFA-PL through VLDL, or by a reduced PUFA-PL transport from peripheral tissues to the liver via HDL. I therefore investigated further this paradigm by separating the lipoprotein fractions HDL and VLDL and then performing lipidomic analyses.

● Male, no T2D ▲ Male, T2D
● Female, no T2D ▲ Female, T2D



● Male, no T2D ▲ Male, T2D
● Female, no T2D ▲ Female, T2D



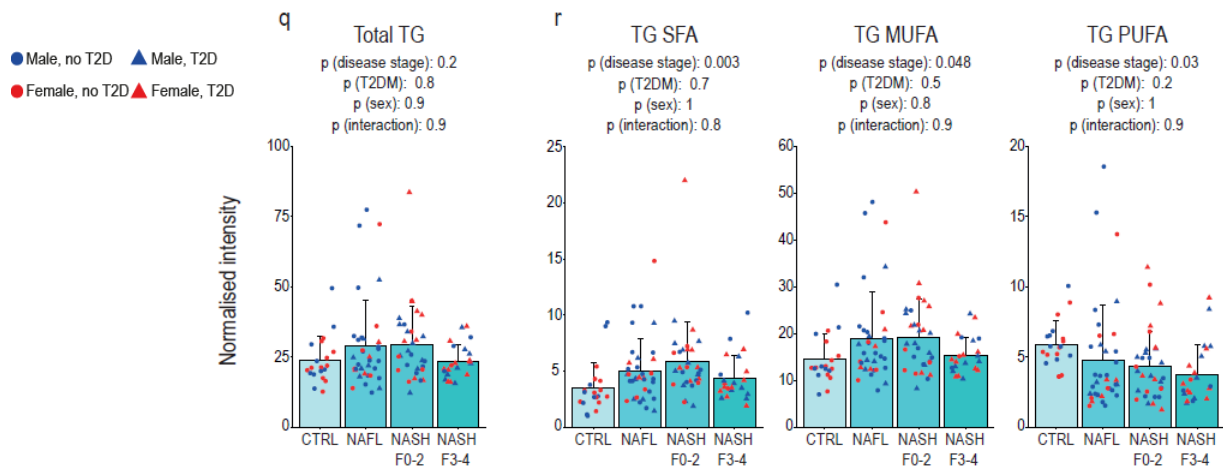


Figure 1. Whole serum lipidomic signature of NAFLD. (a,b) PC, (c,d) PE, (e,f) PG, were reduced across the NAFLD spectrum. (g,h) LPC were qualitatively increased, and (i,j) LPE qualitatively reduced in NAFLD compared to controls. (k-n) SM and Cer were unchanged and (o,p,q,r) FFA and TG showed increased SFA, MUFA, and reduced PUFA as compared to controls. All lipid species were analysed by LC-MS. Statistical significance was assessed using three-way ANOVA controlling for sex, presence of T2DM and interaction between sex, T2DM and disease state, with a P-value <0.05 considered significant. Data are mean \pm standard deviation. In Supplementary Table 3 are reported the specific lipid species analysed highlighting whether they were considered saturated, monounsaturated and polyunsaturated.

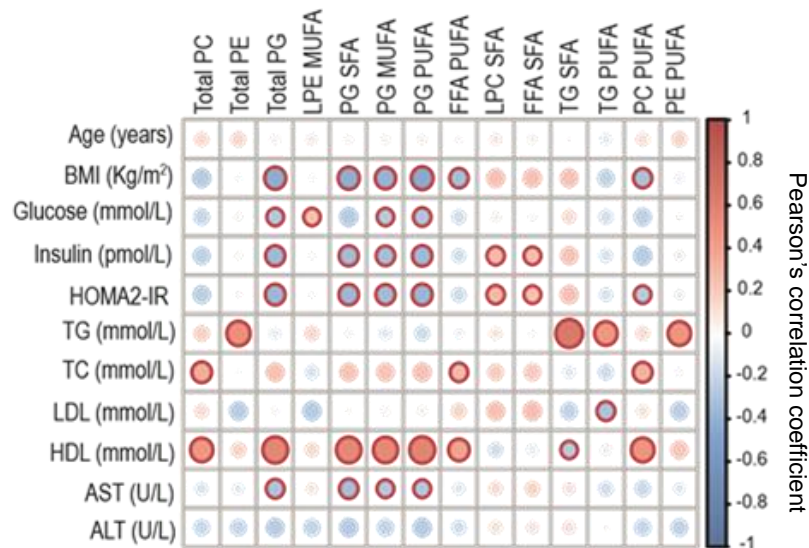


Figure 2. Heatmap of a correlation matrix, Pearson's correlation coefficient, among significantly changed lipid species and clinical data in NAFLD and healthy controls. Data are plotted based on whether they are positively (red) or negatively (blue) correlated, with a red circle highlighting the significant correlation with a p-value <0.01.

4.4.2 HDL lipidomics of NAFLD patients suggest a reduced reverse PUFA transport from peripheral tissues to the liver

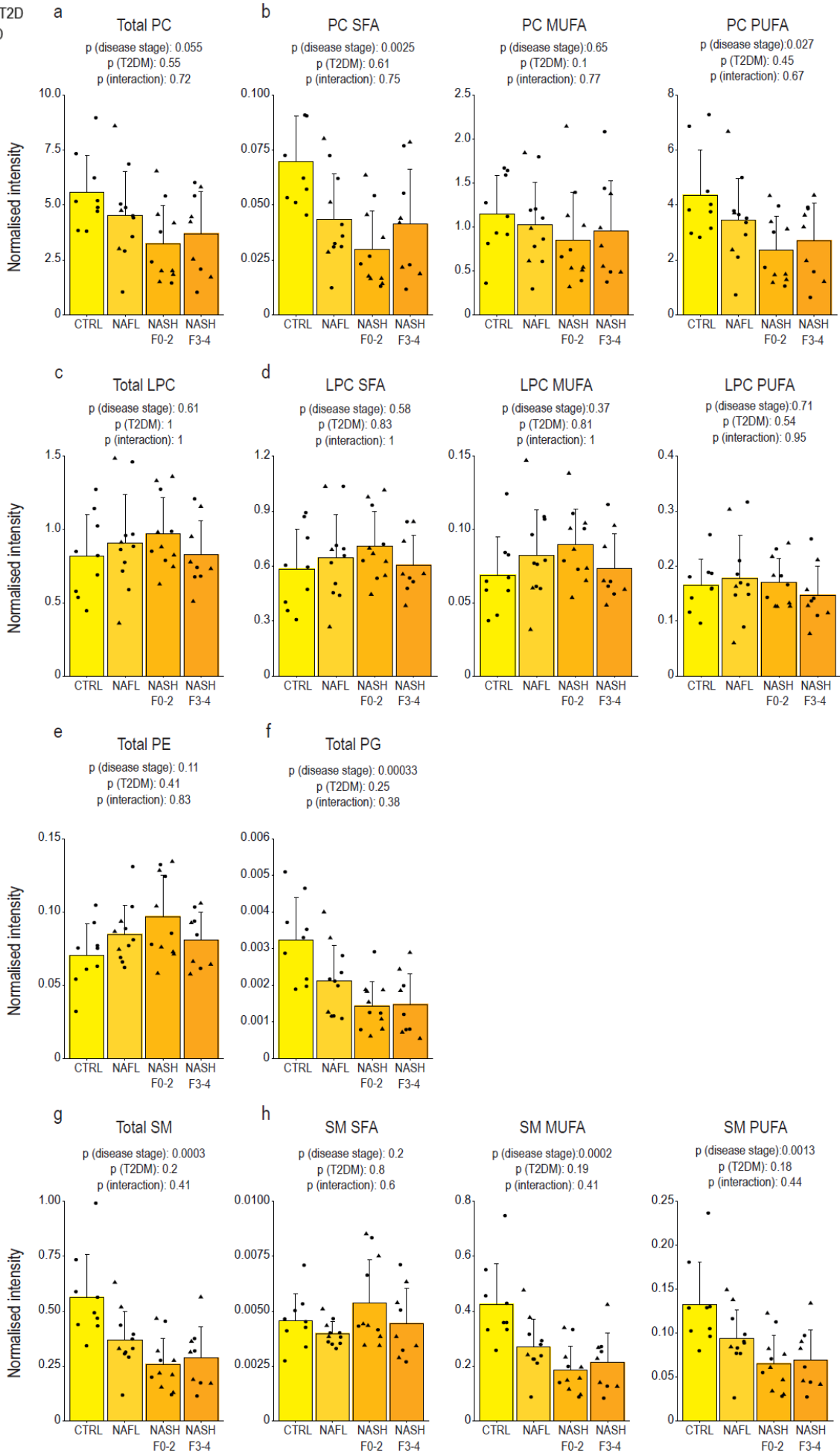
The strong correlation observed between whole serum lipidomics and HDL-C suggested a potential key role of HDL particles in carrying less PL and PUFA from

peripheral tissues to the liver. To confirm this observation, I isolated HDL and studied their lipidome from a subpopulation of our cohort, which included 40 age-matched males distributed as follows: 9 healthy, 11 NAFL, 11 mild NASH, and 9 NASH with moderate/advanced fibrosis (Supplementary Table 2). The lipoprotein lipidomics was performed on a smaller subgroup because of the reduced time available in the lab due to the lockdown related with the COVID-19 pandemic. I particularly focused on male participants to reduce the variability attributable to sex differences. Because NAFLD patients were characterised by low HDL-C levels as compared to controls, it was reasonable to assume that HDL lipoproteins were reduced in the NAFLD group and so would be the other lipids since cholesterol account for ~40% of total lipids within HDL. To account for this difference, the lipidomic data of the HDL fractions, after the internal standard lipid normalisation, were further normalised for the ApoA-I abundance (Supplementary Figure 1), since the latter is the most abundant protein found within HDL particles, accounting for ~70% of its protein content (Dominiczak & Caslake, 2011). In light of these considerations, the further normalisation for ApoA-I was considered a reasonable way to overcome the issue related to different levels of HDL-C. Of note, it has been shown that after a meal, HDL temporarily increases its ApoA-I levels (Averill et al, 2020; Burnap et al, 2021) without changing its total mass. In this scenario, a normalisation for total protein content, providing albumin is depleted from the HDL fraction, would provide a much better normalisation matrix.

Compared to controls, the HDL lipidomic profile of NAFLD patients was characterised by decreased PC levels, mainly driven by their PUFA content (Figure 3 a,b). These results suggested, after lipid normalisation (absolute values) to Apo1, that the HDL fractions showed reduced PUFA-PC. Reduced PC and, especially their PUFA content, have been reported in peripheral tissues of IR obese patients: peripheral tissues including AT provide lipids such as PL to HDL (Borkman et al, 1993; Ferrara et al, 2021; Pietilainen et al, 2011). LPC and PE did not show significant changes between the groups, while total PG were dramatically reduced in NAFLD patients (Figure 3 c-f). PG represent a minor component of the HDL lipidome, however, it can influence the HDL cholesterol efflux capacity (Camont et al, 2013). Furthermore, when compared with controls, the NAFLD group showed a reduced total SM (mostly MUFA and PUFA), increased levels of SFA Cer, and no changes in the TG fraction (Figure 3 g-l). Within the HDL-TG, it is worth noticing how the NASH F2-3 behave differently from the previous stages (being closer to control). This has been previously shown by

others (in whole serum) and attributable to lower functionality of the liver in advanced stages of NASH (Guerra et al, 2021). Moreover, this is also supported at gene expression levels (i.e. gene related with lipid synthesis) performed on liver biopsies of a cohort of NASH patients partially overlapping with this one (Azzu et al, 2021). Reduced SM levels have also been associated with a decreased HDL efflux capacity (Sano et al, 2007), while increased HDL Cer have been less investigated. The liver is the main site of synthesis of Cer, and they have been found increased in liver of patients with NAFLD (Samuel & Shulman, 2018), my data suggest that HDL might also be contributing to this increase. Surprisingly, T2DM did not show a significant effect in any of the lipids studied within the HDL fraction, this suggesting that the changes observed were mainly driven by the NAFLD state. To further assess the extent to which the HDL lipidome related with metabolic parameters, I correlated the significantly changed lipids between NAFLD and healthy controls with key clinical metabolic data (Figure 4). Pearson correlation analysis showed that the lipid species significantly reduced in the NAFLD group were negatively correlated with insulin resistance and, within these species, (Total, MUFA, and PUFA) SM having the strongest correlation; on the other hand, SFA Cer had an opposite trend (Figure 4). Furthermore, the latter was also positively correlated with liver enzymes, with AST showing the strongest correlation (Figure 4). In summary, these data show that independently of the low HDL-C levels, in NAFLD, HDL is characterised by reduced PUFA PL and increased SFA Cer levels and that IR is intimately related to these changes. The fact that the liver largely reuses HDL-derived PL either incorporating them into membranes or converting them into different lipid classes has been previously suggested with tracer experiments (van der Veen et al, 2012): my observational results show in real-life data from HDL from patients with NAFLD, that the HDL lipidome carries the hepatic lipidomic signatures previously described in NAFLD patients, thus pointing at HDL composition as a partial contributor in the pathogenesis of NAFLD. Together with the more studied FFA, HDL might therefore be a largely understudied but equally important player in the “reverse (phospho)lipid transport” from peripheral organs able to influence liver function and pathophysiology in hepatic metabolic diseases.

● No T2D
▲ T2D



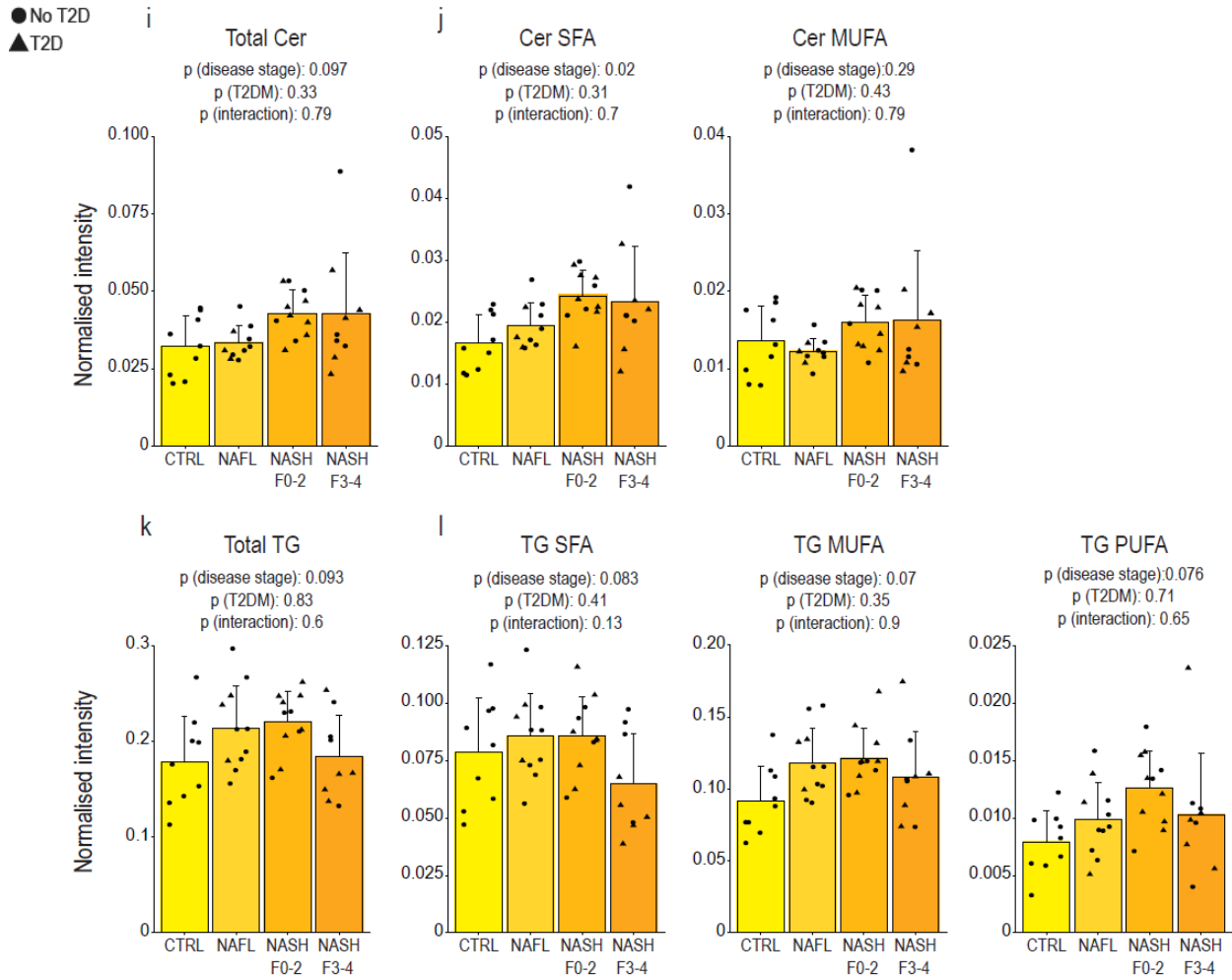


Figure 3. HDL lipidomic signature of NAFLD. (a,b) PC were reduced in NAFLD as compared to controls while (c,d,e) LPC and PE did not show any changes. (f,g,h) PG and SM were reduced across the NAFLD spectrum, whereas (i,j) Cer increased qualitatively and no changes were observed among the (k,l) TG. All lipid species were analysed by LC-MS and normalised to its internal standard as with whole serum, in addition to the ApoA-I concentration (Supplementary Figure 1). Statistical significance was assessed using two-way ANOVA controlling for presence of T2DM and interaction between T2DM and disease state, with a P-value <0.05 considered significant. Data are mean \pm standard deviation. In Supplementary Table 4 are reported the specific lipid species analysed within the HDL fraction.

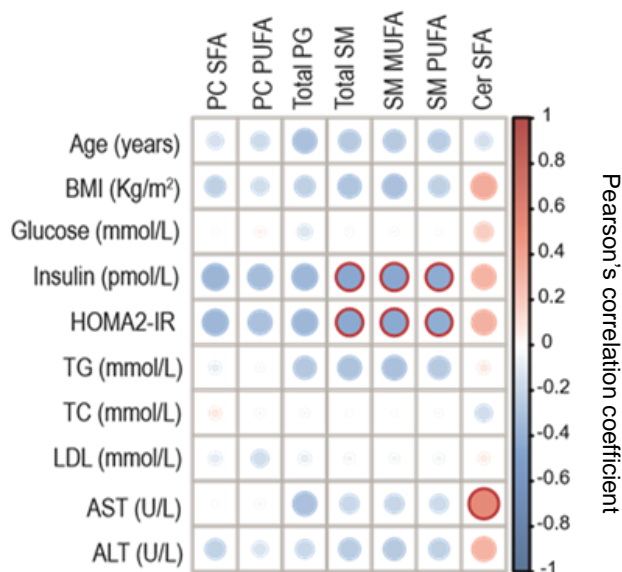


Figure 4. HDL heatmap correlation matrix, Pearson's correlation coefficient, among significantly changed lipid species and clinical data in NAFLD and healthy controls. Data are plotted based on whether they are positively (red) or negatively (blue) correlated, with a red circle highlighting the significant correlation with a p-value <0.01.

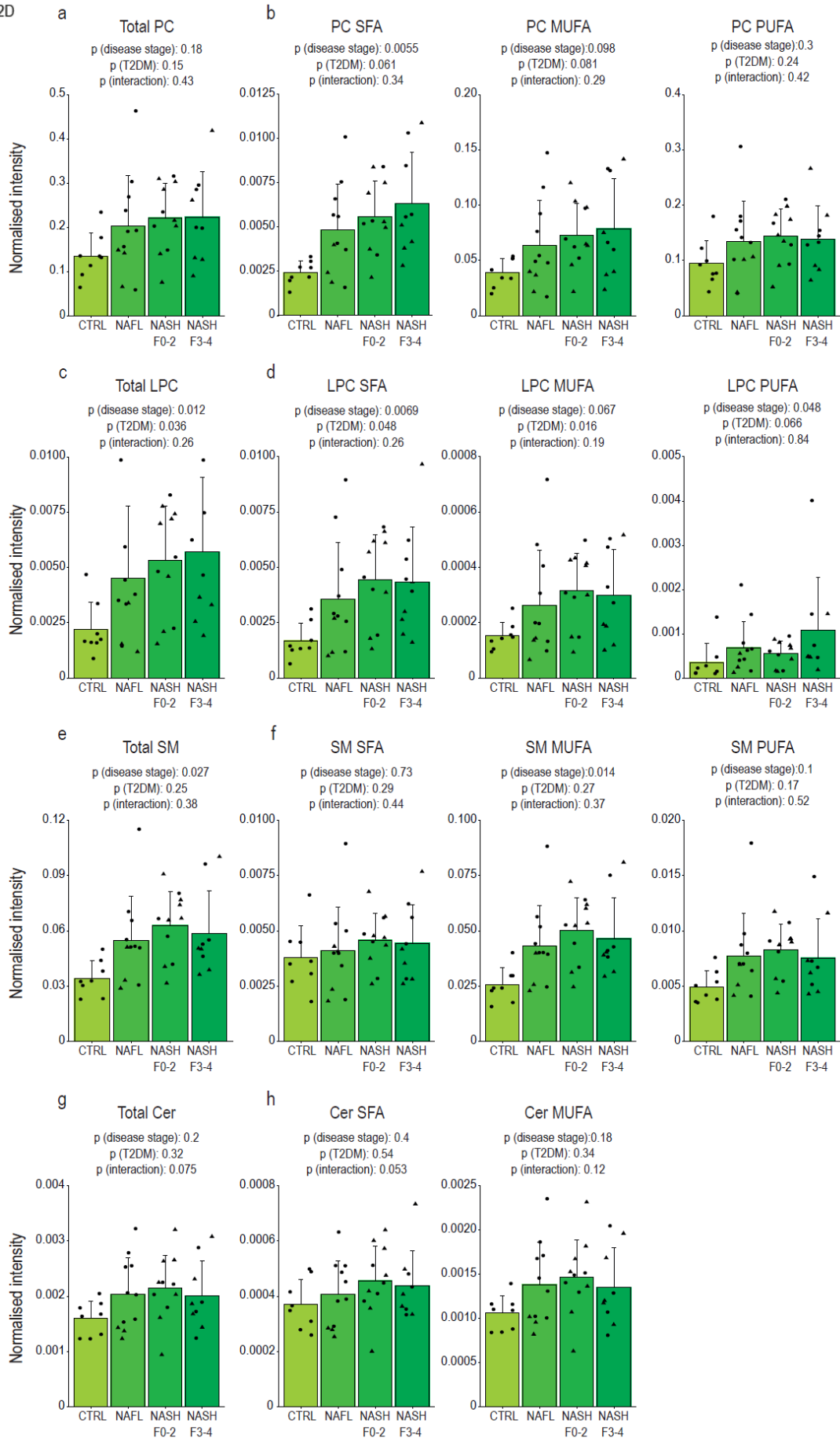
4.4.3 VLDL lipidomics of NAFLD patients shows an enhanced SFA export from the liver to peripheral tissues

VLDL fractions are an important biological matrix for the study of liver diseases because of their intimate connection with this organ. While the remodelling of the VLDL-TG has been widely investigated, less is known about other major lipid classes. In an attempt to fill this gap, I analysed the lipidomic profile of separated VLDL fractions belonging to the sub-cohort described above (Supplementary Table 2). As compared to controls, NAFLD patients showed a generalised increase in PC, which reached significance only for the SFA fraction (Figure 5a,b), whereas total LPC were markedly increased, mostly driven by their SFA content (Figure 5c,d). Moreover, the NAFLD group showed increased levels of total SM, driven by their MUFA content, and no significant differences were observed among the Cer (Figure 5e-h). With regards to TG, the most striking results were observed in their PUFA content which were depleted in the NAFLD as compared to controls (Figure 5i-j). The presence of T2DM had a significant effect only on the LPC fraction, whereas none of the analyses performed showed a significant interaction between disease state and T2DM (Figure 5). To further study the association between clinical data and significantly changed VLDL lipids (NAFLD vs controls), I performed a correlation analysis. Specifically, Pearson

correlation showed that among all the selected lipids, the strongest association was with circulating liver enzymes, particularly AST, which was positive for all lipids except for the PUFA TG (inversely correlated) (Figure 6). These data indicate that the VLDL lipidome was strongly related to hepatocyte cytotoxicity more than with markers of metabolic impairment; however, the lack of fibrosis-associated changes in the data tempts me to speculate that the reshaping of hepatocytes metatabolic programs in NAFLD might not be a sole and sufficient driver of liver disease progression.

Also, most of the changes observed in VLDL were due to SFA-containing lipids, which is in line with the increased arrival to the liver of saturated FFA, alongside the enhanced DNL characterising NAFLD (Donnelly et al, 2005). Taken together these data show that, in NAFLD, VLDL are crucial contributors of the SFA and MUFA plasma pool within several lipids classes while having a minimal role, except for the TG, in the observed PUFA depletion that cannot be only interpreted as a sole consequence of the relative increase of DNL-like products. My data therefore point to the fact that the reduced circulating lipidome described in the whole serum lipidomics of NAFLD patients results from a combination of events driven by both HDL (PUFA-PL) and hepatic secretion of VLDL (PUFA-TG).

● No T2D
▲ T2D



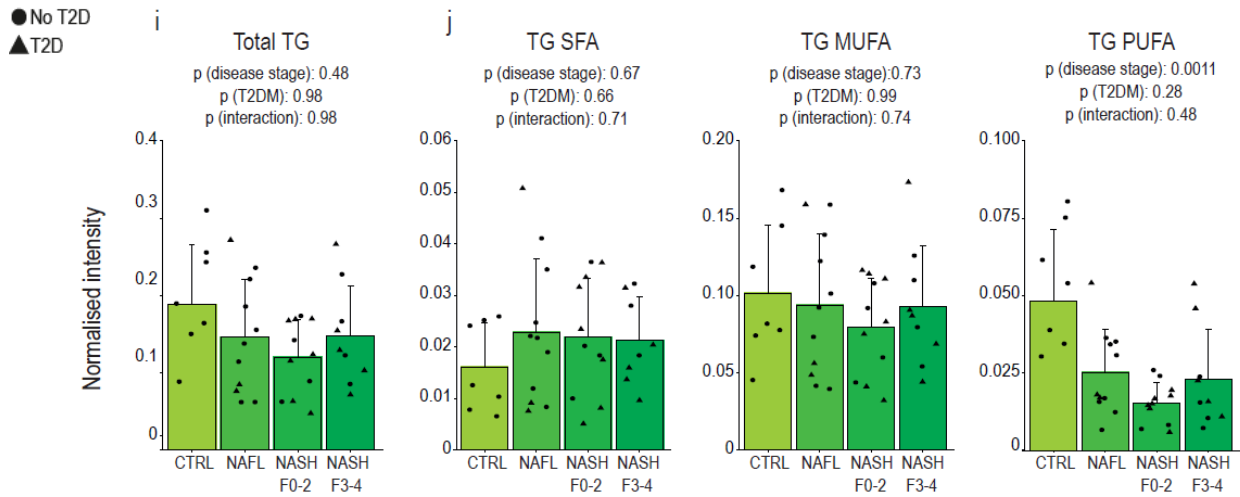


Figure 5. VLDL lipidomic signature of NAFLD. (a,b,c,d,e,f) PC, LPC and SM showed both a quantitative and qualitative generalised increase in NAFLD as compared to controls. (g,h) Cer were not significantly changed whereas (i,j) TG were qualitatively depleted in the NAFLD as compared to controls. All lipid species were analysed by LC-MS and normalised to its internal standard as with whole serum, in addition to the ApoB-100 concentration (Supplementary Figure 2). Statistical significance was assessed using two-way ANOVA controlling for presence of T2DM and interaction between T2DM and disease state, with a P-value <0.05 considered significant. Data are mean \pm standard deviation. In Supplementary Table 5 are reported the specific lipid species analysed within the VLDL fraction.

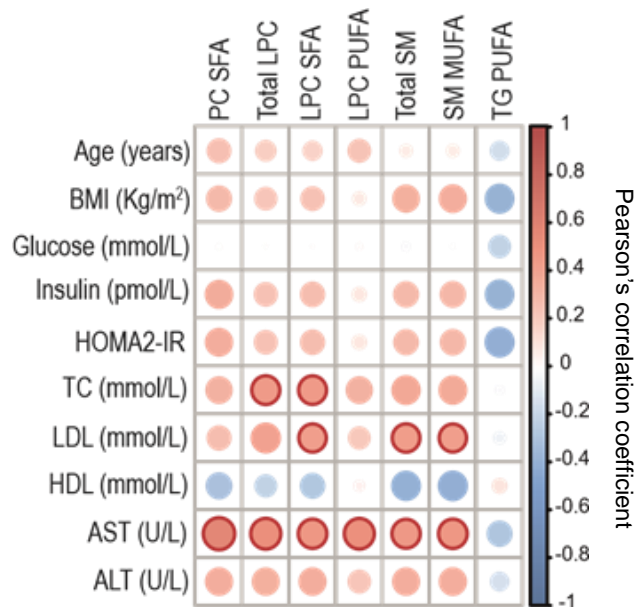


Figure 6. VLDL heatmap correlation matrix, Pearson's correlation coefficient, among significantly changed lipid species and clinical data in NAFLD and healthy controls. Data are plotted based on whether they are positively (red) or negatively (blue) correlated, with a red circle highlighting the significant correlation with a p-value <0.01.

4.4.4 Discussion

The liver is a key player in regulating lipoprotein metabolism. The latter is due to the liver's role in VLDL, LDL, and HDL synthesis and clearance. An imbalance between the influx and efflux of these particles is considered crucial in the pathogenesis of NAFLD (Donnelly et al, 2005).

Different studies have coherently reported a hepatic lipidomic signature of NAFLD (Araya et al, 2004; Chiappini et al, 2017; Musso et al, 2018). On the other hand, whole serum lipidomic studies have produced conflicting results, often discordant with the liver findings (Mannisto et al, 2019; Puri et al, 2009). Discrepant findings have indeed been reported even among major lipidomic classes: For instance, in morbidly obese women with NASH, Anjani et al. found elevated levels of PC, PE, and PG when compared to healthy females (Anjani et al, 2015). Likewise, increased levels of PC and SM in NAFL and NASH compared to healthy subjects were reported by Tiwari-Heckler et al. (Tiwari-Heckler et al, 2018). On the other hand, Zhou et al. reported reduced levels of PC and LPC in NALF and NASH compared to controls (Zhou et al, 2016). In line with the previous findings, decreased levels of LPC in NAFLD compared to controls were also reported by Oresic et al. (Oresic et al, 2013). Increased levels of SM in NAFL and NASH compared to controls have been reported by some authors (Tiwari-Heckler et al, 2018), while others found no significant changes (Anjani et al, 2015) or reduced levels (Zhou et al, 2016). It is therefore clear that the current approaches to investigate the circulating lipidome requires different strategies to find a unifying signature of plasma NAFLD.

Mass-spectrometry-based lipoprotein lipidomics of NAFLD has mainly focused on VLDL (Boon et al, 2013; Carlier et al, 2020; Kotronen et al, 2009b), with limited information regarding the other lipoprotein fractions. In this chapter, I first described the whole serum lipidomic features of NAFLD compared to healthy controls. The latter showed that NAFLD is characterised by a depletion in PL (PC, PE, PG) and specifically in their PUFA fraction. Moreover, NAFLD patients had increased saturated and decreased polyunsaturated FFA. Circulating FFA are released by the AT, and elevated levels of FFA have been attributed to AT-IR-driven enhanced lipolysis (Azzu et al, 2020). Elevated FFA play a major role in the onset and development of NAFLD (Bevilacqua et al, 1987; Lomonaco et al, 2012). The FFA changes observed in serum are broadly in line with the results previously observed in liver biopsies (Chiappini et

al, 2017; Puri et al, 2007) and previous literature in whole serum lipidomics (de Almeida et al, 2002; Feng et al, 2017; Gambino et al, 2016) despite the reduction of polyunsaturated FFA is a debated finding (de Almeida et al, 2002; Feng et al, 2017; Gambino et al, 2016). It is worth mentioning that the view of obesity as a driver for elevated FFA due to increased lipolysis in AT has however been challenged by recent re-evaluation of the literature (Hodson & Karpe, 2019; Karpe et al, 2011). A closer look at the matter suggests that obese people have reduced lipolysis per unit of fat mass, so when normalising FFA release per body fat, obese people show reduced lipolysis. In this view, the conflicting literature on FFA changes might be due to the different inclusion criteria among studies.

While the mechanism by which our NAFLD cohort displayed reduced polyunsaturated FFA levels is not inferable from our data, the reduced PUFA TG in VLDL suggests a strong cross-talk between liver and AT. I think that the discrepant results also previously reported in whole lipidome studies for complex lipids are due, at least in part, to the fact that the whole serum lipidome provides averaged information of lipoproteins concentration and composition varying according to disease state, dietary habits, fasting/fed states, sex and many other factors (Ding & Rexrode, 2020; Kontush et al, 2013). I therefore wonder, if as it happens for cholesterol, where the different biological significance of its concentration in VLDL/LDL and HDL is differentially studied, this approach should also be used for other lipid classes.

Since NAFLD liver biopsies are depleted in PUFA in multiple lipid classes (Kartsoli et al, 2020), and I observed a generalised PUFA reduction in the whole serum, I sought to understand whether whole serum levels were reflecting “hepatic input”, i.e. lipids deriving from peripheral tissues via HDL to the liver, or “output”, i.e. liver VLDL export. To better understand these changes, I employed FPLC to isolate HDL and VLDL fractions, where I then performed LC-MS lipidomic analyses. HDL lipidome showed a generalised reduction in PC and PUFA across different lipid classes. These changes have shown to affect HDL’s functionality as decreased PC levels in reconstituted HDL (in vitro experiments) have been associated with reduced cholesterol efflux capacity, thus rendering these particles potentially less atheroprotective (Jebari-Benslaiman et al, 2020; Schwendeman et al, 2015). Moreover, the lipid profile of these HDL are in line with reduced PL and PUFA content of peripheral tissues, such as skeletal muscles and AT (both providing lipids to HDL), of obese and IR patients (Borkman et al, 1993; Ferrara et al, 2021; Pietilainen et al, 2011). These findings are particularly relevant as

they highlight an often overlooked role of HDL in NAFLD, which is its transport of lipids from peripheral tissues to the liver beyond its cholesterol content (van der Veen et al, 2012). Indeed, much attention has been given to reverse cholesterol transport but not to HDL PL content and function, despite the elevated content of PL within HDL (Kontush et al, 2013). This chapter therefore introduces the new paradigm that HDL, whose PL content has been mainly studied with regards to consequences in HDL physical properties, might be also acting as carriers of a “reverse phospholipid transport” from periphery to the liver.

This concept emphasises the impaired lipid inter-organ cross-talk occurring in IR and NAFLD and might be of help to better understand the pathophysiology of NAFLD.

Lastly, to investigate the role of the liver to the circulating lipidome, I studied the isolated VLDL lipidome. In this regard, I observed, a different trend in the different lipid classes. Indeed, as compared to control, NAFLD’s VLDL were enriched in PC and SM (mostly driven by their SFA and MUFA content while their PUFA levels were unchanged). Of note, while the contribution of the DNL, FFA, and dietary fat to VLDL TG has been investigated, their contribution to the synthesis of other lipids (i.e PL and sphingolipids) is not currently established. Although some studies have investigated the VLDL lipidome of obese and IR subjects, there is very little information on the biological role of these changes in the pathophysiology of IR, NAFLD and on lipoprotein functions (Boon et al, 2013; Carlier et al, 2020; Kotronen et al, 2009b). These results align with the increased SFA arrival to the liver from FFA and the already described enhanced DNL in NAFLD (de Almeida et al, 2002; Donnelly et al, 2005; Puri et al, 2007; Sanders et al, 2018). However, the extent to which de novo vs. peripheral lipid recycling contribute to the PL and other lipid classes remodelling in NAFLD has not been systematically investigated yet. Previous studies suggested that HDL PL can be used to build up membranes and/or disassembled to use FA which were esterified into TG (van der Veen et al, 2012). This hypothesis is really fascinating and I am tempted to speculate that the reduced PUFA-TG pool could be, at least in part, influenced by reduced transport of polyunsaturated FFA and HDL PUFA PL to the liver. However, this hypothesis requires further validation with stable isotopes approaches.

In conclusion, by using mass-spectrometry-based lipidomics, this chapter suggests that NAFLD is characterised by an impaired reverse PL/PUFA transport (via FFA and

HDL) from peripheral tissues to the liver that, in turn exports mainly SFA and MUFA enriched lipids through VLDL. More studies are needed to understand the metabolic basis of this observation in terms of hepatic lipid fluxes, which of the two events is cause or consequence, and the pathophysiological consequences of these altered lipid fluxes in NAFLD progression.

4.4.5 Limitations

The findings in this chapter are subject to different limitations. First, as an exploratory analysis, I used data from the highest number of available participants and no formal sample size calculation was performed. This implies that results must be interpreted with caution. Second, the observational nature of the study does not allow to draw causality among the changes observed. Third, I could only see differences among healthy and diseased participants without being able to distinguish patients according to disease severity. Fourth, variables not significantly different because of low effect size should be interpreted with caution because of the risk of false negatives due to the low power. Lastly, our study described a real-life cohort where medications such as statins and metformin were not used as exclusion criteria. The latter medications were present in the NAFLD spectrum but not in the controls, thus potentially further confounding our results of circulating lipidome (data on medication were only present for a subset of patients, thus rendering a further sub-analysis more complex due to smaller numbers). These results thus warrant further confirmations in cohorts where patients are not medically treated.

Supplementary materials

	Healthy controls n = 20	NAFL n = 36	NASH n = 31	NASH Fibrosis n = 22	P
Gender (M/F)	9/11	25/11	17/14	11/11	NS
Age (years)	54 ± 13	54 ± 12	55 ± 11	60 ± 9	NS
BMI (Kg/m ²)	25.1 ± 4.2	31.4 ± 3.5 ^a	33.9 ± 5.9 ^a	31.6 ± 3.8 ^a	<0.001
Glucose (mmol/L)	4.8 ± 0.7	5.9 ± 2.2	6.8 ± 2 ^{ab}	7.3 ± 1.7 ^{ab}	<0.001
Insulin (pmol/L)	37.8 ± 20	100.7 ± 45 ^a	143.9 ± 91.2 ^a	132.6 ± 66.7 ^a	<0.001
HOMA2-IR	0.7 ± 0.3	1.9 ± 0.8 ^a	2.8 ± 1.7 ^a	2.6 ± 1.3 ^a	<0.001
TG (mmol/L)	1.1 ± 0.4	1.7 ± 0.8	1.8 ± 0.7 ^a	1.3 ± 0.5	<0.001
TC (mmol/L)	4.8 ± 0.8	4.6 ± 1.4	4.4 ± 0.9	4.2 ± 0.9	NS
LDL-C (mmol/L)	2.7 ± 0.6	2.8 ± 1.3	2.6 ± 0.9	2.6 ± 0.8	NS
HDL-C (mmol/L)	1.6 ± 0.5	1 ± 0.3 ^a	1 ± 0.2 ^a	1 ± 0.3 ^a	<0.001
AST (IU/L)	22 ± 5	37 ± 20 ^a	47 ± 29 ^a	54 ± 25 ^a	<0.001
ALT (IU/L)	31 ± 10	63 ± 38 ^a	64 ± 29 ^a	71 ± 32 ^a	<0.001
Diabetes, n (%)	0	11 (31)	18 (58)	17 (77)	<0.001
Statin, n (%)	0	11 (45)	9 (34)	11 (68)	<0.001
Metformin, n (%)	0	7 (43)	10 (59)	11 (85)	<0.001

Supplementary Table 1. Clinical characteristics of the BIONASH cohort. Data are mean ± SD and n (%). Statistical tests are ANOVA-test, followed by Bonferroni correction and Pearson χ^2 test, as appropriate. M = Male, F = Female, BMI = Body Mass Index, HOMA2-IR = Homeostasis Model Assessment 2 of Insulin Resistance, TG = Triglycerides, TC = Total Cholesterol, HDL-C = High-density lipoprotein cholesterol, LDL-C = Low-density lipoprotein cholesterol, AST = Aspartate aminotransaminase, ALT = Alanine aminotransaminase. “a” means different from “healthy controls”, “b” means different from “NAFL”.

	Healthy controls n = 9	NAFL n = 11	NASH n = 11	NASH Fibrosis n = 9	P
Age (years)	47 ± 12	49 ± 12	52 ± 14	60 ± 10	NS
BMI (Kg/m ²)	25.3 ± 2.6	30.2 ± 2.5 ^a	31.8 ± 4.1 ^a	30.2 ± 3.1 ^a	0.0004
Glucose (mmol/L)	5 ± 0.7	5.7 ± 0.7 ^a	6.7 ± 2 ^a	6.5 ± 1.6 ^a	0.03
Insulin (pmol/L)	41.8 ± 20.5	97 ± 38.1 ^a	102.9 ± 44.7 ^a	118.4 ± 57 ^a	0.002
HOMA2-IR	0.8 ± 0.3	1.8 ± 0.7 ^a	2 ± 0.9 ^a	2.2 ± 0.9 ^a	0.0007
TG (mmol/L)	1.1 ± 0.6	1.6 ± 0.7	1.6 ± 0.6	1.5 ± 0.5	NS
TC (mmol/L)	4.6 ± 0.7	3.9 ± 1.1	4.2 ± 0.6	4.2 ± 0.9	NS
LDL-C (mmol/L)	2.8 ± 0.5	2.2 ± 1	2.5 ± 0.9	2.5 ± 1	NS
HDL-C (mmol/L)	1.3 ± 0.3	1 ± 0.2	0.9 ± 0.2 ^a	1 ± 0.4	0.007
AST (IU/L)	23 ± 7	37 ± 12	51 ± 37	62 ± 27 ^a	0.01
ALT (IU/L)	38 ± 10	72 ± 37 ^a	64 ± 35	89 ± 36 ^a	0.05
Diabetes, n (%)	0	3 (25)	7 (58)	5 (56)	0.01
Statin, n (%)	0	5 (55)	3 (30)	5 (70)	0.02
Metformin, n (%)	0	1 (12.5)	4 (66.7)	4 (66.7)	0.01

Supplementary Table 2. Clinical characteristics of the BIONASH sub-cohort. Data are mean ± SD and n (%). Statistical tests are ANOVA-test, followed by Bonferroni correction and Pearson χ^2 test, as appropriate. BMI = Body Mass Index, HOMA2-IR = Homeostasis Model Assessment 2 of Insulin Resistance, TG = Triglycerides, TC = Total Cholesterol, HDL-C = High-density lipoprotein cholesterol, LDL-C = Low-density lipoprotein cholesterol, AST = Aspartate aminotransaminase, ALT = Alanine aminotransaminase. “a” means different from “healthy controls”.

Supplementary Table 3. Average value for lipid species in the whole serum of Healthy and NAFLD participants (all stages grouped together). Lipids classified as saturated are not highlighted, lipids classified as monounsaturated are highlighted in yellow while lipids classified as polyunsaturated are highlighted in green.

Whole serum lipidome	Average normalised peak intensity - Healthy	Average normalised peak intensity - NAFLD	p value	FDR
PG 36 0	0.014748201	0.005179818	4.22158E-10	6.54345E-08
LPC 18 0	0.171692782	0.30997664	8.07312E-10	6.25667E-08
FA 18 0	379.2858021	682.6838731	1.46962E-09	7.59305E-08
PC 40 3	0.014297539	0.0067915	5.75396E-09	2.22966E-07
PC 40 4	0.056544391	0.031717683	1.02056E-08	3.16372E-07
SM 36 0	0.011812975	0.020500518	3.8519E-08	9.95073E-07
LPC 20 3	0.053765111	0.0806669	4.30925E-08	9.54191E-07
PG 34 0	0.034846243	0.012994663	6.72028E-08	1.30205E-06
PC 36 3	2.137494094	1.415853174	2.14785E-07	3.69907E-06
FA 16 0	942.9547552	1394.123296	2.5921E-07	4.01776E-06
Cer 36 0	0.008456599	0.019749949	3.75514E-07	5.29134E-06
PG 36 1	0.02765252	0.010054597	3.78198E-07	4.88506E-06
PG 36 2	0.016776836	0.004994688	9.7554E-07	1.16314E-05
LPE 18 0	0.000359174	0.000570023	1.38961E-06	1.53849E-05
PC 40 5	0.118727491	0.071905907	1.82108E-06	1.88178E-05
LPC 20 5	0.046482622	0.028819538	2.26199E-06	2.1913E-05
LPC 16 0	0.4996007	0.672453364	2.43387E-06	2.21912E-05
PC 37 4	0.032959614	0.015358542	2.51935E-06	2.16944E-05
PC 38 4	1.295007127	0.916974658	5.09316E-06	4.15495E-05
PC 38 6	1.359269863	0.591195805	7.29985E-06	5.65738E-05
PC 36 4	2.12967252	1.375102926	1.00297E-05	7.4029E-05
PC 34 2	6.811594223	4.581828431	1.48476E-05	0.000104608
PC 40 7	0.003904402	0.002694416	2.79448E-05	0.000188323
PC 37 2	0.016597678	0.008354148	2.89966E-05	0.00018727
LPC 18 2	0.143743901	0.08905674	3.88665E-05	0.000240973
TG 56 7	0.384708987	0.146362584	5.55915E-05	0.000331411
TG 56 6	0.329124615	0.176450535	6.51753E-05	0.000374154
PC 40 6	0.352494449	0.185670388	6.63943E-05	0.00036754
PC 40 2	0.001762744	0.000958538	7.12518E-05	0.000380828
PC 35 2	0.179878633	0.098529668	8.17349E-05	0.000422297
TG 58 7	0.048293371	0.015221884	9.4929E-05	0.000474645
TG 54 2	0.471921768	0.673406027	0.000121986	0.000590872
LPC 18 3	0.130961449	0.159659379	0.000126492	0.000594129
SM 34 1	1.701129358	1.316848081	0.000135461	0.000617541
PC 34 0	0.047653084	0.03458482	0.000136753	0.000605619
SM 33 5	1.829952174	1.414013775	0.000139817	0.000601989
TG 58 9	0.058068907	0.01495279	0.000155005	0.000649346
PC 36 2	3.678560323	2.610111306	0.0001606	0.000655079
PC 34 3	0.356582789	0.233711842	0.000190129	0.00075564
TG 58 8	0.08240187	0.018608729	0.000252734	0.000979344
SM 40 2	0.298696337	0.223489711	0.00026105	0.000986895

PC 38 5	0.352628075	0.166031886	0.000300813	0.001110142
SM 34 0	0.075556586	0.055711834	0.000370318	0.001334866
PC 35 1	0.082458649	0.055512795	0.000392795	0.001383711
FA 18 2	329.6861672	215.5474681	0.000548402	0.00188894
TG 54 5	1.059217064	0.715614653	0.000652886	0.002199942
PC 33 2	0.05846998	0.033434261	0.000706675	0.002330525
PC 38 2	0.055368122	0.039913992	0.000800529	0.002585042
PE 36 2	0.000375027	0.006689366	0.000925772	0.002928462
PE 38 6	0.042240911	0.021048568	0.000958848	0.00297243
TG 54 6	0.507911836	0.295730154	0.000973446	0.002958513
TG 52 1	0.487064832	0.763458754	0.001213994	0.003618635
SM 39 1	0.062874069	0.043825517	0.002229345	0.006519781
TG 50 1	1.621117601	2.442823402	0.002311435	0.006634675
TG 55 4	0.010164041	0.007456292	0.002504056	0.007056885
SM 38 4	1.014174888	0.8327084	0.002672551	0.00739724
PE 36 4	0.029040167	0.017546235	0.002993897	0.0081413
PC 32 0	0.258742029	0.210212061	0.003120848	0.008340198
PC 33 0	0.018504835	0.012530957	0.003549836	0.009325841
SM 35 1	0.042782193	0.033584709	0.004581632	0.011835882
SM 38 2	0.077144951	0.064668715	0.005029367	0.012779538
PC 35 0	0.001093739	0.000703513	0.005422184	0.013555461
TG 53 4	0.078399038	0.058923079	0.006028379	0.014831726
Cer 42 1	0.368421738	0.295529379	0.006035074	0.014616195
TG 52 2	4.924785129	6.378896703	0.006708683	0.015997628
SM 35 2	0.00905709	0.006859068	0.007603464	0.017856619
TG 55 1	0.011231395	0.01594091	0.007886216	0.018244231
TG 50 2	2.162033725	3.037472134	0.010370271	0.023638119
SM 40 1	0.365680519	0.311965229	0.010397079	0.023355758
PE 38 4	0.068963139	0.048708654	0.012544773	0.027777712
SM 36 3	0.002015663	0.001565165	0.012751561	0.027837916
LPE 18 3	0.000100289	0.000142343	0.01570424	0.033807739
PC 32 2	0.047240408	0.033790582	0.01791477	0.03803821
PC 33 1	0.06973977	0.051307991	0.019239685	0.04029934
FA 20 3	23.16625311	28.38401948	0.020478851	0.042322959
PC 31 0	0.018639458	0.012848567	0.021474323	0.043796316
TG 48 1	0.712691074	1.066147329	0.025374494	0.051078528
TG 54 4	1.586045512	1.293319848	0.025820765	0.051310494
SM 40 0	0.006597577	0.008343683	0.026108764	0.051226057
PC 34 1	3.875880386	3.420680493	0.02656267	0.051465174
SM 38 0	0.005011409	0.006210849	0.029640868	0.056720179
TG 46 1	0.197976916	0.299050733	0.030136271	0.056964902
PC 38 3	0.511548876	0.424514255	0.030853664	0.057618288
TG 53 2	0.123605181	0.156476199	0.03157715	0.05826736
TG 51 4	0.043387531	0.033037759	0.033839288	0.061706938
SM 38 0	0.278119378	0.242951991	0.039494924	0.071182711
Cer 38 0	0.019795919	0.025148434	0.04410776	0.078582791
PE 36 1	0.006039451	0.008090838	0.046778831	0.082394532
LPC 20 0	0.000883901	0.001037751	0.050977364	0.088780802

TG 51 1	0.097711733	0.135934903	0.051003672	0.087839658
FA 17 0	18.75606812	23.21320572	0.051186727	0.087186184
LPC 17 1	0.001519162	0.001165227	0.053344317	0.089873578
SM 38 3	0.00037632	0.00055999	0.054060133	0.090100221
TG 52 3	4.16136592	4.890910516	0.057620101	0.095011869
LPC 19 0	0.000736451	0.000880904	0.060349524	0.098465013
LPE 18 1	0.00016746	0.000137501	0.061458795	0.099230346
SM 38 1	0.195680778	0.171537605	0.068750023	0.109858284
SM 33 0	0.001426946	0.001010083	0.112862627	0.178507216
TG 48 2	0.583440119	0.751996778	0.114072625	0.178598555
Cer 40 1	0.076138956	0.066939959	0.115000602	0.178250933
SM 36 2	0.168274169	0.152689324	0.119172875	0.182889065
PC 36 1	0.645693803	0.574379417	0.128152073	0.194740895
TG 51 2	0.257213028	0.319187716	0.130720519	0.196715344
LPC 17 0	0.010530699	0.012240134	0.147281183	0.219505609
TG 55 6	0.001591285	0.001247413	0.150801893	0.222612318
TG 44 1	0.055972231	0.074357854	0.171576459	0.250890105
TG 46 2	0.106103849	0.13505879	0.187510301	0.271627071
TG 49 1	0.136225244	0.171783481	0.224032474	0.321528088
PC 34 4	0.013789747	0.015578987	0.243746934	0.346612612
LPC 20 4	0.053524631	0.050064085	0.248855344	0.350659804
TG 36 0	0.002210239	0.00283418	0.251518342	0.351219307
LPC 22 5	0.002424331	0.002656169	0.268273739	0.371271692
TG 45 2	0.004564572	0.005761857	0.271011196	0.371741021
FA 16 1	23.50909592	25.79354486	0.280760255	0.381735435
FA 20 5	9.716240896	8.380809181	0.304505575	0.410420557
PC 30 0	0.031726939	0.027817631	0.305906705	0.408754649
TG 55 3	0.012260371	0.013568166	0.313309919	0.415068697
FA 20 0	2.023399641	1.7895456	0.319994999	0.420332414
TG 50 3	0.994422187	1.124475927	0.332915581	0.433629539
FA 22 6	21.49378451	20.01904109	0.437775157	0.565459578
SM 36 0	0.466111983	0.448381576	0.485122122	0.621437429
FFA 18 1	265.0450125	279.6138833	0.488633653	0.620805051
SM 36 1	0.284009176	0.273626569	0.51036215	0.643139294
TG 53 3	0.142474067	0.150757901	0.521631262	0.652039078
TG 51 0	0.015856844	0.01483812	0.526995528	0.653474455
TG 45 1	0.008921788	0.010128522	0.555892662	0.683836211
LPE 20 3	0.001036273	0.000976271	0.571096811	0.697007919
LPE 17 0	0.004698619	0.004498117	0.58426526	0.707508713
TG 55 5	0.004808685	0.004519492	0.584745523	0.70260121
LPC 14 0	0.004697222	0.004498589	0.587587657	0.700585283
TG 52 4	1.708569832	1.611895384	0.599481036	0.709309623
TG 47 1	0.039755673	0.044500191	0.600716923	0.705387296
TG 51 3	0.147955213	0.139405562	0.615217102	0.716982337
PG 40 8	7.41952E-05	6.38839E-05	0.6179688	0.714814657
TG 48 3	0.17420052	0.188341371	0.635775514	0.729964479
TG 47 2	0.016519234	0.018034179	0.653110791	0.744354211
TG 48 0	0.083973661	0.089417022	0.671094178	0.759267136

TG 47 0	0.012234878	0.013336855	0.680200471	0.763993283
FA 15 0	7.286185265	7.579770547	0.688512616	0.767765867
Cer 40 0	0.121337589	0.126324167	0.690230699	0.764183988
LPC 18 4	0.003775193	0.003632668	0.707727787	0.777998631
TG 49 2	0.102614755	0.109312505	0.712023805	0.777209083
SM 41 0	0.002207009	0.002132269	0.714596223	0.77456234
LPC 22 6	0.009051539	0.008824695	0.748542917	0.805723279
FA 20 4	67.0786296	68.40998139	0.762806895	0.815414267
LPC 16 1	0.011428513	0.011679651	0.798254515	0.847461985
PC 30 1	0.004854268	0.004649218	0.801534555	0.845155483
TG 49 0	0.010699581	0.01029592	0.822109425	0.860992979
TG 49 3	0.028759009	0.027870656	0.844841365	0.878861823
LPC 18 1	0.131916	0.130171544	0.848305029	0.876581864
Cer 42 0	0.194352039	0.198117391	0.850721456	0.873257123
TG 45 0	0.005677316	0.005998039	0.853520013	0.870365803
LPC 15 0	0.003861245	0.003816067	0.901685994	0.91347274
TG 53 0	0.005240329	0.005176851	0.902781942	0.908644162
PC 32 1	0.328226925	0.329184533	0.981004724	0.981004724

Supplementary Table 4. Average value for lipid species within the HDL fractions of Healthy and NAFLD participants (all stages grouped together).

HDL	Average normalised peak intensity - Healthy	Average normalised peak intensity - NAFLD	P-value	FDR
PC 32 0	0.05085952	0.02769058	0.000410406	0.053763125
SM 38 2	0.014903302	0.00661459	0.001090314	0.071415553
PC 34 0	0.006525886	0.002699913	0.001602173	0.069961541
SM 34 1	0.374719877	0.185130709	0.00253388	0.082984554
SM 42 2	0.064525964	0.035238397	0.002684714	0.070339512
TG 47 2	0.006736223	0.008350617	0.003530756	0.077088181
PC 40 7	0.008322957	0.004108538	0.005373129	0.100554272
PC 37 6	0.00112323	0.000529108	0.006219044	0.10183685
PC 35 2	0.029028764	0.016692424	0.006981667	0.101622041
PC 35 4	0.004018736	0.002291535	0.007575312	0.099236581
PG 34 0	0.001571234	0.000579927	0.008777752	0.104535042
PC 35 3	0.002811492	0.001317773	0.009766183	0.106614163
PC 33 2	0.013372644	0.007879047	0.009988851	0.100656879
PC 38 5	0.176164556	0.091061586	0.011621184	0.108741074
Cer 40 0	0.0002682	0.000438229	0.011913793	0.104047122
PG 40 3	0.000403659	0.000149143	0.016245732	0.133011929
TG 58 7	0.006086781	0.008566875	0.018006103	0.138752908
Cer 48 0	0.00091826	0.001523649	0.020050576	0.145923635
PC 33 0	0.001051196	0.000461825	0.020780006	0.143272674
TG 57 0	0.000697469	0.000898659	0.020825665	0.136408106
PC 38 6	0.209794713	0.123996832	0.020831395	0.129948225
TG 55 4	0.000243245	0.000567363	0.022260658	0.132552099
SM 33 1	0.01057071	0.006482438	0.023960053	0.136468128
TG 55 0	0.001140398	0.001469393	0.024081906	0.131447071
PC 37 3	0.002124625	0.001123846	0.024335873	0.127519973
SM 36 2	0.017858075	0.010028779	0.024436482	0.123122276
TG 56 1	0.001422822	0.001866669	0.02554961	0.123962921
TG 52 1	0.052041468	0.066044327	0.026708773	0.124958903
PC 31 0	0.002873701	0.000988602	0.026921938	0.121612894
PC 37 4	0.004772476	0.002259412	0.030959684	0.13519062
Cer 34 0	0.002496829	0.00375933	0.034072717	0.143984706
TG 55 1	0.000811525	0.001064585	0.03445897	0.14106641
Cer 46 0	0.000869744	0.001592473	0.035023552	0.139032887
SM 35 2	0.000692432	0.000416835	0.03507376	0.135137132
Cer 48 0	0.000462525	0.000753895	0.03751466	0.140412012
PC 36 3	0.468446937	0.272827832	0.037615925	0.13688017
TG 56 0	0.001329916	0.001673076	0.039046567	0.138245954
PC 35 1	0.014485887	0.006535817	0.039158132	0.134992509
PG 40 4	0.000210055	0.000109974	0.039575149	0.132931911
PC 40 4	0.005265963	0.002682494	0.041418015	0.135643998
PE 34 2	0.068024704	0.086362548	0.041747403	0.133388042

PC 34 2	1.848612215	1.095762999	0.043856345	0.136790028
TG 54 1	0.010248092	0.013082273	0.044493144	0.135548881
Cer 38 0	0.002177946	0.002815909	0.044822177	0.133447844
PC 34 1	1.066324225	0.806822323	0.053682771	0.156276513
Cer 47 0	0.000352289	0.000580778	0.053944319	0.153624038
PE 38 6	0.002188674	0.001170495	0.054967785	0.153208081
SM 34 1	0.00030193	0.000143185	0.055103002	0.150385276
TG 45 1	0.005946912	0.00902467	0.057175417	0.152856728
TG 47 1	0.012083555	0.014750736	0.058417672	0.153054301
PC 37 5	0.001463517	0.000451129	0.058682049	0.150732322
SM 36 3	0.00085933	0.000452718	0.059683234	0.150355838
Cer 47 0	0.000742792	0.001127729	0.059761853	0.14771326
PG 40 2	0.001060883	0.000854005	0.061722016	0.149733038
PC 40 6	0.058079051	0.040437512	0.061819915	0.147243798
Cer 45 0	0.000636864	0.001328443	0.062689476	0.146648596
Cer 46 0	0.001560305	0.002571366	0.067665067	0.155510944
PC 33 1	0.010670792	0.00550487	0.072598892	0.163973359
SM 40 1	0.038154012	0.030172651	0.072981884	0.162044521
PC 40 5	0.021481642	0.013801563	0.074462304	0.162576031
PC 36 1	0.123948226	0.076838214	0.082241525	0.176617045
SM 34 2	0.033069178	0.023532713	0.09425912	0.1991604
LPC 20 0	0.002650322	0.002058234	0.094617216	0.196743735
PC 34 3	0.063140735	0.045552233	0.095505434	0.195487685
PC 36 0	0.00203329	0.001086177	0.095990602	0.193457982
Cer 45 0	0.000556893	0.000987656	0.096686469	0.191907992
PC 36 4	0.427986686	0.309426209	0.097197927	0.190043708
SM 30 1	0.001156955	0.001486407	0.097258226	0.187365112
PC 38 3	0.097072817	0.067185527	0.102889526	0.195340984
TG 53 1	0.002658631	0.00318575	0.118204448	0.221211182
TG 45 0	0.00747789	0.009436071	0.122803768	0.2265816
PC 36 2	0.66462548	0.472585073	0.122956756	0.223712987
Cer 44 0	0.000942936	0.001937748	0.126453874	0.226924075
SM 37 2	0.000157081	0.00020828	0.13375016	0.236773932
Cer 46 2	0.000415948	0.000820583	0.159514812	0.278619206
Cer 50 0	0.000331418	0.00053406	0.16019855	0.276131711
PC 39 6	0.000583222	0.000265312	0.174623413	0.297086586
Cer 44 2	0.000614002	0.002040343	0.175799761	0.295253445
Cer 44 1	0.00058102	0.001856446	0.175998605	0.291845788
LPC 16 0	0.271583998	0.340535084	0.176833964	0.289565616
Cer 37 0	0.003350846	0.003906992	0.177119012	0.286451736
Cer 48 1	0.000338548	0.000673484	0.177371262	0.283361406
Cer 47 1	0.000337619	0.000593188	0.180902078	0.285520147
Cer 45 1	0.000424347	0.000936705	0.181339496	0.282803262
Cer 46 1	0.000683785	0.001595733	0.184293277	0.284028462
Cer 42 0	0.000573395	0.001524667	0.187367337	0.285408386
Cer 44 1	0.000907713	0.00251857	0.188233859	0.283432592
PC 38 4	0.307278372	0.251030266	0.194427491	0.289431833
LPC 18 1	0.068863495	0.082299971	0.199065126	0.293005971

Cer 50 2	0.00011764	0.000214472	0.205499604	0.299116091
Cer 38 0	0.00011096	0.000352217	0.218922529	0.315152212
SM 40 0	0.000867028	0.000995811	0.221038585	0.314739724
Cer 38 1	0.000231363	0.000594209	0.233190991	0.328473332
LPC 18 2	0.025584271	0.020252743	0.240767767	0.335538058
Cer 45 1	0.000229777	0.000600876	0.246756046	0.3402636
TG 58 10	0.00158694	0.001808095	0.247698548	0.338005311
PC 30 0	0.005665716	0.0044129	0.24989518	0.337487305
Cer 43 1	0.000199657	0.000769718	0.251326995	0.335957514
Cer 45 2	0.000230362	0.000599635	0.25417787	0.336336374
PC 34 4	0.002902288	0.00219471	0.277265979	0.363218433
Cer 34 1	9.66E-05	0.00060191	0.283405777	0.367585711
Cer 41 2	5.25E-05	0.000267954	0.301482808	0.387198509
TG 47 0	0.015521254	0.017713545	0.317365541	0.403639669
Cer 43 1	0.000816992	0.001430037	0.324614575	0.408889513
Cer 37 1	0.003357093	0.003757293	0.333692808	0.416321504
LPC 18 3	0.058635942	0.06837232	0.333697267	0.412399452
Cer 43 0	0.000272674	0.000647105	0.334489313	0.409514953
Cer 43 2	0.000366229	0.001095554	0.335696666	0.407187623
LPC 17 0	0.008115858	0.009252024	0.337868757	0.406062451
SM 42 0	0.000865978	0.000966307	0.368553471	0.438913679
TG 52 0	0.011744753	0.010090233	0.380963317	0.449605357
PE 34 1	0.000420276	0.000503506	0.391600389	0.458032598
Cer 50 1	0.000232988	0.000350105	0.409336678	0.47454075
PC 30 1	0.00113586	0.001453306	0.429073963	0.493058676
PC 38 2	0.009704364	0.007720001	0.436390973	0.497106239
SM 40 0	0.000599772	0.000531182	0.441948236	0.499096715
LPC 20 4	0.018976849	0.020816203	0.445179159	0.49844846
TG 49 0	0.007797999	0.008680456	0.487472758	0.541177384
LPC 20 3	0.06199402	0.057138466	0.504842927	0.555751458
Cer 39 1	8.42E-05	0.000150757	0.507115275	0.553600842
TG 48 0	0.028411831	0.025552231	0.630091534	0.682165214
Cer 41 1	0.001123668	0.001381184	0.632048507	0.678675036
Cer 42 1	0.003408553	0.003934894	0.689872192	0.734741928
PC 28 0	0.000656556	0.000594263	0.756596046	0.799307114
PC 32 1	0.048536816	0.045397828	0.791463516	0.829453765
TG 53 0	0.001399954	0.001440666	0.795537843	0.827106805
TG 51 0	0.003078209	0.003176127	0.810334644	0.835856995
SM 33 0	0.001930055	0.001961189	0.918122958	0.939641465
LPC 18 0	0.302046828	0.304767406	0.939637594	0.954205619
Cer 40 1	0.000477375	0.000484648	0.961649446	0.969046749
PC 32 2	0.010488942	0.010425302	0.968044067	0.968044067

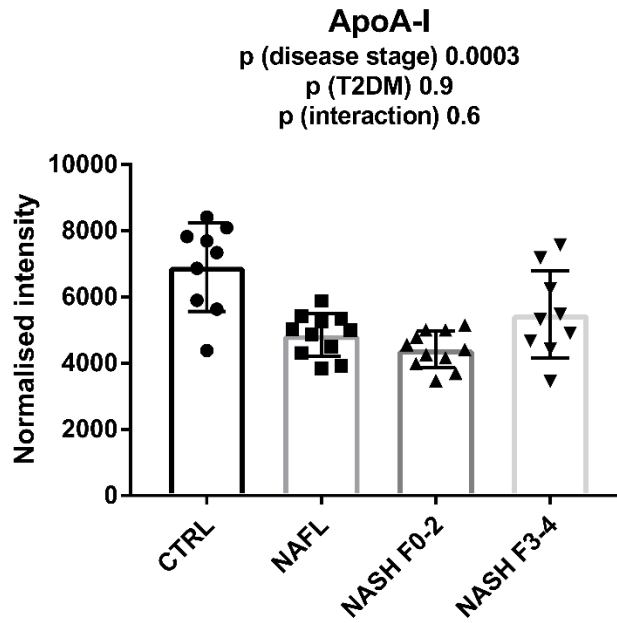
Supplementary Table 5. Average value for lipid species within the VLDL fractions of Healthy and NAFLD participants (all stages grouped together).

VLDL	Average normalised peak intensity - Healthy	Average normalised peak intensity - NAFLD	P-value	FDR
SM 38 0	1.64E-05	5.90E-05	0.000725908	0.103078998
SM 36 0	0.000118311	0.000296425	0.002462228	0.174818164
PC 36 0	0.000120779	0.000299941	0.003337048	0.157953596
PC 32 0	0.002282174	0.00409094	0.005229781	0.185657229
SM 32 0	1.85E-05	3.64E-05	0.007697312	0.218603656
SM 30 1	1.52E-05	3.91E-05	0.009326217	0.220720474
SM 32 1	0.001231918	0.002055163	0.009742023	0.19762389
SM 42 1	0.002200887	0.003664717	0.010568205	0.187585639
PC 34 0	0.000317408	0.000590306	0.011338917	0.178902917
SM 36 1	0.003014769	0.005194076	0.01229138	0.174537595
SM 38 1	0.001865159	0.003201536	0.013756776	0.177587478
TG 54 6	0.007253429	0.001557512	0.015267723	0.180668059
Cer 42 0	3.11E-05	5.46E-05	0.01994314	0.217840451
SM 40 1	0.003280978	0.004872498	0.021782806	0.220939886
TG 54 5	0.010891758	0.003286594	0.022404919	0.212099897
SM 34 1	0.017287935	0.02599398	0.027295636	0.242248767
SM 33 0	0.001355826	0.000339181	0.027486423	0.229592473
TG 56 8	0.0021035	0.000307393	0.028550824	0.225234275
TG 54 4	0.014081464	0.00533033	0.029703566	0.22199507
TG 58 7	0.000711575	0.000195432	0.029835832	0.211834409
SM 35 1	0.000313305	0.00053147	0.036530803	0.24701781
SM 38 2	0.000716539	0.001124055	0.045110114	0.291165282
TG 51 4	0.000518805	0.000173617	0.046419712	0.286591268
SM 44 1	0.000286624	6.04E-05	0.055187822	0.326527948
TG 53 4	0.000656809	0.000261498	0.061595775	0.349864002
Cer 36 0	4.32E-05	5.23E-05	0.062780787	0.342879685
TG 56 3	0.000247314	0.000115154	0.064418784	0.338795086
TG 52 4	0.02094862	0.009924854	0.066712281	0.338326567
TG 58 9	0.000414199	6.12E-05	0.066989418	0.328017149
LPC 16 0	0.000822757	0.001539891	0.074331903	0.351837675
SM 36 3	1.39E-05	2.60E-05	0.074428726	0.340931584
TG 56 6	0.003713296	0.00079967	0.080371001	0.356646319
SM 34 0	0.000563524	0.00082278	0.082301229	0.354144681
Cer 36 1	1.53E-05	2.63E-05	0.08285178	0.346028021
TG 55 5	0.000129901	2.80E-05	0.09244864	0.375077338
Cer 40 0	7.75E-06	1.62E-05	0.09414458	0.371348065
TG 58 10	0.00022681	2.49E-05	0.108574809	0.416692511
TG 51 3	0.001508399	0.000682267	0.110133616	0.411551935
PC 33 0	5.87E-05	9.98E-05	0.112947492	0.411244715
TG 53 3	0.001332957	0.000598287	0.116176495	0.412426557
TG 54 3	0.011789519	0.007093287	0.119602708	0.414233769
TG 52 3	0.04727754	0.025458108	0.123194471	0.41651464

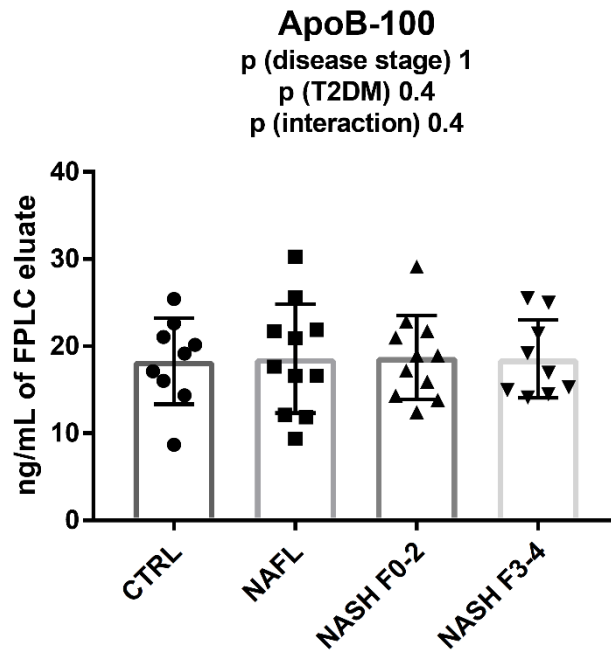
TG 49 3	0.000476086	0.000179315	0.127520985	0.421115811
PC 36 1	0.005654631	0.008234784	0.13276145	0.428457407
TG 47 2	0.000399637	0.00019667	0.146511756	0.462325984
SM 34 2	0.001288182	0.001770359	0.15113638	0.466551434
PC 38 2	0.000370736	0.000528636	0.164290046	0.496365672
TG 55 3	7.32E-05	2.74E-05	0.169947128	0.502760253
TG 51 2	0.002711071	0.001185441	0.173602076	0.503091732
TG 45 1	0.000253797	0.000141791	0.176613851	0.501583338
Cer 46 1	1.47E-05	7.97E-06	0.178000419	0.49560901
LPC 18 1	0.000204534	0.000291911	0.181958627	0.496887021
TG 56 7	0.002701672	0.000607087	0.186193723	0.498858655
TG 49 2	0.001219126	0.000571831	0.186975833	0.491677191
TG 55 4	8.46E-05	2.20E-05	0.188444226	0.48652873
PC 31 0	0.000124441	0.000189325	0.188866165	0.478910633
TG 48 3	0.002606029	0.001093743	0.189321376	0.471642727
TG 46 4	9.36E-05	2.75E-05	0.193701662	0.474235103
Cer 45 1	8.37E-06	5.44E-06	0.194050447	0.467036669
TG 50 3	0.012366626	0.00621292	0.198459254	0.469686901
TG 49 1	0.001577092	0.00066469	0.202455819	0.471290596
SM 36 2	0.000710086	0.001020051	0.210232542	0.481500338
PC 36 2	0.022462112	0.029938416	0.222651821	0.501850137
SM 40 0	0.002141875	0.002697262	0.228044857	0.505974526
PC 30 0	0.000163443	0.000244546	0.229218712	0.500754725
TG 53 2	0.000966699	0.000440526	0.237360521	0.510684758
Cer 47 0	8.20E-06	6.33E-06	0.23850698	0.505492405
TG 47 1	0.000623068	0.000329739	0.243801517	0.509114932
PC 34 1	0.043380747	0.058753576	0.248249666	0.510890617
SM 34 0	1.29E-05	1.80E-05	0.253433724	0.514108412
SM 40 2	0.003211464	0.003926275	0.254049782	0.508099564
PC 38 3	0.003417012	0.004806974	0.264511169	0.521674806
TG 52 2	0.045966498	0.029146265	0.266586926	0.518566349
TG 48 2	0.008406837	0.004188476	0.270296832	0.518677705
TG 53 1	0.00010632	5.48E-05	0.276945135	0.524349456
TG 51 1	0.000888865	0.000376012	0.285535452	0.53350045
TG 46 2	0.001926717	0.000940073	0.288628023	0.532275056
TG 45 2	0.000142335	8.59E-05	0.292791843	0.533031304
Cer 46 0	1.48E-05	1.06E-05	0.292966201	0.526597475
TG 50 0	0.001294721	0.000748263	0.297469409	0.5280082
Cer 48 0	1.54E-05	1.08E-05	0.305400444	0.535393371
Cer 47 1	4.76E-06	2.94E-06	0.30955713	0.536062348
TG 50 2	0.025864674	0.014963728	0.310040655	0.530431
PC 30 1	3.62E-05	5.28E-05	0.318600618	0.538586759
PC 32 2	0.000262703	0.000344008	0.329245018	0.550032853
TG 56 2	8.23E-05	5.62E-05	0.338395283	0.5587457
SM 40 0	0.000137659	7.67E-05	0.34051691	0.555786221
TG 44 1	0.00110792	0.000582715	0.34755793	0.560832114
TG 46 1	0.003223549	0.001700473	0.348255493	0.555643596
TG 48 0	0.003183064	0.00208503	0.34861262	0.550033245

Cer 42 1	0.000408799	0.000521489	0.352211975	0.5496055
LPC 18 2	3.48E-05	4.67E-05	0.382033288	0.589660075
TG 48 1	0.009331883	0.005341443	0.38292265	0.584677594
Cer 44 0	1.72E-05	1.30E-05	0.383658506	0.579569232
Cer 38 1	1.46E-05	1.94E-05	0.404152063	0.604100978
SM 35 2	3.14E-05	3.87E-05	0.406492636	0.601270358
TG 54 2	0.002740124	0.002026569	0.411315337	0.602131731
Cer 42 0	5.46E-05	7.15E-05	0.422114427	0.61163519
TG 50 1	0.016634978	0.011168324	0.445998603	0.639715168
SM 37 2	1.29E-05	1.68E-05	0.456267902	0.647900421
LPC 17 0	2.20E-05	3.27E-05	0.478494018	0.672734164
TG 52 1	0.003693083	0.002434799	0.479390481	0.667386748
Cer 40 1	0.000102664	0.000130243	0.480834756	0.662898402
PC 38 6	0.004243898	0.003277305	0.482727466	0.659108655
PC 38 5	0.001515105	0.001098437	0.484330202	0.65499894
LPC 18 0	0.001939338	0.002520599	0.497906314	0.667006571
PC 32 1	0.002266018	0.002929076	0.501122582	0.665041184
LPC 18 3	0.000217798	0.000300851	0.562226283	0.739223446
Cer 45 0	5.72E-06	4.70E-06	0.566192448	0.73760851
PC 37 3	8.77E-05	7.24E-05	0.58449671	0.754532116
TG 54 1	0.000228347	0.000182819	0.589935329	0.754692042
PC 40 5	0.000634337	0.00050541	0.592426974	0.751112771
Cer 41 1	0.000118245	0.000138361	0.596826607	0.749994497
PC 35 1	0.000589558	0.000693357	0.602699645	0.750731137
Cer 37 0	0.000122097	0.00011145	0.606448142	0.748831619
Cer 43 1	6.68E-05	7.45E-05	0.611576216	0.748653643
Cer 37 1	0.000121854	0.000111452	0.614018663	0.745219232
Cer 39 1	7.88E-06	9.53E-06	0.615933145	0.741207682
PC 34 2	0.052485566	0.059834824	0.630243515	0.752055287
Cer 44 1	3.31E-05	2.94E-05	0.642375872	0.760144782
PC 33 2	0.000267724	0.000297702	0.691534383	0.811552747
LPC 20 4	7.55E-05	8.45E-05	0.749745875	0.872655035
PC 37 2	4.13E-05	3.60E-05	0.764644898	0.882760777
PC 40 4	0.000216256	0.000181847	0.767755297	0.879203646
Cer 47 0	2.59E-06	2.26E-06	0.793408132	0.901311638
PC 36 4	0.011704723	0.010650792	0.794283663	0.895145081
Cer 38 0	5.59E-05	5.79E-05	0.802063052	0.896794909
SM 33 1	0.000920576	0.000960887	0.808104388	0.896490806
Cer 35 1	0.000338189	0.000325308	0.812418315	0.894289928
PC 40 6	0.001801183	0.00167113	0.823975417	0.900034686
TG 61 12	2.53E-05	2.71E-05	0.834277463	0.904331295
LPC 20 3	0.000356414	0.000319264	0.869336661	0.935195499
PC 36 3	0.012801294	0.012351956	0.903062197	0.964171669
PC 33 1	0.000415532	0.000433378	0.923070797	0.978179501
Cer 41 0	8.83E-06	9.11E-06	0.92870562	0.976860726
PC 34 3	0.001637708	0.001590517	0.939706352	0.981163985
Cer 43 0	8.75E-06	8.60E-06	0.956174461	0.991071339
Cer 48 0	4.15E-06	4.08E-06	0.968987409	0.997074

PC 38 4	0.00976357	0.009819216	0.98540401	1.006671722
PC 35 2	0.001074877	0.001077542	0.991660455	1.005827033
PC 40 7	0.000493895	0.000492985	0.996335056	1.003401262
PC 34 4	0.000127041	0.000127335	0.997301532	0.997301532



Supplementary figure 1. HDL ApoA-I levels in healthy and NAFLD participants. ApoA-I levels were significantly reduced within isolated HDL fractions of NAFLD patients compared to controls independently from the presence of type 2 diabetes mellitus (T2DM). ApoA-I was analysed by LC-MS and normalised to bovine serum albumin as detailed in the method section. Statistical significance was assessed using two-way ANOVA controlling for presence of T2DM and interaction between T2DM and disease state, with a P-value <0.05 considered significant. Data are mean \pm standard deviation.



Supplementary figure 2. VLDL ApoB-100 levels in healthy and NAFLD participants. ApoB-100 levels were not significantly different within isolated VLDL fractions of NAFLD patients compared to controls. ApoB-100 was analysed by an ELISA kit as detailed in the method section. Statistical significance was assessed using two-way ANOVA controlling for presence of T2DM and interaction between T2DM and disease state, with a P-value <0.05 considered significant. Data are mean \pm standard deviation.

Chapter 5. Conclusion

5.1 Summary and conclusion

The epidemic spread of obesity has rendered this condition a public health priority. Obesity and AT dysfunction promote IR, and together they increase the risk for NAFLD, T2DM, and CVD. Lipoprotein dysmetabolism is believed to be a key mediator in this process. However, most of the studies conducted thus far have focused on their LDL/HDL cholesterol levels or triglycerides in VLDL, thus leaving largely unexplored multiple other lipid classes and their changes in health and disease.

In this thesis, I sought to understand the lipoprotein remodelling occurring in obesity-related metabolic disorders, the MetS and NAFLD, since they are well known to be associated to altered lipoprotein metabolism and dyslipidaemia.

Studies investigating the whole serum/plasma lipidome of MetS and NAFLD have reported conflicting findings (Kartsoli et al, 2020; Monnerie et al, 2020) and there currently lacks an accepted mechanistic explanation as to why certain lipoprotein changes are associated with MetS and NAFLD. Part of these discrepancies are due to the fact that whole serum/plasma lipidome is an average of lipid signals from different lipoprotein fractions thus being highly influenced by the recruitment criteria and characteristics of the study population.

In chapter 3, I first profiled the major lipidomic classes in the whole serum of healthy and MetS patients. In addition to the expected increased levels of TG and DG in MetS compared with controls, the most intriguing results were attributable to increased PC and reduced LPC levels, alongside a decreased CE/FC ratio in MetS compared to controls. By using a lipidomic index as an indirect measure of enzyme activity, termed the Q index (Gerl et al, 2018), my data suggested that LCAT, the only circulating enzyme capable of esterifying CE from FC, could be responsible for the changes observed. The use of enzyme activity assays confirmed a reduced activity of LCAT in MetS compared with controls while ruling out the contribution of the other major enzyme involved in plasma PC metabolism, namely PLPA2. The whole serum targeted proteomic data further supported the hypothesis of reduced activity of LCAT in MetS compared with controls since ApoA-I, the predominant activator of LCAT, was significantly reduced, and ApoC-III, a potent *in vitro* inhibitor of LCAT, was markedly

increased in MetS (Cho, 2009; Sorci-Thomas et al, 2009). Gerl et al. demonstrated that the Q index was reduced in patients with CVD (Gerl et al, 2018). In line with their study, I also showed that in patients at high CVD risk, the Q index is also reduced, thus suggesting that it could possibly serve as an early marker of CVD risk also in primary prevention. Of note, I also validated the utility of the Q index as a surrogate LCAT activity marker correlating it with the direct measurement of LCAT. Whether MetS patients experience elevated CVD risk via LCAT is yet to be established: although the role of LCAT in CVD has been already investigated, conflicting results directly linking LCAT activity to CVD have been reported in both clinical and pre-clinical studies (Norum et al, 2020). While our small cohort does not address the clinical implication of LCAT in CVD it strongly suggests that LCAT is an important player in regulating the plasma lipidome. This chapter demonstrates how combined omics approaches along with fluorometric assays can provide a clearer picture of the lipoprotein remodelling in metabolic diseases. Although promising, these results require further validations in larger cohorts designed to confirm the clinical implications of our findings.

In chapter 4, I investigated the lipoprotein remodelling occurring in NAFLD. Several studies have coherently reported a reduction of PUFA in the liver of NAFLD patients. However, the circulating lipidomic studies found conflicting results which do not always match the liver findings (Kartsoli et al, 2020). In this chapter, I showed that the whole serum lipidome of NAFLD patients was indeed characterised by a reduction of PUFA lipids and specifically in the PL species. Furthermore, increased levels of saturated and reduced polyunsaturated FFA in NAFLD compared with controls, suggested that AT is an important player in the hepatic lipid composition of NAFLD, this being in line with previous research (Donnelly et al, 2005). To understand whether the PUFA reduction in circulation was led by a reduced hepatic “input” (HDL and FFA) or a consequence of reduced PUFA export from the liver (VLDL), I isolated the lipoprotein fractions to study in more detail their lipidomic profile. These data showed that NAFLD’s HDL were depleted in PL and specifically in PUFA lipids, suggesting that the peripheral tissues provide less PL and PUFA to the liver also via HDL. These findings go alongside previous literature showing that AT and skeletal muscle biopsies of obese and IR subjects are depleted in PL and PUFA (Borkman et al, 1993; Ferrara et al, 2021; Pietilainen et al, 2011). Intriguingly, with tracer experiments, previous

literature suggested that the liver largely re-uses HDL-derived PL either incorporating them into membranes or converting them into TG (van der Veen et al, 2012); this seems to be confirmed in my VLDL data where the VLDL lipidome of NAFLD patients appears depleted in PUFA-TG compared to controls. Besides TG, the remaining lipids had unchanged PUFA levels and increased SFA and MUFA lipids in several PL classes probably reflecting a well-known upregulation of DNL and lipid remodeling occurring in NAFLD. These results indicated that the plasma PL depletion observed in NAFLD could be driven, at least in part, by the HDL lipid composition; however, it cannot be excluded that peripheral organs become PUFA-depleted because they receive less PUFA-TG from the liver (VLDL). Another intriguing hypothesis is that PUFA-PL might also be depleted as a consequence of their utilisation for the production of bioactive lipid species, such as eicosanoids, which exert signalling functions (Musso et al, 2018) either in the liver or in peripheral tissues. However, it should be said that these are only speculations and that the extent to which AT influences the liver lipidome and vice versa is not inferable from our data, thus warranting further investigation with stable isotope approaches to measure fluxes. The strong correlation between VLDL lipidome and circulating liver enzymes confirms the role of the hepatic lipidome in driving hepatocyte lipotoxicity; however, the lack of stepwise changes with the severity of the disorder suggest that other factors might be also influencing disease progression.

The hypothesis of HDL as a nexus of peripheral and hepatic lipid disorders has been largely unexplored except for its cholesterol content or in mouse studies (van der Veen et al, 2012). This chapter therefore introduces a new paradigm where HDL, whose PL content has been mainly studied with regards to consequences in HDL physical properties, might be also acting as carriers of a “reverse phospholipid transport” from the periphery to the liver.

The reader might have noticed some differences in the findings between the MetS (Chapter 4) and NAFLD (Chapter 5) cohorts, despite these disorders being both obesity-driven. This could be attributable to the different criteria of recruitment in the two studies leading to pretty different metabolic profiles of the NAFLD/MetS groups. The MetS patients inclusion criteria was the presence of 3 ATPIII criteria for MetS, in the case of NAFLD the diagnosis is clinically made irrespectively of the metabolic

background. Also, the nutritional background between the 2 cohorts was completely different as the MetS patients were recruited in Southern Italy (in a region characterised by a high dietary consumption of extra-virgin olive oil and fish) while the NAFLD cohort was recruited in the UK therefore possibly being less exposed to nutritional PUFA and potentially more prone to depletion. In this work, I could not rule out the influence of the dietary habits of these two cohorts. It is thus essential for future lipidomic studies to also account for dietary habits.

In conclusion, the work done in this thesis highlighted a novel role for the circulating lipoprotein remodelling enzyme LCAT in shaping the plasma lipidome in MetS patients alongside providing a new role for HDL in the pathogenesis of NAFLD. If confirmed, both findings could lead to novel therapeutic strategies.

5.2 Future directions

The work presented in this thesis has highlighted future areas of research that would increase the understanding of lipoprotein metabolism in obesity-related metabolic disorders and potentially lead to new drug targets.

In chapter 3, I identified LCAT as a putative modulator of the PL and cholesterol dysmetabolism observed. A follow-up experiment would be to profile the serum lipidome of patients with genetic LCAT deficiency. The latter would provide evidence of the plasma remodelling occurring as a consequence of LCAT deficiency while excluding the influence of other factors characterising the MetS, which could also be involved in the lipid changes observed. In parallel, a further question to answer would be to assess if the use of recombinant LCAT, which has proven to restore the HDL cholesterol levels in LCAT deficient patients (Simonelli et al, 2013), would also rescue the changes in the lipidomic phenotype described in this chapter. In terms of functionality, it would also be relevant to characterise how the changes in the Q index affects the cholesterol efflux capacity (with in vitro experiments), thus providing a functional relevance of these lipids for HDL function and CVD. Lastly, larger prospective cohorts would also be necessary to confirm the role of the Q index as a hallmark of cardiometabolic risk. While these findings are still preliminary, my work also supports the increasingly established role of shorter and more saturated TG as hallmark of IR and MetS. Because increased levels of these TG are already present at early stages of IR, my work also suggests that the use of a specific set of TG, measured through liquid chromatography mass-spectrometry, might prove a better identifying criteria for the MetS as compared to total TG.

In chapter 4, I found that HDL lipid composition matches the profile described in the liver of NAFLD patients. Interestingly, the contribution of de novo vs. dietary FA in promoting lipotoxic species such as ceramides in different tissues is still poorly described, and a better understanding of these pathways in clinical and pre-clinical models would improve our understanding of the NAFLD pathophysiology.

The use of stable isotopes in mice with humanised livers (mouse models which better recapitulate the human lipoprotein metabolism) placed on western-style diets (high-fat, high-cholesterol diets enriched in refined carbohydrates either in the form of

sucrose or fructose) with different ratios between PUFA and MUFA/SFA, would allow to study if the defective reverse PUFA/PL transport observed in NASH patients and likely due to a reduced accumulation of PUFA in peripheral tissues (AT, skeletal muscle) is secondary to reduced PUFA intake, increased PUFA consumption in different organs, or rather an event secondary to the enhanced de novo hepatic FA synthesis. These settings would also allow to characterise in parallel gene/protein expression of enzymes involved in FA metabolism in different tissues to inform whether the elongation and desaturation of preformed essential PUFA is a primary liver event or rather a peripheral event leading to the PL depletion. These findings could also be translated clinically via the administration of stable isotopes to patients scheduled for liver biopsy to study hepatic fluxes of different lipid classes, and to investigate if lipotoxic species (i.e. ceramides) are products of intra-hepatic de novo synthesis. Lastly, profiling of eicosanoids in tissues and plasma would shed light on the contribution of these pathways to the PL and its PUFA remodelling across the NAFLD spectrum. Despite the preliminary nature of the results provided here, our data highlights that whole serum lipidomics is highly influenced by lipoprotein remodelling and that can provide useful insights into these processes; however, the use of lipoprotein lipidomics will ultimately be necessary to allow a better understanding of the biology underlying lipoprotein metabolism and remodelling.

Reference

(2019) The path of biomolecular mass spectrometry into open research. *Nature communications* **10**: 4029

(Gov.UK national statistics, 2017)

(World Health Organization, 2018) Obesity and overweight.

Adiels M, Olofsson SO, Taskinen MR, Boren J (2008) Overproduction of very low-density lipoproteins is the hallmark of the dyslipidemia in the metabolic syndrome. *Arteriosclerosis, thrombosis, and vascular biology* **28**: 1225-1236

Adiels M, Taskinen MR, Packard C, Caslake MJ, Soro-Paavonen A, Westerbacka J, Vehkavaara S, Hakkinen A, Olofsson SO, Yki-Jarvinen H, Boren J (2006) Overproduction of large VLDL particles is driven by increased liver fat content in man. *Diabetologia* **49**: 755-765

Al-Serri A, Anstee QM, Valenti L, Nobili V, Leathart JB, Dongiovanni P, Patch J, Fracanzani A, Fargion S, Day CP, Daly AK (2012) The SOD2 C47T polymorphism influences NAFLD fibrosis severity: evidence from case-control and intra-familial allele association studies. *Journal of hepatology* **56**: 448-454

Albers JJ, Vuletic S, Cheung MC (2012) Role of plasma phospholipid transfer protein in lipid and lipoprotein metabolism. *Biochimica et biophysica acta* **1821**: 345-357

Alberti KG, Eckel RH, Grundy SM, Zimmet PZ, Cleeman JI, Donato KA, Fruchart JC, James WP, Loria CM, Smith SC, Jr., International Diabetes Federation Task Force on E, Prevention, National Heart L, Blood I, American Heart A, World Heart F, International Atherosclerosis S, International Association for the Study of O (2009) Harmonizing the metabolic syndrome: a joint interim statement of the International Diabetes Federation Task Force on Epidemiology and Prevention; National Heart, Lung, and Blood Institute; American Heart Association; World Heart Federation; International Atherosclerosis Society; and International Association for the Study of Obesity. *Circulation* **120**: 1640-1645

Alberti KG, Zimmet PZ (1998) Definition, diagnosis and classification of diabetes mellitus and its complications. Part 1: diagnosis and classification of diabetes mellitus provisional report of a WHO consultation. *Diabetic medicine : a journal of the British Diabetic Association* **15**: 539-553

Allard JP, Aghdassi E, Mohammed S, Raman M, Avand G, Arendt BM, Jalali P, Kandasamy T, Prayitno N, Sherman M, Guindi M, Ma DW, Heathcote JE (2008) Nutritional assessment and hepatic fatty acid composition in non-alcoholic fatty liver disease (NAFLD): a cross-sectional study. *Journal of hepatology* **48**: 300-307

Altomonte J, Cong L, Harbaran S, Richter A, Xu J, Meseck M, Dong HH (2004) Foxo1 mediates insulin action on apoC-III and triglyceride metabolism. *The Journal of clinical investigation* **114**: 1493-1503

Angelini R, Vortmeier G, Corcelli A, Fuchs B (2014) A fast method for the determination of the PC/LPC ratio in intact serum by MALDI-TOF MS: an easy-to-follow lipid biomarker of inflammation. *Chemistry and physics of lipids* **183**: 169-175

Anjani K, Lhomme M, Sokolovska N, Poitou C, Aron-Wisniewsky J, Bouillot JL, Lesnik P, Bedossa P, Kontush A, Clement K, Dugail I, Tordjman J (2015) Circulating phospholipid profiling identifies portal contribution to NASH signature in obesity. *Journal of hepatology* **62**: 905-912

Annema W, Dijkers A, de Boer JF, van Greevenbroek MMJ, van der Kallen CJH, Schalkwijk CG, Stehouwer CDA, Dullaart RPF, Tietge UJF (2016) Impaired HDL cholesterol efflux in metabolic syndrome is unrelated to glucose tolerance status: the CODAM study. *Scientific reports* **6**: 27367

Apostolopoulou M, Gordillo R, Koliaki C, Gancheva S, Jelenik T, De Filippo E, Herder C, Markgraf D, Jankowiak F, Esposito I, Schlensak M, Scherer PE, Roden M (2018) Specific Hepatic Sphingolipids Relate to Insulin Resistance, Oxidative Stress, and Inflammation in Nonalcoholic Steatohepatitis. *Diabetes Care* **41**: 1235-1243

Araya J, Rodrigo R, Videla LA, Thielemann L, Orellana M, Pettinelli P, Poniachik J (2004) Increase in long-chain polyunsaturated fatty acid n - 6/n - 3 ratio in relation to hepatic steatosis in patients with non-alcoholic fatty liver disease. *Clinical science* **106**: 635-643

Argo CK, Caldwell SH (2009) Epidemiology and natural history of non-alcoholic steatohepatitis. *Clinics in liver disease* **13**: 511-531

Arner P, Bernard S, Salehpour M, Possnert G, Liebl J, Steier P, Buchholz BA, Eriksson M, Arner E, Hauner H, Skurk T, Ryden M, Frayn KN, Spalding KL (2011) Dynamics of human adipose lipid turnover in health and metabolic disease. *Nature* **478**: 110-113

Azzu V, Vacca M, Kamzolas I, Hall Z, Leslie J, Carobbio S, Virtue S, Davies SE, Lukasik A, Dale M, Bohlooly YM, Acharjee A, Linden D, Bidault G, Petsalaki E, Griffin JL, Oakley F, Allison MED, Vidal-Puig A (2021) Suppression of insulin-induced gene 1 (INSIG1) function promotes hepatic lipid remodelling and restrains NASH progression. *Molecular metabolism* **48**: 101210

Azzu V, Vacca M, Virtue S, Allison M, Vidal-Puig A (2020) Adipose Tissue-Liver Cross Talk in the Control of Whole-Body Metabolism: Implications in Nonalcoholic Fatty Liver Disease. *Gastroenterology* **158**: 1899-1912

Barr J, Vazquez-Chantada M, Alonso C, Perez-Cormenzana M, Mayo R, Galan A, Caballeria J, Martin-Duce A, Tran A, Wagner C, Luka Z, Lu SC, Castro A, Le Marchand-Brustel Y,

- Martinez-Chantar ML, Veyrie N, Clement K, Tordjman J, Gual P, Mato JM (2010) Liquid chromatography-mass spectrometry-based parallel metabolic profiling of human and mouse model serum reveals putative biomarkers associated with the progression of nonalcoholic fatty liver disease. *Journal of proteome research* **9**: 4501-4512
- Bedossa P, Poitou C, Veyrie N, Bouillot JL, Basdevant A, Paradis V, Tordjman J, Clement K (2012) Histopathological algorithm and scoring system for evaluation of liver lesions in morbidly obese patients. *Hepatology* **56**: 1751-1759
- Beliard S, Nogueira JP, Maraninchi M, Lairon D, Nicolay A, Giral P, Portugal H, Vialettes B, Valero R (2009) Parallel increase of plasma apoproteins C-II and C-III in Type 2 diabetic patients. *Diabetic medicine : a journal of the British Diabetic Association* **26**: 736-739
- Benhamed F, Denechaud PD, Lemoine M, Robichon C, Moldes M, Bertrand-Michel J, Ratziu V, Serfaty L, Housset C, Capeau J, Girard J, Guillou H, Postic C (2012) The lipogenic transcription factor ChREBP dissociates hepatic steatosis from insulin resistance in mice and humans. *The Journal of clinical investigation* **122**: 2176-2194
- Berenson GS, Srinivasan SR, Bao W, Newman WP, 3rd, Tracy RE, Wattigney WA (1998) Association between multiple cardiovascular risk factors and atherosclerosis in children and young adults. The Bogalusa Heart Study. *The New England journal of medicine* **338**: 1650-1656
- Berneis KK, Krauss RM (2002) Metabolic origins and clinical significance of LDL heterogeneity. *Journal of lipid research* **43**: 1363-1379
- Berrington de Gonzalez A, Hartge P, Cerhan JR, Flint AJ, Hannan L, MacInnis RJ, Moore SC, Tobias GS, Anton-Culver H, Freeman LB, Beeson WL, Clipp SL, English DR, Folsom AR, Freedman DM, Giles G, Hakansson N, Henderson KD, Hoffman-Bolton J, Hoppin JA, Koenig KL, Lee IM, Linet MS, Park Y, Pocobelli G, Schatzkin A, Sesso HD, Weiderpass E, Willcox BJ, Wolk A, Zeleniuch-Jacquotte A, Willett WC, Thun MJ (2010) Body-mass index and mortality among 1.46 million white adults. *The New England journal of medicine* **363**: 2211-2219
- Bevilacqua S, Bonadonna R, Buzzigoli G, Boni C, Ciociaro D, Maccari F, Giorico MA, Ferrannini E (1987) Acute elevation of free fatty acid levels leads to hepatic insulin resistance in obese subjects. *Metabolism: clinical and experimental* **36**: 502-506
- Bhatt DL, Steg PG, Miller M, Brinton EA, Jacobson TA, Ketchum SB, Doyle RT, Jr., Juliano RA, Jiao L, Granowitz C, Tardif JC, Ballantyne CM, Investigators R-I (2019) Cardiovascular Risk Reduction with Icosapent Ethyl for Hypertriglyceridemia. *The New England journal of medicine* **380**: 11-22
- Boon J, Hoy AJ, Stark R, Brown RD, Meex RC, Henstridge DC, Schenk S, Meikle PJ, Horowitz JF, Kingwell BA, Bruce CR, Watt MJ (2013) Ceramides contained in LDL are

elevated in type 2 diabetes and promote inflammation and skeletal muscle insulin resistance. *Diabetes* **62**: 401-410

Boren J, Chapman MJ, Krauss RM, Packard CJ, Bentzon JF, Binder CJ, Daemen MJ, Demer LL, Hegele RA, Nicholls SJ, Nordestgaard BG, Watts GF, Bruckert E, Fazio S, Ference BA, Graham I, Horton JD, Landmesser U, Laufs U, Masana L, Pasterkamp G, Raal FJ, Ray KK, Schunkert H, Taskinen MR, van de Sluis B, Wiklund O, Tokgozoglul L, Catapano AL, Ginsberg HN (2020) Low-density lipoproteins cause atherosclerotic cardiovascular disease: pathophysiological, genetic, and therapeutic insights: a consensus statement from the European Atherosclerosis Society Consensus Panel. *European heart journal* **41**: 2313-2330

Boren J, Taskinen MR, Adiels M (2012) Kinetic studies to investigate lipoprotein metabolism. *Journal of internal medicine* **271**: 166-173

Boren J, Watts GF, Adiels M, Soderlund S, Chan DC, Hakkarainen A, Lundbom N, Matikainen N, Kahri J, Verges B, Barrett PH, Taskinen MR (2015) Kinetic and Related Determinants of Plasma Triglyceride Concentration in Abdominal Obesity: Multicenter Tracer Kinetic Study. *Arteriosclerosis, thrombosis, and vascular biology* **35**: 2218-2224

Borkman M, Storlien LH, Pan DA, Jenkins AB, Chisholm DJ, Campbell LV (1993) The relation between insulin sensitivity and the fatty-acid composition of skeletal-muscle phospholipids. *The New England journal of medicine* **328**: 238-244

Boucher J, Kleinridders A, Kahn CR (2014) Insulin receptor signaling in normal and insulin-resistant states. *Cold Spring Harbor perspectives in biology* **6**

Brunt EM, Wong VW, Nobili V, Day CP, Sookoian S, Maher JJ, Bugianesi E, Sirlin CB, Neuschwander-Tetri BA, Rinella ME (2015) Nonalcoholic fatty liver disease. *Nature reviews Disease primers* **1**: 15080

Bui HH, Leohr JK, Kuo MS (2012) Analysis of sphingolipids in extracted human plasma using liquid chromatography electrospray ionization tandem mass spectrometry. *Analytical biochemistry* **423**: 187-194

Buzzetti E, Pinzani M, Tsochatzis EA (2016) The multiple-hit pathogenesis of non-alcoholic fatty liver disease (NAFLD). *Metabolism: clinical and experimental* **65**: 1038-1048

Byrne CD, Targher G (2020) NAFLD as a driver of chronic kidney disease. *Journal of hepatology* **72**: 785-801

Calabresi L, Baldassarre D, Simonelli S, Gomaschi M, Amato M, Castelnuovo S, Frigerio B, Ravani A, Sansaro D, Kauhanen J, Rauramaa R, de Faire U, Hamsten A, Smit AJ, Mannarino E, Humphries SE, Giral P, Veglia F, Sirtori CR, Franceschini G, Tremoli E (2011) Plasma lecithin:cholesterol acyltransferase and carotid intima-media thickness in European individuals at high cardiovascular risk. *Journal of lipid research* **52**: 1569-1574

Camara NO, Iseki K, Kramer H, Liu ZH, Sharma K (2017) Kidney disease and obesity: epidemiology, mechanisms and treatment. *Nature reviews Nephrology* **13**: 181-190

Camont L, Lhomme M, Rached F, Le Goff W, Negre-Salvayre A, Salvayre R, Calzada C, Lagarde M, Chapman MJ, Kontush A (2013) Small, dense high-density lipoprotein-3 particles are enriched in negatively charged phospholipids: relevance to cellular cholesterol efflux, antioxidative, antithrombotic, anti-inflammatory, and antiapoptotic functionalities. *Arteriosclerosis, thrombosis, and vascular biology* **33**: 2715-2723

Cao J, Dai DL, Yao L, Yu HH, Ning B, Zhang Q, Chen J, Cheng WH, Shen W, Yang ZX (2012) Saturated fatty acid induction of endoplasmic reticulum stress and apoptosis in human liver cells via the PERK/ATF4/CHOP signaling pathway. *Molecular and cellular biochemistry* **364**: 115-129

Capel F, Bongard V, Malpuech-Brugere C, Karoly E, Michelotti GA, Rigaudiere JP, Jouve C, Ferrieres J, Marmonier C, Sebedio JL (2020) Metabolomics reveals plausible interactive effects between dairy product consumption and metabolic syndrome in humans. *Clinical nutrition* **39**: 1497-1509

Carlier A, Phan F, Szpigiel A, Hajduch E, Salem JE, Gautheron J, Le Goff W, Guerin M, Lachkar F, Ratzu V, Hartemann A, Ferre P, Foufelle F, Bourron O (2020) Dihydroceramides in Triglyceride-Enriched VLDL Are Associated with Nonalcoholic Fatty Liver Disease Severity in Type 2 Diabetes. *Cell reports Medicine* **1**: 100154

Chapman MJ, Goldstein S, Lagrange D, Laplaud PM (1981) A density gradient ultracentrifugal procedure for the isolation of the major lipoprotein classes from human serum. *Journal of lipid research* **22**: 339-358

Chapman MJ, Le Goff W, Guerin M, Kontush A (2010) Cholesteryl ester transfer protein: at the heart of the action of lipid-modulating therapy with statins, fibrates, niacin, and cholesteryl ester transfer protein inhibitors. *European heart journal* **31**: 149-164

Charidemou E, Ashmore T, Li X, McNally BD, West JA, Liggi S, Harvey M, Orford E, Griffin JL (2019) A randomized 3-way crossover study indicates that high-protein feeding induces de novo lipogenesis in healthy humans. *JCI insight* **4**

Chavez JA, Knotts TA, Wang LP, Li G, Dobrowsky RT, Florant GL, Summers SA (2003) A role for ceramide, but not diacylglycerol, in the antagonism of insulin signal transduction by saturated fatty acids. *The Journal of biological chemistry* **278**: 10297-10303

Chavez JA, Summers SA (2012) A ceramide-centric view of insulin resistance. *Cell metabolism* **15**: 585-594

Cheung MC, Albers JJ (1984) Characterization of lipoprotein particles isolated by immunoaffinity chromatography. Particles containing A-I and A-II and particles containing A-I but no A-II. *The Journal of biological chemistry* **259**: 12201-12209

Chiappini F, Coilly A, Kadar H, Gual P, Tran A, Desterke C, Samuel D, Duclos-Vallee JC, Touboul D, Bertrand-Michel J, Brunelle A, Guettier C, Le Naour F (2017) Metabolism dysregulation induces a specific lipid signature of nonalcoholic steatohepatitis in patients. *Scientific reports* **7**: 46658

Cho KH (2009) Synthesis of reconstituted high density lipoprotein (rHDL) containing apoA-I and apoC-III: the functional role of apoC-III in rHDL. *Molecules and cells* **27**: 291-297

Christinat N, Masoodi M (2017) Comprehensive Lipoprotein Characterization Using Lipidomics Analysis of Human Plasma. *J Proteome Res* **16**: 2947-2953

Cohen DE, Fisher EA (2013) Lipoprotein metabolism, dyslipidemia, and nonalcoholic fatty liver disease. *Seminars in liver disease* **33**: 380-388

Cornier MA, Dabelea D, Hernandez TL, Lindstrom RC, Steig AJ, Stob NR, Van Pelt RE, Wang H, Eckel RH (2008) The metabolic syndrome. *Endocrine reviews* **29**: 777-822

D'Amore S, Hardfeldt J, Cariello M, Graziano G, Copetti M, Di Tullio G, Piglionica M, Scialpi N, Sabba C, Palasciano G, Vacca M, Moschetta A (2018) Identification of miR-9-5p as direct regulator of ABCA1 and HDL-driven reverse cholesterol transport in circulating CD14+ cells of patients with metabolic syndrome. *Cardiovascular research* **114**: 1154-1164

de Almeida IT, Cortez-Pinto H, Fidalgo G, Rodrigues D, Camilo ME (2002) Plasma total and free fatty acids composition in human non-alcoholic steatohepatitis. *Clinical nutrition* **21**: 219-223

DeFilippis AP, Blaha MJ, Martin SS, Reed RM, Jones SR, Nasir K, Blumenthal RS, Budoff MJ (2013) Nonalcoholic fatty liver disease and serum lipoproteins: the Multi-Ethnic Study of Atherosclerosis. *Atherosclerosis* **227**: 429-436

DeFronzo RA, Ferrannini E, Groop L, Henry RR, Herman WH, Holst JJ, Hu FB, Kahn CR, Raz I, Shulman GI, Simonson DC, Testa MA, Weiss R (2015) Type 2 diabetes mellitus. *Nature reviews Disease primers* **1**: 15019

Denechaud PD, Dentin R, Girard J, Postic C (2008) Role of ChREBP in hepatic steatosis and insulin resistance. *FEBS letters* **582**: 68-73

Dentin R, Benhamed F, Hainault I, Fauveau V, Foufelle F, Dyck JR, Girard J, Postic C (2006) Liver-specific inhibition of ChREBP improves hepatic steatosis and insulin resistance in ob/ob mice. *Diabetes* **55**: 2159-2170

Diffenderfer MR, Schaefer EJ (2014) The composition and metabolism of large and small LDL. *Current opinion in lipidology* **25**: 221-226

Ding M, Rexrode KM (2020) A Review of Lipidomics of Cardiovascular Disease Highlights the Importance of Isolating Lipoproteins. *Metabolites* **10**

Diraison F, Yankah V, Letexier D, Dusserre E, Jones P, Beylot M (2003) Differences in the regulation of adipose tissue and liver lipogenesis by carbohydrates in humans. *Journal of lipid research* **44**: 846-853

Dominiczak MH, Caslake MJ (2011) Apolipoproteins: metabolic role and clinical biochemistry applications. *Annals of clinical biochemistry* **48**: 498-515

Donnelly KL, Smith CI, Schwarzenberg SJ, Jessurun J, Boldt MD, Parks EJ (2005) Sources of fatty acids stored in liver and secreted via lipoproteins in patients with nonalcoholic fatty liver disease. *The Journal of clinical investigation* **115**: 1343-1351

Dullaart RP, Perton F, Sluiter WJ, de Vries R, van Tol A (2008) Plasma lecithin: cholesterol acyltransferase activity is elevated in metabolic syndrome and is an independent marker of increased carotid artery intima media thickness. *The Journal of clinical endocrinology and metabolism* **93**: 4860-4866

Eberle D, Hegarty B, Bossard P, Ferre P, Foufelle F (2004) SREBP transcription factors: master regulators of lipid homeostasis. *Biochimie* **86**: 839-848

Eckel RH, Grundy SM, Zimmet PZ (2005) The metabolic syndrome. *Lancet* **365**: 1415-1428

Edgerton DS, Kraft G, Smith M, Farmer B, Williams PE, Coate KC, Printz RL, O'Brien RM, Cherrington AD (2017) Insulin's direct hepatic effect explains the inhibition of glucose production caused by insulin secretion. *JCI insight* **2**: e91863

Emerging Risk Factors C, Sarwar N, Gao P, Seshasai SR, Gobin R, Kaptoge S, Di Angelantonio E, Ingelsson E, Lawlor DA, Selvin E, Stampfer M, Stehouwer CD, Lewington S, Pennells L, Thompson A, Sattar N, White IR, Ray KK, Danesh J (2010) Diabetes mellitus, fasting blood glucose concentration, and risk of vascular disease: a collaborative meta-analysis of 102 prospective studies. *Lancet* **375**: 2215-2222

Engelking LJ, Kuriyama H, Hammer RE, Horton JD, Brown MS, Goldstein JL, Liang G (2004) Overexpression of Insig-1 in the livers of transgenic mice inhibits SREBP processing and reduces insulin-stimulated lipogenesis. *The Journal of clinical investigation* **113**: 1168-1175

Eslam M, Newsome PN, Sarin SK, Anstee QM, Targher G, Romero-Gomez M, Zelber-Sagi S, Wai-Sun Wong V, Dufour JF, Schattenberg JM, Kawaguchi T, Arrese M, Valenti L, Shiha G, Tiribelli C, Yki-Jarvinen H, Fan JG, Gronbaek H, Yilmaz Y, Cortez-Pinto H, Oliveira CP,

Bedossa P, Adams LA, Zheng MH, Fouad Y, Chan WK, Mendez-Sanchez N, Ahn SH, Castera L, Bugianesi E, Ratziu V, George J (2020a) A new definition for metabolic dysfunction-associated fatty liver disease: An international expert consensus statement. *Journal of hepatology* **73**: 202-209

Eslam M, Sanyal AJ, George J, International Consensus P (2020b) MAFLD: A Consensus-Driven Proposed Nomenclature for Metabolic Associated Fatty Liver Disease. *Gastroenterology* **158**: 1999-2014 e1991

Fadaei R, Poustchi H, Meshkani R, Moradi N, Golmohammadi T, Merat S (2018) Impaired HDL cholesterol efflux capacity in patients with non-alcoholic fatty liver disease is associated with subclinical atherosclerosis. *Scientific reports* **8**: 11691

Feng R, Luo C, Li C, Du S, Okekunle AP, Li Y, Chen Y, Zi T, Niu Y (2017) Free fatty acids profile among lean, overweight and obese non-alcoholic fatty liver disease patients: a case - control study. *Lipids in health and disease* **16**: 165

Ference BA, Ginsberg HN, Graham I, Ray KK, Packard CJ, Bruckert E, Hegele RA, Krauss RM, Raal FJ, Schunkert H, Watts GF, Boren J, Fazio S, Horton JD, Masana L, Nicholls SJ, Nordestgaard BG, van de Sluis B, Taskinen MR, Tokgozoglu L, Landmesser U, Laufs U, Wiklund O, Stock JK, Chapman MJ, Catapano AL (2017) Low-density lipoproteins cause atherosclerotic cardiovascular disease. 1. Evidence from genetic, epidemiologic, and clinical studies. A consensus statement from the European Atherosclerosis Society Consensus Panel. *European heart journal* **38**: 2459-2472

Fernandes Messias MC, Mecatti GC, Figueiredo Angolini CF, Eberlin MN, Credidio L, Real Martinez CA, Rodrigues Coy CS, de Oliveira Carvalho P (2017) Plasma Lipidomic Signature of Rectal Adenocarcinoma Reveals Potential Biomarkers. *Frontiers in oncology* **7**: 325

Ferrara PJ, Rong X, Maschek JA, Verkerke AR, Siripoksup P, Song H, Green TD, Krishnan KC, Johnson JM, Turk J, Houmard JA, Lusic AJ, Drummond MJ, McClung JM, Cox JE, Shaikh SR, Tontonoz P, Holland WL, Funai K (2021) Lysophospholipid acylation modulates plasma membrane lipid organization and insulin sensitivity in skeletal muscle. *The Journal of clinical investigation* **131**

Flood C, Gustafsson M, Pitas RE, Arnaboldi L, Walzem RL, Boren J (2004) Molecular mechanism for changes in proteoglycan binding on compositional changes of the core and the surface of low-density lipoprotein-containing human apolipoprotein B100. *Arteriosclerosis, thrombosis, and vascular biology* **24**: 564-570

Folch J, Lees M, Sloane Stanley GH (1957) A simple method for the isolation and purification of total lipides from animal tissues. *The Journal of biological chemistry* **226**: 497-509

Furtado JD, Yamamoto R, Melchior JT, Andraski AB, Gamez-Guerrero M, Mulcahy P, He Z, Cai T, Davidson WS, Sacks FM (2018) Distinct Proteomic Signatures in 16 HDL (High-

Density Lipoprotein) Subspecies. *Arteriosclerosis, thrombosis, and vascular biology* **38**: 2827-2842

Gambino R, Bugianesi E, Rosso C, Mezzabotta L, Pinach S, Alemanno N, Saba F, Cassader M (2016) Different Serum Free Fatty Acid Profiles in NAFLD Subjects and Healthy Controls after Oral Fat Load. *International journal of molecular sciences* **17**: 479

Gastaldelli A, Cusi K (2019) From NASH to diabetes and from diabetes to NASH: Mechanisms and treatment options. *JHEP reports : innovation in hepatology* **1**: 312-328

Gelissen IC, Harris M, Rye KA, Quinn C, Brown AJ, Kockx M, Cartland S, Packianathan M, Kritharides L, Jessup W (2006) ABCA1 and ABCG1 synergize to mediate cholesterol export to apoA-I. *Arteriosclerosis, thrombosis, and vascular biology* **26**: 534-540

Gerl MJ, Vaz WLC, Domingues N, Klose C, Surma MA, Sampaio JL, Almeida MS, Rodrigues G, Araujo-Goncalves P, Ferreira J, Borbinha C, Marto JP, Viana-Baptista M, Simons K, Vieira OV (2018) Cholesterol is Inefficiently Converted to Cholesteryl Esters in the Blood of Cardiovascular Disease Patients. *Scientific reports* **8**: 14764

Ginsberg HN, Packard CJ, Chapman MJ, Boren J, Aguilar-Salinas CA, Averna M, Ference BA, Gaudet D, Hegele RA, Kersten S, Lewis GF, Lichtenstein AH, Moulin P, Nordestgaard BG, Remaley AT, Staels B, Stroes ESG, Taskinen MR, Tokgozoglul LS, Tybjaerg-Hansen A, Stock JK, Catapano AL (2021) Triglyceride-rich lipoproteins and their remnants: metabolic insights, role in atherosclerotic cardiovascular disease, and emerging therapeutic strategies-a consensus statement from the European Atherosclerosis Society. *European heart journal*

Gorden DL, Myers DS, Ivanova PT, Fahy E, Maurya MR, Gupta S, Min J, Spann NJ, McDonald JG, Kelly SL, Duan J, Sullards MC, Leiker TJ, Barkley RM, Quehenberger O, Armando AM, Milne SB, Mathews TP, Armstrong MD, Li C, Melvin WV, Clements RH, Washington MK, Mendonsa AM, Witztum JL, Guan Z, Glass CK, Murphy RC, Dennis EA, Merrill AH, Jr., Russell DW, Subramaniam S, Brown HA (2015) Biomarkers of NAFLD progression: a lipidomics approach to an epidemic. *Journal of lipid research* **56**: 722-736

Griffin JL, Atherton H, Shockcor J, Atzori L (2011) Metabolomics as a tool for cardiac research. *Nature reviews Cardiology* **8**: 630-643

Group HTRC, Bowman L, Hopewell JC, Chen F, Wallendszus K, Stevens W, Collins R, Wiviott SD, Cannon CP, Braunwald E, Sammons E, Landray MJ (2017) Effects of Anacetrapib in Patients with Atherosclerotic Vascular Disease. *The New England journal of medicine* **377**: 1217-1227

Guerra S, Mocciaro G, Gastaldelli A (2021) "Adipose tissue insulin resistance and lipidome alterations are the characterizing factors of NASH". *European journal of clinical investigation*: e13695

Hafiane A, Genest J (2015) High density lipoproteins: Measurement techniques and potential biomarkers of cardiovascular risk. *BBA clinical* **3**: 175-188

Hammad SM, Pierce JS, Soodavar F, Smith KJ, Al Gadban MM, Rembiesa B, Klein RL, Hannun YA, Bielawski J, Bielawska A (2010) Blood sphingolipidomics in healthy humans: impact of sample collection methodology. *Journal of lipid research* **51**: 3074-3087

Han J, Kaufman RJ (2016) The role of ER stress in lipid metabolism and lipotoxicity. *Journal of lipid research* **57**: 1329-1338

Han S, Flattery AM, McLaren D, Raubertas R, Lee SH, Mendoza V, Rosa R, Geoghagen N, Castro-Perez JM, Roddy TP, Forrest G, Johns D, Hubbard BK, Li J (2012) Comparison of lipoprotein separation and lipid analysis methodologies for human and cynomolgus monkey plasma samples. *Journal of cardiovascular translational research* **5**: 75-83

Harwood HJ, Jr. (2005) Treating the metabolic syndrome: acetyl-CoA carboxylase inhibition. *Expert opinion on therapeutic targets* **9**: 267-281

Havel RJ, Eder HA, Bragdon JH (1955) The distribution and chemical composition of ultracentrifugally separated lipoproteins in human serum. *The Journal of clinical investigation* **34**: 1345-1353

He S, McPhaul C, Li JZ, Garuti R, Kinch L, Grishin NV, Cohen JC, Hobbs HH (2010) A sequence variation (I148M) in PNPLA3 associated with nonalcoholic fatty liver disease disrupts triglyceride hydrolysis. *The Journal of biological chemistry* **285**: 6706-6715

Hill NR, Fatoba ST, Oke JL, Hirst JA, O'Callaghan CA, Lasserson DS, Hobbs FD (2016) Global Prevalence of Chronic Kidney Disease - A Systematic Review and Meta-Analysis. *PloS one* **11**: e0158765

Hilvo M, Meikle PJ, Pedersen ER, Tell GS, Dhar I, Brenner H, Schottker B, Laaperi M, Kauhanen D, Koistinen KM, Jylha A, Huynh K, Mellett NA, Tonkin AM, Sullivan DR, Simes J, Nestel P, Koenig W, Rothenbacher D, Nygard O, Laaksonen R (2020) Development and validation of a ceramide- and phospholipid-based cardiovascular risk estimation score for coronary artery disease patients. *European heart journal* **41**: 371-380

Hilvo M, Salonurmi T, Havulinna AS, Kauhanen D, Pedersen ER, Tell GS, Meyer K, Teeriniemi AM, Laatikainen T, Jousilahti P, Savolainen MJ, Nygard O, Salomaa V, Laaksonen R (2018) Ceramide stearic to palmitic acid ratio predicts incident diabetes. *Diabetologia* **61**: 1424-1434

Hinz C, Liggi S, Mocciaro G, Jung S, Induruwa I, Pereira M, Bryant CE, Meckelmann SW, O'Donnell VB, Farndale RW, Fjeldsted J, Griffin JL (2019) A Comprehensive UHPLC Ion Mobility Quadrupole Time-of-Flight Method for Profiling and Quantification of Eicosanoids, Other Oxylipins, and Fatty Acids. *Analytical chemistry* **91**: 8025-8035

Hodson L, Karpe F (2019) Hyperinsulinaemia: does it tip the balance toward intrahepatic fat accumulation? *Endocrine connections* **8**: R157-R168

Holleboom AG, Kuivenhoven JA, Vergeer M, Hovingh GK, van Miert JN, Wareham NJ, Kastelein JJ, Khaw KT, Boekholdt SM (2010) Plasma levels of lecithin:cholesterol acyltransferase and risk of future coronary artery disease in apparently healthy men and women: a prospective case-control analysis nested in the EPIC-Norfolk population study. *Journal of lipid research* **51**: 416-421

Hu Q, Noll RJ, Li H, Makarov A, Hardman M, Graham Cooks R (2005) The Orbitrap: a new mass spectrometer. *Journal of mass spectrometry : JMS* **40**: 430-443

Hurt-Camejo E, Camejo G (2018) ApoB-100 Lipoprotein Complex Formation with Intima Proteoglycans as a Cause of Atherosclerosis and Its Possible Ex Vivo Evaluation as a Disease Biomarker. *Journal of cardiovascular development and disease* **5**

Huuskonen J, Olkkonen VM, Jauhiainen M, Ehnholm C (2001) The impact of phospholipid transfer protein (PLTP) on HDL metabolism. *Atherosclerosis* **155**: 269-281

Iizuka K, Horikawa Y (2008) ChREBP: a glucose-activated transcription factor involved in the development of metabolic syndrome. *Endocrine journal* **55**: 617-624

Innis-Whitehouse W, Li X, Brown WV, Le NA (1998) An efficient chromatographic system for lipoprotein fractionation using whole plasma. *Journal of lipid research* **39**: 679-690

Ivanova EA, Myasoedova VA, Melnichenko AA, Grechko AV, Orekhov AN (2017) Small Dense Low-Density Lipoprotein as Biomarker for Atherosclerotic Diseases. *Oxidative medicine and cellular longevity* **2017**: 1273042

Jebari-Benslaiman S, Uribe KB, Benito-Vicente A, Galicia-Garcia U, Larrea-Sebal A, Alloza I, Vandembroeck K, Ostolaza H, Martin C (2020) Cholesterol Efflux Efficiency of Reconstituted HDL Is Affected by Nanoparticle Lipid Composition. *Biomedicines* **8**

Jensen MK, Aroner SA, Mukamal KJ, Furtado JD, Post WS, Tsai MY, Tjonneland A, Polak JF, Rimm EB, Overvad K, McClelland RL, Sacks FM (2018) High-Density Lipoprotein Subspecies Defined by Presence of Apolipoprotein C-III and Incident Coronary Heart Disease in Four Cohorts. *Circulation* **137**: 1364-1373

Jonas A (2000) Lecithin cholesterol acyltransferase. *Biochimica et biophysica acta* **1529**: 245-256

Kahn CR, Wang G, Lee KY (2019) Altered adipose tissue and adipocyte function in the pathogenesis of metabolic syndrome. *The Journal of clinical investigation* **129**: 3990-4000

- Kamagate A, Qu S, Perdomo G, Su D, Kim DH, Slusher S, Meseck M, Dong HH (2008) FoxO1 mediates insulin-dependent regulation of hepatic VLDL production in mice. *The Journal of clinical investigation* **118**: 2347-2364
- Karpe F, Dickmann JR, Frayn KN (2011) Fatty acids, obesity, and insulin resistance: time for a reevaluation. *Diabetes* **60**: 2441-2449
- Kartsoli S, Kostara CE, Tsimihodimos V, Bairaktari ET, Christodoulou DK (2020) Lipidomics in non-alcoholic fatty liver disease. *World journal of hepatology* **12**: 436-450
- Kawai T, Akira S (2007) TLR signaling. *Seminars in immunology* **19**: 24-32
- Kay RG, Gregory B, Grace PB, Pleasance S (2007) The application of ultra-performance liquid chromatography/tandem mass spectrometry to the detection and quantitation of apolipoproteins in human serum. *Rapid communications in mass spectrometry : RCM* **21**: 2585-2593
- Kim JK, Gavrilova O, Chen Y, Reitman ML, Shulman GI (2000) Mechanism of insulin resistance in A-ZIP/F-1 fatless mice. *The Journal of biological chemistry* **275**: 8456-8460
- Kindel T, Lee DM, Tso P (2010) The mechanism of the formation and secretion of chylomicrons. *Atherosclerosis Supplements* **11**: 11-16
- Kofeler HC, Fauland A, Rechberger GN, Trotsmuller M (2012) Mass spectrometry based lipidomics: an overview of technological platforms. *Metabolites* **2**: 19-38
- Koliaki C, Szendroedi J, Kaul K, Jelenik T, Nowotny P, Jankowiak F, Herder C, Carstensen M, Krausch M, Knoefel WT, Schlensak M, Roden M (2015) Adaptation of hepatic mitochondrial function in humans with non-alcoholic fatty liver is lost in steatohepatitis. *Cell metabolism* **21**: 739-746
- Kontush A, Lhomme M, Chapman MJ (2013) Unraveling the complexities of the HDL lipidome. *Journal of lipid research* **54**: 2950-2963
- Kotronen A, Peltonen M, Hakkarainen A, Sevastianova K, Bergholm R, Johansson LM, Lundbom N, Rissanen A, Ridderstrale M, Groop L, Orho-Melander M, Yki-Jarvinen H (2009a) Prediction of non-alcoholic fatty liver disease and liver fat using metabolic and genetic factors. *Gastroenterology* **137**: 865-872
- Kotronen A, Velagapudi VR, Yetukuri L, Westerbacka J, Bergholm R, Ekroos K, Makkonen J, Taskinen MR, Oresic M, Yki-Jarvinen H (2009b) Serum saturated fatty acids containing triacylglycerols are better markers of insulin resistance than total serum triacylglycerol concentrations. *Diabetologia* **52**: 684-690

Krauss RM (2010) Lipoprotein subfractions and cardiovascular disease risk. *Current opinion in lipidology* **21**: 305-311

Krssak M, Falk Petersen K, Dresner A, DiPietro L, Vogel SM, Rothman DL, Roden M, Shulman GI (1999) Intramyocellular lipid concentrations are correlated with insulin sensitivity in humans: a ¹H NMR spectroscopy study. *Diabetologia* **42**: 113-116

Kuai R, Li D, Chen YE, Moon JJ, Schwendeman A (2016) High-Density Lipoproteins: Nature's Multifunctional Nanoparticles. *ACS nano* **10**: 3015-3041

Kulkarni H, Meikle PJ, Mamtani M, Weir JM, Barlow CK, Jowett JB, Bellis C, Dyer TD, Johnson MP, Rainwater DL, Almasy L, Mahaney MC, Comuzzie AG, Blangero J, Curran JE (2013a) Plasma lipidomic profile signature of hypertension in Mexican American families: specific role of diacylglycerols. *Hypertension* **62**: 621-626

Kulkarni H, Meikle PJ, Mamtani M, Weir JM, Barlow CK, Jowett JB, Bellis C, Dyer TD, Johnson MP, Rainwater DL, Almasy L, Mahaney MC, Comuzzie AG, Blangero J, Curran JE (2013b) Variability in associations of phosphatidylcholine molecular species with metabolic syndrome in Mexican-American families. *Lipids* **48**: 497-503

Kumari M, Schoiswohl G, Chitraju C, Paar M, Cornaciu I, Rangrez AY, Wongsiriroj N, Nagy HM, Ivanova PT, Scott SA, Knittelfelder O, Rechberger GN, Birner-Gruenberger R, Eder S, Brown HA, Haemmerle G, Oberer M, Lass A, Kershaw EE, Zimmermann R, Zechner R (2012) Adiponutrin functions as a nutritionally regulated lysophosphatidic acid acyltransferase. *Cell metabolism* **15**: 691-702

Kumashiro N, Erion DM, Zhang D, Kahn M, Beddow SA, Chu X, Still CD, Gerhard GS, Han X, Dziura J, Petersen KF, Samuel VT, Shulman GI (2011) Cellular mechanism of insulin resistance in nonalcoholic fatty liver disease. *Proceedings of the National Academy of Sciences of the United States of America* **108**: 16381-16385

Kylin E (1923) On clinical determination of capillary tension. *J Intern Med* **57**, 566–586.

Lan YL, Lou JC, Lyu W, Zhang B (2019) Update on the synergistic effect of HSL and insulin in the treatment of metabolic disorders. *Therapeutic advances in endocrinology and metabolism* **10**: 2042018819877300

Law SH, Chan ML, Marathe GK, Parveen F, Chen CH, Ke LY (2019) An Updated Review of Lysophosphatidylcholine Metabolism in Human Diseases. *International journal of molecular sciences* **20**

Lewis GF, Uffelman KD, Szeto LW, Weller B, Steiner G (1995) Interaction between free fatty acids and insulin in the acute control of very low density lipoprotein production in humans. *The Journal of clinical investigation* **95**: 158-166

Lomonaco R, Ortiz-Lopez C, Orsak B, Webb A, Hardies J, Darland C, Finch J, Gastaldelli A, Harrison S, Tio F, Cusi K (2012) Effect of adipose tissue insulin resistance on metabolic parameters and liver histology in obese patients with nonalcoholic fatty liver disease. *Hepatology* **55**: 1389-1397

Lopez-Vicario C, Gonzalez-Periz A, Rius B, Moran-Salvador E, Garcia-Alonso V, Lozano JJ, Bataller R, Cofan M, Kang JX, Arroyo V, Claria J, Totos E (2014) Molecular interplay between Delta5/Delta6 desaturases and long-chain fatty acids in the pathogenesis of non-alcoholic steatohepatitis. *Gut* **63**: 344-355

Lucero D, Sviridov D, Freeman L, Lopez GI, Fassio E, Remaley AT, Schreier L (2015) Increased cholesterol efflux capacity in metabolic syndrome: Relation with qualitative alterations in HDL and LCAT. *Atherosclerosis* **242**: 236-242

Lusis AJ (2000) Atherosclerosis. *Nature* **407**: 233-241

Luukkonen PK, Zhou Y, Sadevirta S, Leivonen M, Arola J, Oresic M, Hyotylainen T, Yki-Jarvinen H (2016) Hepatic ceramides dissociate steatosis and insulin resistance in patients with non-alcoholic fatty liver disease. *Journal of hepatology* **64**: 1167-1175

Mack E, Ziv E, Reuveni H, Kalman R, Niv MY, Jorns A, Lenzen S, Shafrir E (2008) Prevention of insulin resistance and beta-cell loss by abrogating PKCepsilon-induced serine phosphorylation of muscle IRS-1 in Psammomys obesus. *Diabetes/metabolism research and reviews* **24**: 577-584

Magkos F, Mohammed BS, Mittendorfer B (2009) Plasma lipid transfer enzymes in non-diabetic lean and obese men and women. *Lipids* **44**: 459-464

Magkos F, Su X, Bradley D, Fabbri E, Conte C, Eagon JC, Varela JE, Brunt EM, Patterson BW, Klein S (2012) Intrahepatic diacylglycerol content is associated with hepatic insulin resistance in obese subjects. *Gastroenterology* **142**: 1444-1446 e1442

Mahley RW, Ji ZS (1999) Remnant lipoprotein metabolism: key pathways involving cell-surface heparan sulfate proteoglycans and apolipoprotein E. *Journal of lipid research* **40**: 1-16

Mann M, Kelleher NL (2008) Precision proteomics: the case for high resolution and high mass accuracy. *Proceedings of the National Academy of Sciences of the United States of America* **105**: 18132-18138

Mannisto V, Kaminska D, Karja V, Tiainen M, de Mello VD, Hanhineva K, Soinen P, Ala-Korpela M, Pihlajamaki J (2019) Total liver phosphatidylcholine content associates with non-alcoholic steatohepatitis and glycine N-methyltransferase expression. *Liver international : official journal of the International Association for the Study of the Liver* **39**: 1895-1905

Marathe GK, Pandit C, Lakshmikanth CL, Chaithra VH, Jacob SP, D'Souza CJ (2014) To hydrolyze or not to hydrolyze: the dilemma of platelet-activating factor acetylhydrolase. *Journal of lipid research* **55**: 1847-1854

Mayo R, Crespo J, Martinez-Arranz I, Banales JM, Arias M, Minchola I, Aller de la Fuente R, Jimenez-Aguero R, Alonso C, de Luis DA, Vitek L, Stritesky J, Caballeria J, Romero-Gomez M, Martin-Duce A, Muguerza Huguet JM, Busteros-Moraza JI, Idowu MO, Castro A, Martinez-Chantar ML, Ortiz P, Bruha R, Lu SC, Bedossa P, Noureddin M, Sanyal AJ, Mato JM (2018) Metabolomic-based noninvasive serum test to diagnose nonalcoholic steatohepatitis: Results from discovery and validation cohorts. *Hepatology communications* **2**: 807-820

Mielke MM, Bandaru VV, Han D, An Y, Resnick SM, Ferrucci L, Haughey NJ (2015) Demographic and clinical variables affecting mid- to late-life trajectories of plasma ceramide and dihydroceramide species. *Aging cell* **14**: 1014-1023

Mikkelsen J, Hojrup P, Rasmussen MM, Roepstorff P, Knudsen J (1985) Amino acid sequence around the active-site serine residue in the acyltransferase domain of goat mammary fatty acid synthetase. *The Biochemical journal* **227**: 21-27

Mittendorfer B, Yoshino M, Patterson BW, Klein S (2016) VLDL Triglyceride Kinetics in Lean, Overweight, and Obese Men and Women. *The Journal of clinical endocrinology and metabolism* **101**: 4151-4160

Miura K, Yang L, van Rooijen N, Brenner DA, Ohnishi H, Seki E (2013) Toll-like receptor 2 and palmitic acid cooperatively contribute to the development of nonalcoholic steatohepatitis through inflammasome activation in mice. *Hepatology* **57**: 577-589

Monnerie S, Comte B, Ziegler D, Morais JA, Pujos-Guillot E, Gaudreau P (2020) Metabolomic and Lipidomic Signatures of Metabolic Syndrome and its Physiological Components in Adults: A Systematic Review. *Scientific reports* **10**: 669

Morigny P, Boucher J, Arner P, Langin D (2021) Lipid and glucose metabolism in white adipocytes: pathways, dysfunction and therapeutics. *Nature reviews Endocrinology* **17**: 276-295

Mottillo S, Filion KB, Genest J, Joseph L, Pilote L, Poirier P, Rinfret S, Schiffrin EL, Eisenberg MJ (2010) The metabolic syndrome and cardiovascular risk a systematic review and meta-analysis. *Journal of the American College of Cardiology* **56**: 1113-1132

Muralidharan S, Shimobayashi M, Ji S, Burla B, Hall MN, Wenk MR, Torta F (2021) A reference map of sphingolipids in murine tissues. *Cell reports* **35**: 109250

Murao K, Wada Y, Nakamura T, Taylor AH, Mooradian AD, Wong NC (1998) Effects of glucose and insulin on rat apolipoprotein A-I gene expression. *The Journal of biological chemistry* **273**: 18959-18965

Musso G, Cassader M, Paschetta E, Gambino R (2018) Bioactive Lipid Species and Metabolic Pathways in Progression and Resolution of Nonalcoholic Steatohepatitis. *Gastroenterology* **155**: 282-302 e288

Nakhjavani M, Asgharani F, Khalilzadeh O, Esteghamati A, Ghaneei A, Morteza A, Anvari M (2011) Oxidized low-density lipoprotein is negatively correlated with lecithin-cholesterol acyltransferase activity in type 2 diabetes mellitus. *The American journal of the medical sciences* **341**: 92-95

Noble RP (1968) Electrophoretic separation of plasma lipoproteins in agarose gel. *Journal of lipid research* **9**: 693-700

Norheim F, Bjellaas T, Hui ST, Chella Krishnan K, Lee J, Gupta S, Pan C, Hasin-Brumshtein Y, Parks BW, Li DY, Bui HH, Mosier M, Wu Y, Huertas-Vazquez A, Hazen SL, Gundersen TE, Mehrabian M, Tang WHW, Hevener AL, Drevon CA, Lusis AJ (2018) Genetic, dietary, and sex-specific regulation of hepatic ceramides and the relationship between hepatic ceramides and IR. *Journal of lipid research* **59**: 1164-1174

Norum KR, Remaley AT, Miettinen HE, Strom EH, Balbo BEP, Sampaio C, Wiig I, Kuivenhoven JA, Calabresi L, Tesmer JJ, Zhou M, Ng DS, Skeie B, Karathanasis SK, Manthei KA, Retterstol K (2020) Lecithin:cholesterol acyltransferase: symposium on 50 years of biomedical research from its discovery to latest findings. *Journal of lipid research* **61**: 1142-1149

Ooi EM, Chan DC, Hodson L, Adiels M, Boren J, Karpe F, Fielding BA, Watts GF, Barrett PH (2016) Triglyceride-rich lipoprotein metabolism in women: roles of apoC-II and apoC-III. *European journal of clinical investigation* **46**: 730-736

Ooi GJ, Meikle PJ, Huynh K, Earnest A, Roberts SK, Kemp W, Parker BL, Brown W, Burton P, Watt MJ (2021) Hepatic lipidomic remodeling in severe obesity manifests with steatosis and does not evolve with non-alcoholic steatohepatitis. *J Hepatol* **75**: 524-535

Oresic M, Hyotylainen T, Kotronen A, Gopalacharyulu P, Nygren H, Arola J, Castillo S, Mattila I, Hakkarainen A, Borra RJ, Honka MJ, Verrijken A, Francque S, Iozzo P, Leivonen M, Jaser N, Juuti A, Sorensen TI, Nuutila P, Van Gaal L, Yki-Jarvinen H (2013) Prediction of non-alcoholic fatty-liver disease and liver fat content by serum molecular lipids. *Diabetologia* **56**: 2266-2274

Osei M, Griffin JL, Koulman A (2015) Hyphenating size-exclusion chromatography with electrospray mass spectrometry; using on-line liquid-liquid extraction to study the lipid composition of lipoprotein particles. *Rapid communications in mass spectrometry : RCM* **29**: 1969-1976

Ossoli A, Pavanello C, Calabresi L (2016a) High-Density Lipoprotein, Lecithin: Cholesterol Acyltransferase, and Atherosclerosis. *Endocrinology and metabolism* **31**: 223-229

Ossoli A, Simonelli S, Varrenti M, Morici N, Oliva F, Stucchi M, Gomasaschi M, Strazzella A, Arnaboldi L, Thomas MJ, Sorci-Thomas MG, Corsini A, Veglia F, Franceschini G, Karathanasis SK, Calabresi L (2019) Recombinant LCAT (Lecithin:Cholesterol Acyltransferase) Rescues Defective HDL (High-Density Lipoprotein)-Mediated Endothelial Protection in Acute Coronary Syndrome. *Arteriosclerosis, thrombosis, and vascular biology* **39**: 915-924

Ossoli A, Simonelli S, Vitali C, Franceschini G, Calabresi L (2016b) Role of LCAT in Atherosclerosis. *Journal of atherosclerosis and thrombosis* **23**: 119-127

Ouimet M, Barrett TJ, Fisher EA (2019) HDL and Reverse Cholesterol Transport. *Circulation research* **124**: 1505-1518

Paavola T, Kuusisto S, Jauhiainen M, Kakko S, Kangas-Kontio T, Metso J, Soininen P, Ala-Korpela M, Bloigu R, Hannuksela ML, Savolainen MJ, Salonen T (2017) Impaired HDL2-mediated cholesterol efflux is associated with metabolic syndrome in families with early onset coronary heart disease and low HDL-cholesterol level. *PloS one* **12**: e0171993

Pagadala M, Kasumov T, McCullough AJ, Zein NN, Kirwan JP (2012) Role of ceramides in nonalcoholic fatty liver disease. *Trends in endocrinology and metabolism: TEM* **23**: 365-371

Panarotto D, Remillard P, Bouffard L, Maheux P (2002) Insulin resistance affects the regulation of lipoprotein lipase in the postprandial period and in an adipose tissue-specific manner. *European journal of clinical investigation* **32**: 84-92

Pechlaner R, Tsimikas S, Yin X, Willeit P, Baig F, Santer P, Oberhollenzer F, Egger G, Witztum JL, Alexander VJ, Willeit J, Kiechl S, Mayr M (2017) Very-Low-Density Lipoprotein-Associated Apolipoproteins Predict Cardiovascular Events and Are Lowered by Inhibition of APOC-III. *Journal of the American College of Cardiology* **69**: 789-800

Perry RJ, Camporez JG, Kursawe R, Titchenell PM, Zhang D, Perry CJ, Jurczak MJ, Abudukadier A, Han MS, Zhang XM, Ruan HB, Yang X, Caprio S, Kaech SM, Sul HS, Birnbaum MJ, Davis RJ, Cline GW, Petersen KF, Shulman GI (2015) Hepatic acetyl CoA links adipose tissue inflammation to hepatic insulin resistance and type 2 diabetes. *Cell* **160**: 745-758

Perseghin G, Scifo P, De Cobelli F, Pagliato E, Battezzati A, Arcelloni C, Vanzulli A, Testolin G, Pozza G, Del Maschio A, Luzi L (1999) Intramyocellular triglyceride content is a determinant of in vivo insulin resistance in humans: a 1H-13C nuclear magnetic resonance spectroscopy assessment in offspring of type 2 diabetic parents. *Diabetes* **48**: 1600-1606

Petersen KF, Oral EA, Dufour S, Befroy D, Ariyan C, Yu C, Cline GW, DePaoli AM, Taylor SI, Gorden P, Shulman GI (2002) Leptin reverses insulin resistance and hepatic steatosis in patients with severe lipodystrophy. *The Journal of clinical investigation* **109**: 1345-1350

Petersen MC, Shulman GI (2017) Roles of Diacylglycerols and Ceramides in Hepatic Insulin Resistance. *Trends in pharmacological sciences* **38**: 649-665

Pietilainen KH, Rog T, Seppanen-Laakso T, Virtue S, Gopalacharyulu P, Tang J, Rodriguez-Cuenca S, Maciejewski A, Naukkarinen J, Ruskeepaa AL, Niemela PS, Yetukuri L, Tan CY, Velagapudi V, Castillo S, Nygren H, Hyotylainen T, Rissanen A, Kaprio J, Yki-Jarvinen H, Vattulainen I, Vidal-Puig A, Oresic M (2011) Association of lipidome remodeling in the adipocyte membrane with acquired obesity in humans. *PLoS biology* **9**: e1000623

Postic C, Girard J (2008) Contribution of de novo fatty acid synthesis to hepatic steatosis and insulin resistance: lessons from genetically engineered mice. *The Journal of clinical investigation* **118**: 829-838

Powell DJ, Hajduch E, Kular G, Hundal HS (2003) Ceramide disables 3-phosphoinositide binding to the pleckstrin homology domain of protein kinase B (PKB)/Akt by a PKCzeta-dependent mechanism. *Molecular and cellular biology* **23**: 7794-7808

Puri P, Baillie RA, Wiest MM, Mirshahi F, Choudhury J, Cheung O, Sargeant C, Contos MJ, Sanyal AJ (2007) A lipidomic analysis of nonalcoholic fatty liver disease. *Hepatology* **46**: 1081-1090

Puri P, Wiest MM, Cheung O, Mirshahi F, Sargeant C, Min HK, Contos MJ, Sterling RK, Fuchs M, Zhou H, Watkins SM, Sanyal AJ (2009) The plasma lipidomic signature of nonalcoholic steatohepatitis. *Hepatology* **50**: 1827-1838

Qin S, Song G, Yu Y (2014) Phospholipid transfer protein in diabetes, metabolic syndrome and obesity. *Cardiovascular & hematological disorders drug targets* **14**: 149-153

Rader DJ (2006) Molecular regulation of HDL metabolism and function: implications for novel therapies. *The Journal of clinical investigation* **116**: 3090-3100

Ramakrishanan N, Denna T, Devaraj S, Adams-Huet B, Jialal I (2018) Exploratory lipidomics in patients with nascent Metabolic Syndrome. *Journal of diabetes and its complications* **32**: 791-794

Rashid S, Watanabe T, Sakaue T, Lewis GF (2003) Mechanisms of HDL lowering in insulin resistant, hypertriglyceridemic states: the combined effect of HDL triglyceride enrichment and elevated hepatic lipase activity. *Clinical biochemistry* **36**: 421-429

Rhee CM, Ahmadi SF, Kalantar-Zadeh K (2016) The dual roles of obesity in chronic kidney disease: a review of the current literature. *Current opinion in nephrology and hypertension* **25**: 208-216

Romagnani P, Remuzzi G, Glasscock R, Levin A, Jager KJ, Tonelli M, Massy Z, Wanner C, Anders HJ (2017) Chronic kidney disease. *Nature reviews Disease primers* **3**: 17088

Roth GA, Johnson C, Abajobir A, Abd-Allah F, Abera SF, Abyu G, Ahmed M, Aksut B, Alam T, Alam K, Alla F, Alvis-Guzman N, Amrock S, Ansari H, Arnlov J, Asayesh H, Atey TM, Avila-Burgos L, Awasthi A, Banerjee A, Barac A, Barnighausen T, Barregard L, Bedi N, Belay Ketema E, Bennett D, Berhe G, Bhutta Z, Bitew S, Carapetis J, Carrero JJ, Malta DC, Castaneda-Orjuela CA, Castillo-Rivas J, Catala-Lopez F, Choi JY, Christensen H, Cirillo M, Cooper L, Jr., Criqui M, Cundiff D, Damasceno A, Dandona L, Dandona R, Davletov K, Dharmaratne S, Dorairaj P, Dubey M, Ehrenkranz R, El Sayed Zaki M, Faraon EJA, Esteghamati A, Farid T, Farvid M, Feigin V, Ding EL, Fowkes G, Gebrehiwot T, Gillum R, Gold A, Gona P, Gupta R, Habtewold TD, Hafezi-Nejad N, Hailu T, Hailu GB, Hankey G, Hassen HY, Abate KH, Havmoeller R, Hay SI, Horino M, Hotez PJ, Jacobsen K, James S, Javanbakht M, Jeemon P, John D, Jonas J, Kalkonde Y, Karimkhani C, Kasaeian A, Khader Y, Khan A, Khang YH, Khera S, Khoja AT, Khubchandani J, Kim D, Kolte D, Kosen S, Krohn KJ, Kumar GA, Kwan GF, Lal DK, Larsson A, Linn S, Lopez A, Lotufo PA, El Razek HMA, Malekzadeh R, Mazidi M, Meier T, Meles KG, Mensah G, Meretoja A, Mezgebe H, Miller T, Mirrakhimov E, Mohammed S, Moran AE, Musa KI, Narula J, Neal B, Ngalesoni F, Nguyen G, Obermeyer CM, Owolabi M, Patton G, Pedro J, Qato D, Qorbani M, Rahimi K, Rai RK, Rawaf S, Ribeiro A, Safiri S, Salomon JA, Santos I, Santric Milicevic M, Sartorius B, Schutte A, Sepanlou S, Shaikh MA, Shin MJ, Shishehbor M, Shore H, Silva DAS, Sobngwi E, Stranges S, Swaminathan S, Tabares-Seisdedos R, Tadele Atnafu N, Tesfay F, Thakur JS, Thrift A, Topor-Madry R, Truelsen T, Tyrovolas S, Ukwaja KN, Uthman O, Vasankari T, Vlassov V, Vollset SE, Wakayo T, Watkins D, Weintraub R, Werdecker A, Westerman R, Wiysonge CS, Wolfe C, Workicho A, Xu G, Yano Y, Yip P, Yonemoto N, Younis M, Yu C, Vos T, Naghavi M, Murray C (2017) Global, Regional, and National Burden of Cardiovascular Diseases for 10 Causes, 1990 to 2015. *Journal of the American College of Cardiology* **70**: 1-25

Roumans KHM, Lindeboom L, Veeraiyah P, Remie CME, Phielix E, Havekes B, Bruls YMH, Brouwers M, Stahlman M, Alssema M, Peters HPF, de Mutsert R, Staels B, Taskinen MR, Boren J, Schrauwen P, Schrauwen-Hinderling VB (2020) Hepatic saturated fatty acid fraction is associated with de novo lipogenesis and hepatic insulin resistance. *Nature communications* **11**: 1891

Rousset X, Vaisman B, Amar M, Sethi AA, Remaley AT (2009) Lecithin: cholesterol acyltransferase--from biochemistry to role in cardiovascular disease. *Current opinion in endocrinology, diabetes, and obesity* **16**: 163-171

Ruschenbaum S, Schwarzkopf K, Friedrich-Rust M, Seeger F, Schoelzel F, Martinez Y, Zeuzem S, Bojunga J, Lange CM (2018) Patatin-like phospholipase domain containing 3 variants differentially impact metabolic traits in individuals at high risk for cardiovascular events. *Hepatology communications* **2**: 798-806

Rye KA, Barter PJ (2014) Regulation of high-density lipoprotein metabolism. *Circulation research* **114**: 143-156

Sacks FM (2015) The crucial roles of apolipoproteins E and C-III in apoB lipoprotein metabolism in normolipidemia and hypertriglyceridemia. *Current opinion in lipidology* **26**: 56-63

Salvado L, Palomer X, Barroso E, Vazquez-Carrera M (2015) Targeting endoplasmic reticulum stress in insulin resistance. *Trends in endocrinology and metabolism: TEM* **26**: 438-448

Samuel VT, Liu ZX, Wang A, Beddow SA, Geisler JG, Kahn M, Zhang XM, Monia BP, Bhanot S, Shulman GI (2007) Inhibition of protein kinase Cepsilon prevents hepatic insulin resistance in nonalcoholic fatty liver disease. *The Journal of clinical investigation* **117**: 739-745

Samuel VT, Shulman GI (2012) Mechanisms for insulin resistance: common threads and missing links. *Cell* **148**: 852-871

Samuel VT, Shulman GI (2016) The pathogenesis of insulin resistance: integrating signaling pathways and substrate flux. *The Journal of clinical investigation* **126**: 12-22

Samuel VT, Shulman GI (2018) Nonalcoholic Fatty Liver Disease as a Nexus of Metabolic and Hepatic Diseases. *Cell metabolism* **27**: 22-41

Samuel VT, Shulman GI (2019) Nonalcoholic Fatty Liver Disease, Insulin Resistance, and Ceramides. *The New England journal of medicine* **381**: 1866-1869

Sanders FW, Griffin JL (2016) De novo lipogenesis in the liver in health and disease: more than just a shunting yard for glucose. *Biological reviews of the Cambridge Philosophical Society* **91**: 452-468

Sanders FWB, Acharjee A, Walker C, Marney L, Roberts LD, Imamura F, Jenkins B, Case J, Ray S, Virtue S, Vidal-Puig A, Kuh D, Hardy R, Allison M, Forouhi N, Murray AJ, Wareham N, Vacca M, Koulman A, Griffin JL (2018) Hepatic steatosis risk is partly driven by increased de novo lipogenesis following carbohydrate consumption. *Genome biology* **19**: 79

Sano O, Kobayashi A, Nagao K, Kumagai K, Kioka N, Hanada K, Ueda K, Matsuo M (2007) Sphingomyelin-dependence of cholesterol efflux mediated by ABCG1. *Journal of lipid research* **48**: 2377-2384

Santos-Baez LS, Ginsberg HN (2020) Hypertriglyceridemia-Causes, Significance, and Approaches to Therapy. *Frontiers in endocrinology* **11**: 616

Scherer M, Bottcher A, Liebisch G (2011) Lipid profiling of lipoproteins by electrospray ionization tandem mass spectrometry. *Biochimica et biophysica acta* **1811**: 918-924

Schwarz DS, Blower MD (2016) The endoplasmic reticulum: structure, function and response to cellular signaling. *Cellular and molecular life sciences : CMLS* **73**: 79-94

Schwendeman A, Sviridov DO, Yuan W, Guo Y, Morin EE, Yuan Y, Stonik J, Freeman L, Ossoli A, Thacker S, Killion S, Pryor M, Chen YE, Turner S, Remaley AT (2015) The effect of phospholipid composition of reconstituted HDL on its cholesterol efflux and anti-inflammatory properties. *Journal of lipid research* **56**: 1727-1737

Semple RK, Savage DB, Cochran EK, Gordon P, O'Rahilly S (2011) Genetic syndromes of severe insulin resistance. *Endocrine reviews* **32**: 498-514

Sethi AA, Sampson M, Warnick R, Muniz N, Vaisman B, Nordestgaard BG, Tybjaerg-Hansen A, Remaley AT (2010) High pre-beta1 HDL concentrations and low lecithin: cholesterol acyltransferase activities are strong positive risk markers for ischemic heart disease and independent of HDL-cholesterol. *Clinical chemistry* **56**: 1128-1137

Shi L, Tu BP (2015) Acetyl-CoA and the regulation of metabolism: mechanisms and consequences. *Current opinion in cell biology* **33**: 125-131

Shrestha S, Wu BJ, Guiney L, Barter PJ, Rye KA (2018) Cholesteryl ester transfer protein and its inhibitors. *Journal of lipid research* **59**: 772-783

Simonelli S, Tinti C, Salvini L, Tinti L, Ossoli A, Vitali C, Sousa V, Orsini G, Nolli ML, Franceschini G, Calabresi L (2013) Recombinant human LCAT normalizes plasma lipoprotein profile in LCAT deficiency. *Biologicals : journal of the International Association of Biological Standardization* **41**: 446-449

Singh AK, Kari JA (2013) Metabolic syndrome and chronic kidney disease. *Current opinion in nephrology and hypertension* **22**: 198-203

Solinas G, Becattini B (2017) JNK at the crossroad of obesity, insulin resistance, and cell stress response. *Molecular metabolism* **6**: 174-184

Solinas G, Naugler W, Galimi F, Lee MS, Karin M (2006) Saturated fatty acids inhibit induction of insulin gene transcription by JNK-mediated phosphorylation of insulin-receptor substrates. *Proceedings of the National Academy of Sciences of the United States of America* **103**: 16454-16459

Sorci-Thomas MG, Bhat S, Thomas MJ (2009) Activation of lecithin:cholesterol acyltransferase by HDL ApoA-I central helices. *Clin Lipidol* **4**: 113-124

Sparks JD, Sparks CE, Adeli K (2012) Selective hepatic insulin resistance, VLDL overproduction, and hypertriglyceridemia. *Arteriosclerosis, thrombosis, and vascular biology* **32**: 2104-2112

Speliotes EK, Massaro JM, Hoffmann U, Vasan RS, Meigs JB, Sahani DV, Hirschhorn JN, O'Donnell CJ, Fox CS (2010) Fatty liver is associated with dyslipidemia and dysglycemia independent of visceral fat: the Framingham Heart Study. *Hepatology* **51**: 1979-1987

Stegemann C, Pechlaner R, Willeit P, Langley SR, Mangino M, Mayr U, Menni C, Moayyeri A, Santer P, Rungger G, Spector TD, Willeit J, Kiechl S, Mayr M (2014) Lipidomics profiling and risk of cardiovascular disease in the prospective population-based Bruneck study. *Circulation* **129**: 1821-1831

Stow JL, Kjellen L, Unger E, Hook M, Farquhar MG (1985) Heparan sulfate proteoglycans are concentrated on the sinusoidal plasmalemmal domain and in intracellular organelles of hepatocytes. *The Journal of cell biology* **100**: 975-980

Stratford S, DeWald DB, Summers SA (2001) Ceramide dissociates 3'-phosphoinositide production from pleckstrin homology domain translocation. *The Biochemical journal* **354**: 359-368

Sugino I, Kuboki K, Matsumoto T, Murakami E, Nishimura C, Yoshino G (2011) Influence of fatty liver on plasma small, dense LDL- cholesterol in subjects with and without metabolic syndrome. *Journal of atherosclerosis and thrombosis* **18**: 1-7

Surowiec I, Noordam R, Bennett K, Beekman M, Slagboom PE, Lundstedt T, van Heemst D (2019) Metabolomic and lipidomic assessment of the metabolic syndrome in Dutch middle-aged individuals reveals novel biological signatures separating health and disease. *Metabolomics : Official journal of the Metabolomic Society* **15**: 23

Tabas I (2002) Cholesterol in health and disease. *The Journal of clinical investigation* **110**: 583-590

Targher G, Byrne CD, Lonardo A, Zoppini G, Barbui C (2016) Non-alcoholic fatty liver disease and risk of incident cardiovascular disease: A meta-analysis. *Journal of hepatology* **65**: 589-600

Targher G, Byrne CD, Tilg H (2020) NAFLD and increased risk of cardiovascular disease: clinical associations, pathophysiological mechanisms and pharmacological implications. *Gut* **69**: 1691-1705

Taskinen MR, Boren J (2015) New insights into the pathophysiology of dyslipidemia in type 2 diabetes. *Atherosclerosis* **239**: 483-495

Taskinen MR, Packard CJ, Boren J (2019) Emerging Evidence that ApoC-III Inhibitors Provide Novel Options to Reduce the Residual CVD. *Current atherosclerosis reports* **21**: 27

Ter Horst KW, Gilijsse PW, Versteeg RI, Ackermans MT, Nederveen AJ, la Fleur SE, Romijn JA, Nieuwdorp M, Zhang D, Samuel VT, Vatner DF, Petersen KF, Shulman GI, Serlie MJ (2017) Hepatic Diacylglycerol-Associated Protein Kinase Cepsilon Translocation Links Hepatic Steatosis to Hepatic Insulin Resistance in Humans. *Cell reports* **19**: 1997-2004

- Tilg H, Moschen AR (2010) Evolution of inflammation in nonalcoholic fatty liver disease: the multiple parallel hits hypothesis. *Hepatology* **52**: 1836-1846
- Tiwari-Heckler S, Gan-Schreier H, Stremmel W, Chamulitrat W, Pathil A (2018) Circulating Phospholipid Patterns in NAFLD Patients Associated with a Combination of Metabolic Risk Factors. *Nutrients* **10**
- Toledo FG, Sniderman AD, Kelley DE (2006) Influence of hepatic steatosis (fatty liver) on severity and composition of dyslipidemia in type 2 diabetes. *Diabetes care* **29**: 1845-1850
- Urban PL (2016) Quantitative mass spectrometry: an overview. *Philosophical transactions Series A, Mathematical, physical, and engineering sciences* **374**
- Uyeda K, Repa JJ (2006) Carbohydrate response element binding protein, ChREBP, a transcription factor coupling hepatic glucose utilization and lipid synthesis. *Cell metabolism* **4**: 107-110
- Vacca M, Allison M, Griffin JL, Vidal-Puig A (2015) Fatty Acid and Glucose Sensors in Hepatic Lipid Metabolism: Implications in NAFLD. *Seminars in liver disease* **35**: 250-261
- van Bommel EJ, Muskiet MH, Tonneijck L, Kramer MH, Nieuwdorp M, van Raalte DH (2017) SGLT2 Inhibition in the Diabetic Kidney-From Mechanisms to Clinical Outcome. *Clinical journal of the American Society of Nephrology : CJASN* **12**: 700-710
- van de Sluis B, Wijers M, Herz J (2017) News on the molecular regulation and function of hepatic low-density lipoprotein receptor and LDLR-related protein 1. *Current opinion in lipidology* **28**: 241-247
- van den Berg EH, Gruppen EG, Ebtahaj S, Bakker SJL, Tietge UJF, Dullaart RPF (2018) Cholesterol efflux capacity is impaired in subjects with an elevated Fatty Liver Index, a proxy of non-alcoholic fatty liver disease. *Atherosclerosis* **277**: 21-27
- van der Veen JN, Lingrell S, Vance DE (2012) The membrane lipid phosphatidylcholine is an unexpected source of triacylglycerol in the liver. *The Journal of biological chemistry* **287**: 23418-23426
- van Vliet-Ostapchouk JV, Nuotio ML, Slagter SN, Doiron D, Fischer K, Foco L, Gaye A, Gogele M, Heier M, Hiekkalinna T, Joensuu A, Newby C, Pang C, Partinen E, Reischl E, Schwenbacher C, Tammesoo ML, Swertz MA, Burton P, Ferretti V, Fortier I, Giepmans L, Harris JR, Hillege HL, Holmen J, Jula A, Kootstra-Ros JE, Kvaloy K, Holmen TL, Mannisto S, Metspalu A, Midthjell K, Murtagh MJ, Peters A, Pramstaller PP, Saaristo T, Salomaa V, Stolk RP, Uusitupa M, van der Harst P, van der Klauw MM, Waldenberger M, Perola M, Wolffenbuttel BH (2014) The prevalence of metabolic syndrome and metabolically healthy obesity in Europe: a collaborative analysis of ten large cohort studies. *BMC endocrine disorders* **14**: 9

- Virtue S, Vidal-Puig A (2010) Adipose tissue expandability, lipotoxicity and the Metabolic Syndrome--an allostatic perspective. *Biochimica et biophysica acta* **1801**: 338-349
- Wang H, Eckel RH (2009) Lipoprotein lipase: from gene to obesity. *American journal of physiology Endocrinology and metabolism* **297**: E271-288
- Wang L, Athinarayanan S, Jiang G, Chalasani N, Zhang M, Liu W (2015) Fatty acid desaturase 1 gene polymorphisms control human hepatic lipid composition. *Hepatology* **61**: 119-128
- Warnick GR, Benderson J, Albers JJ (1982) Dextran sulfate-Mg²⁺ precipitation procedure for quantitation of high-density-lipoprotein cholesterol. *Clinical chemistry* **28**: 1379-1388
- Wei Y, Wang D, Topczewski F, Pagliassotti MJ (2006) Saturated fatty acids induce endoplasmic reticulum stress and apoptosis independently of ceramide in liver cells. *American journal of physiology Endocrinology and metabolism* **291**: E275-281
- Wiesner P, Leidl K, Boettcher A, Schmitz G, Liebisch G (2009) Lipid profiling of FPLC-separated lipoprotein fractions by electrospray ionization tandem mass spectrometry. *Journal of lipid research* **50**: 574-585
- Wolska A, Dunbar RL, Freeman LA, Ueda M, Amar MJ, Sviridov DO, Remaley AT (2017) Apolipoprotein C-II: New findings related to genetics, biochemistry, and role in triglyceride metabolism. *Atherosclerosis* **267**: 49-60
- Yang K, Han X (2016) Lipidomics: Techniques, Applications, and Outcomes Related to Biomedical Sciences. *Trends in biochemical sciences* **41**: 954-969
- Yang RX, Hu CX, Sun WL, Pan Q, Shen F, Yang Z, Su Q, Xu GW, Fan JG (2017) Serum Monounsaturated Triacylglycerol Predicts Steatohepatitis in Patients with Non-alcoholic Fatty Liver Disease and Chronic Hepatitis B. *Scientific reports* **7**: 10517
- Yin X, Willinger CM, Keefe J, Liu J, Fernandez-Ortiz A, Ibanez B, Penalvo J, Adourian A, Chen G, Corella D, Pamplona R, Portero-Otin M, Jove M, Courchesne P, van Duijn CM, Fuster V, Ordovas JM, Demirkan A, Larson MG, Levy D (2020) Lipidomic profiling identifies signatures of metabolic risk. *EBioMedicine* **51**: 102520
- Younis N, Charlton-Menys V, Sharma R, Soran H, Durrington PN (2009) Glycation of LDL in non-diabetic people: Small dense LDL is preferentially glycated both in vivo and in vitro. *Atherosclerosis* **202**: 162-168
- Younossi Z, Anstee QM, Marietti M, Hardy T, Henry L, Eslam M, George J, Bugianesi E (2018) Global burden of NAFLD and NASH: trends, predictions, risk factors and prevention. *Nature reviews Gastroenterology & hepatology* **15**: 11-20

Younossi ZM, Koenig AB, Abdelatif D, Fazel Y, Henry L, Wymer M (2016) Global epidemiology of nonalcoholic fatty liver disease-Meta-analytic assessment of prevalence, incidence, and outcomes. *Hepatology* **64**: 73-84

Zannis VI, Fotakis P, Koukos G, Kardassis D, Ehnholm C, Jauhiainen M, Chroni A (2015) HDL biogenesis, remodeling, and catabolism. *Handbook of experimental pharmacology* **224**: 53-111

Zeos P, Renner EL (2014) Liver transplantation and non-alcoholic fatty liver disease. *World journal of gastroenterology* **20**: 15532-15538

Zhang QQ, Lu LG (2015) Nonalcoholic Fatty Liver Disease: Dyslipidemia, Risk for Cardiovascular Complications, and Treatment Strategy. *Journal of clinical and translational hepatology* **3**: 78-84

Zhou JH, Cai JJ, She ZG, Li HL (2019) Noninvasive evaluation of nonalcoholic fatty liver disease: Current evidence and practice. *World journal of gastroenterology* **25**: 1307-1326

Zhou Y, Oresic M, Leivonen M, Gopalacharyulu P, Hyysalo J, Arola J, Verrijken A, Francque S, Van Gaal L, Hyotylainen T, Yki-Jarvinen H (2016) Noninvasive Detection of Nonalcoholic Steatohepatitis Using Clinical Markers and Circulating Levels of Lipids and Metabolites. *Clinical gastroenterology and hepatology : the official clinical practice journal of the American Gastroenterological Association* **14**: 1463-1472 e1466